

# Potential and uncertainty of wind energy in the Swiss Alps

Thèse N° 9350

Présentée le 8 mars 2019

à la Faculté de l'environnement naturel, architectural et construit  
Laboratoire des sciences cryosphériques  
Programme doctoral en génie civil et environnement

pour l'obtention du grade de Docteur ès Sciences

par

**Albertus Christiaan KRUYT**

Acceptée sur proposition du jury

Prof. A. Buttler, président du jury  
Prof. M. Lehning, directeur de thèse  
Dr G. Giudati, rapporteur  
Dr S. Bourgeois, rapporteuse  
Dr J. Fang, rapporteur

2019



*Παντα ρει*

To my parents...



# Acknowledgements

This thesis would not have been possible with the help of many amazing people around me. First of, I'd like to thank Michi Lehning, for putting his trust in me and exploring a relatively new field together. I've learned a great deal from you over the years, thank you for allowing me the freedom to do things my way. The amazing Team Energy at EPFL: Annelen, Jerome and Stuart; you guys are the best. Slowly we will save the world! ;)

Deep gratitude goes to Franziska Gerber and Varun Sharma for helping me with the WRF modeling described in the last chapter of this thesis. If it weren't for your help and patient answers to my countless questions, I am sure that chapter would have looked very different. Similarly, I am grateful for Benoit Gherardi's help with an initial WRF set-up.

The great people at CRYOS in Lausanne have always welcomed me warmly. And although I only made very irregular appearances you all made me feel welcome and part of the team. Thank you Hendrik, Annelen, Jerome, Johan, Varun, Francesco, Tristan, Mahdi, Adrien, Ernesto, Margeaux and all the rest.

These four years in Davos have been an amazing time, largely due to the very inspiring working environment. Thanks to all of the people at the SLF who fed my interest in snow and avalanches with interesting discussions, insights and amazing days in the mountains. The list is too long but thank you Anselm, Achille, Anna, Betty, Beni, Cesar, Chris, Greg, Jürg, Kurt, Marco, Nander, Nathalie, Nena, Philip, Robert, Steffi, Thiemo, and other supercool Davos people: Robi, Fleur, Jenny, Walter, James, Susan, Will, Laubi and Urs.

Most importantly, I want to thank my parents. In this age of the ego, it is tempting to think that all we achieve is solely because of our own efforts (while everything we fail to achieve is because of some lame excuse). I am however very aware that I would be nowhere near where I am today had it not been for you. Throughout my life you have provided all the boundary conditions for me to flourish, without ever being restrictive or directive. I dedicate this thesis to the two of you.

And last but certainly not least, thank you to Quirine. You are my shining light and make me want to be a better person. Some years ago we threw all our possessions in a car and drove off into the unknown. It has been one big adventure ever since and I can't wait to see what is next.

*Davos, December 2018*

B. K.



# Abstract

Switzerland has committed itself to an ambitious energy strategy. It aims to replace the existing nuclear generation capacity with predominantly indigenous renewable resources. Wind power could play a significant role in this transition, yet the wind resource in the mountainous terrain that makes up most of the country is poorly understood. There are indications that this resource could be significant, but studies undertaken so far acknowledge large uncertainties. This is because the complex topography of the mountains influences the flow patterns significantly, and these can become partially decoupled from the synoptic flow aloft. This thesis aims to improve the understanding of the wind resource in highly complex terrain, and thereby contribute to a well informed energy transition in Switzerland.

We start out by investigating the characteristics of the Swiss wind resource based on data from two meteorological measurement networks. From the pair-wise correlation between stations, it is concluded that wind farms across the country can be combined to produce a stable power output. It is also shown that elevation plays an important role in the wind resource, with the likelihood of sustained low wind speeds decreasing as a function of elevation, while mean speeds tend to increase with elevation.

Next, a state of the art Numerical Weather Prediction model is assessed in its ability to simulate wind speeds over the Alps, and is shown to improve drastically upon existing mean wind speed estimates. This same model is then used to calculate the wind turbine capacity that is required to produce significant amounts of wind power, and it is found that the required capacity can be significantly reduced by allowing for wind turbines to be built at high elevations.

In the last part of this thesis, smaller areas of the Alpine domain are simulated at high resolutions, to investigate the effect of increased model resolution on the accuracy and height of resource assessments. While it is found that optimal model parameterization is dependent on weather and terrain, strong indications of higher wind power potential are found with high resolution models compared to a model at lower resolution. This is explained by the fact that high resolutions are required to properly resolve the complex topography, which has a significant influence on the flow patterns and therefore, on the potential energy production.

*Keywords: Wind Energy, Resource Assessment, ES2050, Numerical Weather Prediction, Wind Modeling*





# Zusammenfassung

Die Schweiz hat sich zu einer ambitionierten Energiestrategie verpflichtet. Ziel ist es, die bestehende, nukleare Energieerzeuger durch überwiegend einheimische erneuerbare Ressourcen zu ersetzen. Die Windkraft könnte bei diesem Übergang eine wichtige Rolle spielen, allerdings sind Windressourcen in gebirgigem Gelände, das den größten Teil des Landes ausmacht, kaum verstanden. Vieles deutet darauf hin, dass diese Ressource von Bedeutung sein könnte, aber bisher durchgeführte Studien zeigen große Unsicherheiten. Die komplexe Topographie der Berge beeinflusst die Strömungsmuster erheblich, so dass sie sich zum Teil vom synoptischen Fluss in der Höhe entkoppeln können. Diese Arbeit zielt darauf ab, das Verständnis der Windressource in hochkomplexem Gelände zu verbessern und damit zu einer auf Fakten und Erkenntnissen beruhenden Energiewende in der Schweiz beizutragen. Zunächst untersuchen wir die Eigenschaften der schweizer Windressource anhand von Daten aus zwei meteorologischen Messnetzen. Aus der paarweisen Korrelation zwischen den Stationen wird geschlossen, dass Windparks im ganzen Land zu einer stabilen Stromerzeugung kombiniert werden können. Es wird auch gezeigt, dass die Höhenlage eine wichtige Rolle für die Windenergie spielt: die Wahrscheinlichkeit anhaltend niedriger Windgeschwindigkeiten nimmt mit steigender Höhe ab, während die Durchschnittsgeschwindigkeiten mit der Höhe zunehmen. Als nächstes wird ein numerisches Wettervorhersagemodell in seiner Fähigkeit bewertet, Windgeschwindigkeiten in den Alpen zu simulieren. Hierbei wird eine grosse Verbesserung im Vergleich zu bestehenden Schätzungen der mittleren Windgeschwindigkeit erarbeitet. Das gleiche Modell wird dann verwendet, um die Kapazität zu berechnen, die für die Erzeugung großer Mengen an Windkraft benötigt wird. Die Ergebnisse zeigen, dass die erforderliche Kapazität erheblich reduziert werden kann, wenn der Bau von Windturbinen in hohen Lagen ermöglicht wird. Im letzten Teil dieser Arbeit werden kleinere Bereiche des Alpenraums mit hoher Auflösung simuliert, um die Auswirkungen einer erhöhten Modellauflösung auf die Genauigkeit der Bewertung und auf das Gesamtpotenzial zu untersuchen. Während optimale Modellparametrisierung von Wetter und Gelände abhängt, nimmt mit zunehmender Modellauflösung das Windpotenzial zu. Das lässt sich dadurch erklären, dass für die korrekte Auflösung der komplexen Topographie, die einen wesentlichen Einfluss auf die Strömungsmuster hat, hohe Auflösungen erforderlich sind.



# Contents

<b>Acknowledgements</b>	<b>v</b>
<b>Abstract (English/Français/Deutsch)</b>	<b>vii</b>
<b>List of figures</b>	<b>xiii</b>
<b>List of tables</b>	<b>xvi</b>
<b>1 Introduction</b>	<b>1</b>
1.1 Wind power . . . . .	1
1.1.1 Intermittency and the power system . . . . .	2
1.2 Wind power in Switzerland: Current standings and outlook . . . . .	3
1.2.1 Switzerland's electricity supply . . . . .	3
1.2.2 The Energy Strategy 2050 and the future Swiss power supply . . . . .	4
1.3 Wind resource assessment . . . . .	5
1.4 Wind modeling . . . . .	6
1.4.1 Downscaling: Static vs Dynamic . . . . .	6
1.4.2 Wind modeling and resource assessment for Switzerland . . . . .	7
1.5 Content of the thesis . . . . .	8
<b>2 Potential contributions of wind power to a stable and highly renewable Swiss power supply</b>	<b>11</b>
2.1 Introduction . . . . .	11
2.2 Data and Methods . . . . .	14
2.2.1 Measurement stations . . . . .	14
2.2.2 Missing Data . . . . .	15
2.2.3 Correlation . . . . .	16
2.2.4 Turbine choice . . . . .	16
2.2.5 Height transformation . . . . .	17
2.2.6 Extreme Value Analysis . . . . .	17
2.2.7 Diurnal wind speed patterns . . . . .	19
2.3 Results and Discussion . . . . .	20
2.3.1 Correlation . . . . .	20
2.3.2 Return levels . . . . .	21
	xi

## Contents

---

2.3.3	Seasonal decomposition . . . . .	21
2.3.4	Diurnal patterns . . . . .	22
2.3.5	Elevation . . . . .	26
2.4	Sensitivity and Outlook . . . . .	27
2.5	Conclusion . . . . .	28
2.5.1	Implications and Outlook . . . . .	29
2.6	Acknowledgements . . . . .	30
<b>3</b>	<b>Improvement of wind power assessment in complex terrain: The case of COSMO-1 in the Swiss Alps</b>	<b>31</b>
3.1	Introduction . . . . .	31
3.1.1	Wind resource assessment using NWP	32
3.1.2	Wind resource assessment in the Alps . . . . .	32
3.1.3	Outline and goals . . . . .	33
3.2	Methods . . . . .	34
3.2.1	COSMO-1 . . . . .	34
3.2.2	IMIS network . . . . .	35
3.2.3	Validation of COSMO-1 . . . . .	35
3.2.4	Power transformation . . . . .	36
3.2.5	Wind energy potential . . . . .	36
3.2.6	Modelling Switzerland's power supply . . . . .	37
3.2.7	Required number of wind turbines . . . . .	39
3.3	Results and Discussion . . . . .	40
3.3.1	Validation of COSMO-1 against IMIS weather stations . . . . .	40
3.3.2	Comparison with Wind Atlas . . . . .	42
3.3.3	Capacity factor . . . . .	42
3.3.4	Potential import reduction due to turbine siting . . . . .	43
3.3.5	Required number of turbines . . . . .	46
3.3.6	Swiss wind Energy Concept . . . . .	46
3.3.7	Capacity as function of annual wind power production . . . . .	47
3.3.8	Sensitivity to wind speed errors . . . . .	49
3.4	Conclusions . . . . .	50
3.4.1	Wind resource assessment with COSMO-1 . . . . .	50
3.4.2	Import reduction & wind power . . . . .	51
3.4.3	Required capacity . . . . .	51
3.4.4	Outlook . . . . .	52
3.5	Acknowledgements . . . . .	53
<b>4</b>	<b>Downscaling surface wind speeds over very complex terrain for wind potential iden- tification</b>	<b>55</b>
4.1	Introduction . . . . .	55
4.2	Methods . . . . .	58
4.2.1	Simulated domains . . . . .	58

---

4.2.2	The WRF model setup . . . . .	59
4.2.3	Validation . . . . .	61
4.2.4	Comparison with COSMO-1 and COSMO-2 . . . . .	62
4.3	Results and discussion . . . . .	63
4.3.1	Model performance and validation . . . . .	63
4.3.2	Potential indication . . . . .	72
4.3.3	Power production . . . . .	72
4.4	Conclusions . . . . .	75
4.5	Outlook . . . . .	76
<b>5</b>	<b>Conclusions</b>	<b>79</b>
5.1	Conclusions . . . . .	79
5.2	Outlook . . . . .	83
<b>A</b>	<b>Air density and altitude</b>	<b>85</b>
<b>A</b>	<b>WRF Namelist</b>	<b>87</b>
	<b>Bibliography</b>	<b>106</b>
	<b>Curriculum Vitae</b>	<b>107</b>



# List of Figures

1.1	Global cumulative installed wind capacity . . . . .	1
1.2	Map of current wind turbines in Switzerland. . . . .	4
1.3	The 2016 Swiss wind atlas . . . . .	8
2.1	Map with meteorological stations from the SMN and IMIS networks. . . . .	15
2.2	The Return level as a function of the declustering parameter $k$ . . . . .	19
2.3	correlation between wind speeds in Switzerland . . . . .	20
2.4	Return levels for no power intervals . . . . .	21
2.5	Ratio of return levels in summer vs winter . . . . .	22
2.6	The 10 year return level and parameters of the GEV distribution . . . . .	23
2.7	Diurnal wind speed profiles . . . . .	24
2.8	Seasonal and Diurnal patterns for selected stations . . . . .	25
2.9	Relative increase in mean speeds in winter compared to summer, as a function of elevation . . . . .	26
2.10	Simulated electricity production as a function of elevation . . . . .	27
2.11	Sensitivity of calculated return levels to cut in speeds . . . . .	28
3.1	The IMIS stations . . . . .	35
3.2	Various definitions of wind energy potential . . . . .	37
3.3	Root mean Square errors between IMIS and COSMO-1 wind speeds . . . . .	41
3.4	Mean bias errors between IMIS and COSMO-1 wind speeds . . . . .	41
3.5	Correlations between IMIS and COSMO-1 wind speeds . . . . .	42
3.6	Capacity Factors based on wind speeds from COSMO-1 . . . . .	43
3.7	Required imports for characteristic wind speed time series . . . . .	45
3.8	Required turbine capacity as function of mean turbine elevation . . . . .	47
3.9	Capacity and import as function of turbine location . . . . .	48
3.10	Wind power capacity required to produce 4,6, or 12 TWh/a wind energy . . . . .	48
3.11	MBE for turbine performance ranges . . . . .	50
4.1	WRF simulation domains . . . . .	59
4.2	Root mean square errors of the WRF and COSMO models for the domain around Andermatt . . . . .	64
4.3	Root mean square errors of the WRF and COSMO models for the domain around Andermatt, for wind and snow stations . . . . .	65

## List of Figures

---

4.4	Mean bias errors of the WRF and COSMO models at Andermatt . . . . .	65
4.5	Simulated wind speed time series at Andermatt . . . . .	67
4.6	Root mean square errors of the WRF and COSMO models for the domain around Chur . . . . .	68
4.7	Simulated wind speed time series at Chur . . . . .	69
4.8	Comparison of COSMO-2 and WRF mean wind speeds for the domain around Andermatt . . . . .	73
4.9	Difference between WRF and COSMO2 mean wind speeds for the domain around Andermatt at 100 m above the surface . . . . .	73
4.10	Histograms of the differences between WRF and COSMO2 mean wind speeds .	74





## List of Tables

3.1	COSMO-1 validation against IMIS stations . . . . .	40
4.1	Model comparison for near-surface wind speeds: comparison to IMIS stations. Results per model run. . . . .	70
4.2	Model comparison for hub-height wind speeds: Results per model run. . . . .	71
4.3	Simulated power production as deviation from actual wind turbine production	74



# 1 Introduction

## 1.1 Wind power

Humans have been harnessing the power of the wind since the start of civilization, for example to sail the seas, and later for the pumping of water. The first windmills date back to 200 BC [Carlin, 2003] when they were used to grind grains or pump water. After the invention of electricity the first wind turbines were built at the end of the 19th century, a mere 5 years after the first commercial coal power plant was built<sup>1</sup>. Initial development of wind turbines was slow, and fossil fueled stations were preferred for their ease of dispatch and abundant availability of resources. Towards the end of the 20st century concerns over anthropogenic climate change gained ground, and the interest in wind power as a source of electricity with very low associated carbon emissions surged. As a result, during the 21st century, cumulative installed capacity worldwide increased from 24 GW in 2001 to 539 GW in 2017, i.e. more than 20 fold (see Figure 1.1) [GWEC, 2018, Global WInd Energy Council, 2018].

---

<sup>1</sup>[ethw.org/Pearl\\_Street\\_Station](http://ethw.org/Pearl_Street_Station)

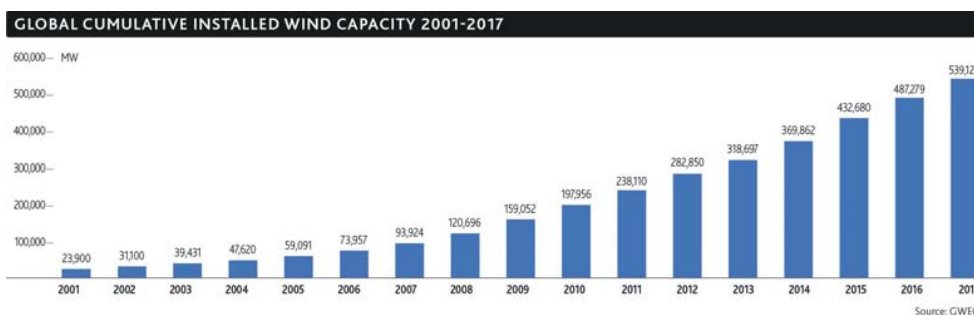


Figure 1.1 – Global cumulative installed wind capacity, from 2001 to 2017. source: GWEC

### 1.1.1 Intermittency and the power system

A noteworthy downside of wind power compared to fossil-based power generation is the intermittent nature of the produced power. Where for hydroelectric, coal- and especially gas-fired power plants power output can be regulated at very small timescales, the power output from a wind turbine is dependent on the weather. Wind energy, together with other renewable electricity sources whose power output cannot be easily regulated, such as PhotoVoltaics (PV), are therefore often referred to as intermittent renewables. Small amounts of such intermittent renewables can easily be integrated into the electricity mix, as other dispatchable sources are able to balance the intermittent character [Brouwer et al., 2014]. As the urgency of climate change becomes more apparent however, people are increasingly looking at ways to allow for higher penetration rates of intermittent renewables. Traditionally, power generators can be divided into base- and peak load, the former being that part of power that is required constantly during the day, and peak load being the positive deviation from the baseload that occurs only at certain times during the day. (usually mornings and late afternoon/early evening). Generators with low fuel cost and/or high capital costs, or whose output can not be easily adjusted (such as nuclear or run of river hydropower) are typically used for baseload power, whereas generators with easily adjustable power output (such as storage hydropower, coal or gas fired power plants) are used for peak load. As there is no way to regulate the output of wind and PV apart from curtailing, they are normally used for baseload power. This also makes sense from an economic perspective, as their marginal costs are low due to the absence of fuel costs. It does however, require other flexible generators in the generating mix in order to respond to the changes in both output and demand. In any power system, with or without renewables, certain power plants are assigned to deal with unforeseen imbalances between supply and demand. This capacity is called *spinning reserve* and *backup capacity*<sup>2</sup> [Ortega-Vazquez and Kirschen, 2009]. This flexible capacity traditionally consists of power plants (gas, hydro or coal), that are operating below their maximum capacity and can be ramped up very quickly.

Further important concepts in the discussion of wind power intermittency are the *capacity factor* (the percentage of power production as a fraction of the nameplate capacity of the wind energy conversion system); the *firm capacity* (the fraction of installed wind capacity that either is online at all times or with a probability similar to the availability of a fossil fuel power plant); and the *capacity credit* (the fraction of installed (renewable) capacity by which the conventional power generation capacity can be reduced without affecting the loss of load probability) [Giebel, 2006].

It is easy to see that the required spinning reserve will increase as the share of intermittent renewables in the supply mix increases. And while uninformed opinions in popular media may occasionally echo sentiments to the contrary, it has been unmistakably shown that wind

---

<sup>2</sup>The difference between the two is related to their response times, where spinning reserve is (by definition) online and able to respond within seconds to minutes, while back-up capacity needs to be cold-started and has typical response times of up to an hour.

## 1.2. Wind power in Switzerland: Current standings and outlook

---

power does offer a capacity credit [Giebel, 2006, Brouwer et al., 2014], i.e. it can displace part of conventional generating capacity without the need for full capacity back-up. Coining the popular saying that 'the wind always blows somewhere', much of the variability can be reduced by combining wind farms over large distances [Giebel, 2000], in part due to the fact that the cross-correlation of the wind speed reduces as a function of distance; An important concept we shall come back to later in this work. As such, it is shown that connecting wind farms over large distances decreases the standard deviation of the combined power output, and the power that can be guaranteed over the year increases [Archer and Jacobson, 2007]. On weekly timescales, weather regimes explain much of the fluctuations in wind power output in Europe, and locating capacity accordingly may alleviate much of the variability, while increasing the minimum (firm) capacity [Grams et al., 2017]. Combining wind power capacity over such large distances does however requires large transmission capacity [Rodriguez, 2014, Becker et al., 2014].

## 1.2 Wind power in Switzerland: Current standings and outlook

### 1.2.1 Switzerland's electricity supply

Switzerland's electricity mix depends heavily on the country's hydropower infrastructure with over 33%<sup>3</sup> of national power production coming from storage hydropower and over 25% from run-of-river hydropower. Another 32% are supplied by the country's five nuclear power plants, and the remaining 9% come from thermal power plants and renewables, with wind power supplying 0.23% (132,6 GWh) [Bundesamt für Energie BFE, 2017, Kaufmann, 2018]. This wind power comes from 37 wind farms with in total 57 turbines and a cumulative capacity of 60.3 MW [Kaufmann, 2018]. The majority of the capacity is located in the Jura mountains, in the northwest of the country (Figure 1.2).

There is a distinct seasonal profile to the Swiss power supply, owing to the seasonality of hydropower. During the summer season, snow melt causes an increase in runoff that leads to an higher run-of-river hydropower production, as well as increased inflow to the storage reservoirs. On the demand side, we see the opposite trend with higher demand during the winter months due to increases in lighting and heating [Dujardin et al., 2017]. Because of the limited storage capacity in the hydropower reservoirs, Switzerland is unable to be fully self sufficient and is a net importer during the winter months, while exporting during summer. These facts alone make a strong case for wind power, since mean wind speeds are known to be higher in winter over north and central Europe [Archer and Jacobson, 2013, Grams et al., 2017, Clark et al., 2017, Graabak and Korpås, 2016, Holttinen, 2005], making wind power an attractive complement to hydropower.

---

<sup>3</sup>numbers given are for the year 2017, and are nett production, meaning that the consumption for pumped storage hydropower has been subtracted.

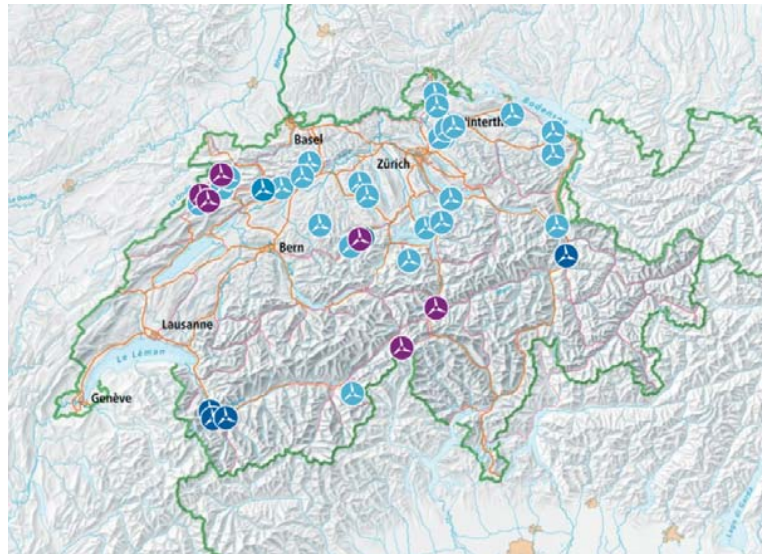


Figure 1.2 – Wind farms in Switzerland. Purple icons indicate wind parks, while the blue icons indicate individual turbines with capacities below (light blue), and equal to or above 1 MW (dark blue). source: Swisstopo, BFE

### 1.2.2 The Energy Strategy 2050 and the future Swiss power supply

The picture painted above is about to change drastically however, as in 2011 following the nuclear disaster in Fukushima, the Swiss Federal Council and Parliament decided on a progressive withdrawal from nuclear energy. This implies that the existing nuclear stations will be shut down at the end of their operating lifetimes and will not be replaced with new nuclear infrastructure [Swiss Federal Office of Energy SFOE, 2018]. The Energy act that followed this decision came into force on January 1st 2018. It envisions, amongst a withdrawal from nuclear and an increase of energy efficiency, a move towards a more indigenous renewables-based electricity supply [Schweizerischen Eidgenossenschaft, 2018].

The 2011 decision to move away from nuclear led many interested parties to publish their vision on the future of the Swiss energy supply [VSE, 2012, Barmettler et al., 2013, Teske, 2013], and produced surge in research on the topic [Prognos, 2012, Weidmann, 2013, Densing et al., 2014, Swiss Academy of Engineering Sciences (SATW), 2012, Bauer et al., 2017]<sup>4</sup>. While for all these studies assumptions and thus outcomes vary (from being unable to cover domestic production without imports or gas [Densing et al., 2014, Redondo and Van Vliet, 2015] to being easily able to meet demand with domestic renewables [Gunzinger, 2015]), one thing they all lack is a proper assessment of wind power potential (by modern means). While some calculations use reanalysis data with a horizontal resolutions of 57 km [Redondo and Van Vliet, 2015], thereby reducing Switzerland to a handful of grid cells, others use average generating days per season [Weidmann, 2013, Gunzinger, 2015]. Most works however, quote one and the same study by Bundesamt für Energie BFE [2004a,b]. This study concludes that the wind

<sup>4</sup>Densing et al. [2014] provide a very good overview of most of these studies.

power potential in Switzerland in the year 2050 amounts to 1.2 TWh from wind farms with an additional 2.8 TWh from individual turbines, which combined forms the often mentioned potential or target of 4 TWh in 2050. This, and other studies for Switzerland are discussed in more detail in section 1.4.2.

### 1.3 Wind resource assessment

Large scale wind resource assessments are often based on reanalysis data with horizontal resolutions in the order of 0.5° to 1° (~50 to ~100 km), and coarse temporal resolutions [Hoogwijk, 2004, Grams et al., 2017, Archer and Jacobson, 2013, 2005]. It is important to realise that at these resolutions it is impossible to resolve the influence of the terrain, nor account for seasonal or diurnal fluctuations [Archer and Jacobson, 2013]. Especially for very complex terrain, the influence of the topography is significant [Mengelkamp, 1999, Clifton et al., 2014]. On the other hand, measurement stations usually offer no reliable alternative, as they are inhomogeneously and sparsely distributed. Regional assessments may give a little more reliability, as model resolutions can be increased. However for very complex terrain such as the Alps, resolutions that capture the complex topography are often unattainable at the country scale, especially as long time series at decent temporal resolution are required to capture the variability at diurnal, seasonal and intra-annual scales.

Further complications arise when translating near surface (~10 m) wind speeds to hub heights (~100 m). The vertical wind profile is often assumed to follow a logarithmic or power law [DeMarrais, Gerard, 1958]. While this may be an acceptable approximation for flat, homogeneous terrain [Brower et al., 2012] over long time averages [Kubik et al., 2013], it is acknowledged that in complex terrain wind shear and thus the vertical profile behave very differently [Cattin et al., 2003, Draxl and Mayr, 2009, Clifton et al., 2014].

Using annual mean speeds as a basis of power potential assessment, several assumptions have to be made. Firstly, as the power produced from any wind turbine is not a linear function of the wind speed, assumptions regarding the distribution of the wind speeds around the mean have to be made if no distributions are available. Secondly assumptions on the surface area available for wind power development have to be made. It is here that we dive into the realm of various potentials. While many different potential definitions exist [Archer and Jacobson, 2013, Hoogwijk and Graus, 2008, Hoogwijk et al., 2004], they all share some similar components. Starting with a theoretical potential that describes the power that can be extracted from the wind, a technical potential then reduces this based on turbine efficiencies and maintenance outages. The largest subjectivities however arise from the assumptions on land availability and political acceptance (often termed geographical potential); costs and competitiveness (economic potential) and integration into the market (market potential). While these are all very relevant parameters, it is important to realize that they vary over time as public opinion or political priorities change (geographic potential), prices or subsidies develop (economic potential) and market regulations and institutional barriers change (market potential).

### 1.4 Wind modeling

Numerical Weather Prediction (NWP) models are used to simulate the physical processes in the atmosphere. Their basic method is to divide the atmosphere into smaller volumes according to a grid, and solve the conservation equations for momentum (otherwise known as the Navier Stokes equations), energy(heat) and mass for each of the grid cells. Amongst atmospheric models, one can distinguish between global, mesoscale (or regional), and microscale models. Mesoscale models, with horizontal resolutions in the order of kilometers, are typically used for weather prediction. Here, fine-scale processes in the boundary layer such as turbulence are parameterized. At the other end of the spectrum are microscale models, with resolutions in the order of meters. With these resolutions, it is possible to explicitly resolve (part of) the turbulent motions. The resolutions that fall in between the meso- and microscale ( $\Delta x \sim 10\text{m} - 10\text{ km}$ ) has been dubbed the 'terra incognita' [Wyngaard, 2004, Mazzaro et al., 2017], or 'Grey zone' [Shin and Dudhia, 2016], a range for which both meso- and microscale models were not designed. The continuous advance in computational power has allowed mesoscale models to be run on increasingly higher resolutions [Gerber et al., 2018, Raderschall et al., 2008], thereby entering this terra incognita. This increase in model resolution can however lead to poorer results, as grid-dependent convection can occur [Zhou et al., 2014].

Wind flows near the earth's surface are a result of both the synoptic scale flow patterns as well as the interactions with the surface. As the topography becomes more complex, the relative influence of the latter increases, to the extent that local flows can deviate significantly from their synoptic drivers, or -in the case of thermal flows- can become completely decoupled [Truhetz, 2010]. This implies that for accurate simulation of the wind speeds over complex terrain, it is imperative to accurately represent the topography.

#### 1.4.1 Downscaling: Static vs Dynamic

The translation of coarse gridded meteorological data to finer grids is called downscaling. This can be done statistically or dynamically, where the latter involves running regional NWP models at finer resolutions with the boundary conditions provided by the coarser model. Statistical downscaling on the other hand relies on correlations between parameters available at the target scale and the parameters at coarser resolution. The downside to statistical downscaling is that the physical processes responsible for these correlations are not taken into account. The upside being that statistical downscaling requires significantly less computational power compared to dynamical downscaling. Downscaling with NWP models requires a lot of computational resources, mainly due to the solving of the (coupled) partial differential equations that make up the governing conservation equations. A third option therefore is to simplify these governing conservation equations. Amongst the model that do this, we can distinguish between linearized, steady-state models such as WASP<sup>5</sup> and non-linear CFD or

---

<sup>5</sup><http://www.wasp.dk>



Reynolds-averaged Navier Stokes (RANS) model such as WindSim<sup>6</sup> [Brower, 2013]. The former, sometimes also called diagnostic models forgo the time-derivatives of the governing equations, thereby assuming a steady-state flow [Truhetz, 2010] and are shown to fall short in complex terrain [Cattin et al., 2006]. For the RANS CFD models the performance in complex terrain is not as unequivocal, with studies concluding their performance to be 'adequate' [Cattin et al., 2006] to clearly outperformed by fully physical NWP models, especially as the distance from measurement towers providing initialization data increases [Brower, 2013]. Both methods are highly sensitive to the initial wind field and the number of observations per simulation area, and are unable to reproduce thermally induced flows [Truhetz, 2010].

### 1.4.2 Wind modeling and resource assessment for Switzerland

As touched upon in section 1.2, the study responsible for the often cited 4 TWh/a in 2050 is the Swiss wind energy concept (*Konzept Windenergie Schweiz*) [Bundesamt für Energie BFE, 2004b,a], not to be confused with the 2017 document with the same name, which only assesses political interests [Bundesamt für Raumentwicklung, 2017]. In the 2004 study, wind flows for several standard situations are calculated, and subsequently weighted with annual means of 103 wind speed measurements from weather stations. Using a topographic model the results are interpolated onto a 100 m by 100 m grid. This geo-spatial method yields annual means with no information on their distributions. As noted by Truhetz [2010] this method has conceptual shortcomings in the Alpine region *Because of the terrain-induced decoupling effects between predictors and predictands*. Nevertheless this method was again used in the Alpine Windharvest project [Cattin et al., 2006, Schaffner and Cattin, 2005, Schaffner and Remund, 2005]. In 2016 roughly the same method was used for an update of the wind map produced in 2004. The resulting 'Swiss Wind Atlas' gives annual mean speeds at heights of 50, 75, 100, 125 and 150 m above the surface, based on the WindSim model mentioned previously, combined with roughly 100 mast measurements at different heights (See Figure 1.3) [Koller and Humar, 2016]. Reported absolute errors in mean annual wind speeds are in the order of 1.0 m/s for valleys and 1.5 m/s for mountains (, although it is unclear if these reported errors are statistically significant or 'example' errors).

Oppliger et al. [2016] applied the CFD model OpenFoam<sup>7</sup> to a small part in the northeast of Switzerland and showed that the uncertainty in the annual means could be reduced with 40% compared to the Swiss wind atlas. In this method, weather is clustered into 9 main classes, based on the pressure differences for valley, hill, and mountain stations (3 each). For each cluster two representative hours in a 24h COSMO-1 forecast are selected and used as boundary conditions for CFD simulations at 200 m resolution<sup>8</sup>. The simulated wind speeds are then scaled to match the speeds at the measurement stations, and Weibull parameters are estimated by averaging over the 9 weather types and stations.

---

<sup>6</sup><https://windsim.com/>

<sup>7</sup>[www.openfoam.com](http://www.openfoam.com)

<sup>8</sup>'detail' simulations with 50 m horizontal resolution were also conducted

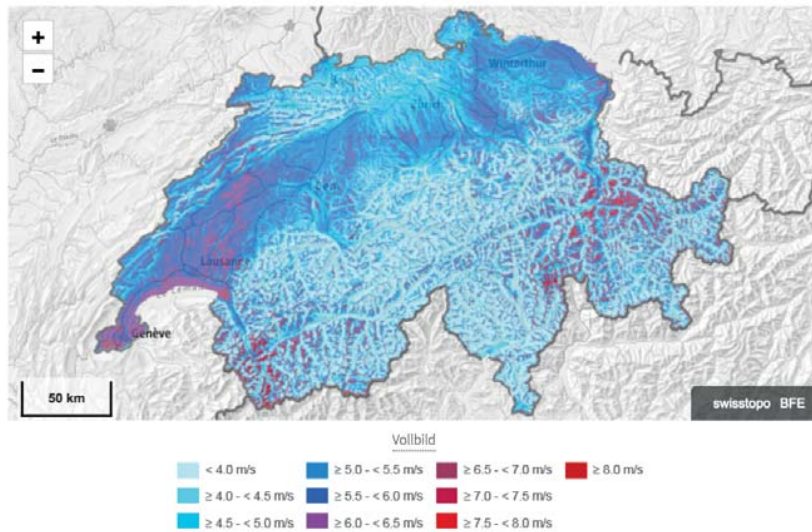


Figure 1.3 – The Swiss wind atlas, available at [www.winddata.ch](http://www.winddata.ch). Shown here are the annual mean speeds at 125 m above the surface. source: Swisstopo, BFE

Notable works from neighboring countries include the works from Draxl and Mayr [2011], who conclude that ridges in the Austrian Alps offer very favorable wind conditions, often with a constant vertical wind profile. All of the sites considered in their work have higher power potential per  $m^2$  than an offshore wind park near the coast of Denmark. A hybrid dynamical/geo-statistical method developed in Truhetz [2010] was used to assess the technical and economical wind power potential in Austria, the upper limit of which was estimated to be around 30 TWh annually [Truhetz et al., 2012]. Including 'political considerations', Winkelmeier et al. [2014] estimate the practical potential for Austria to be around 6649 MW in the year 2030, which could supply around 24% of the country's electricity supply.

## 1.5 Content of the thesis

Given the impending changes to the Swiss power supply, it is remarkable that thus far no in-depth assessment of Swiss wind power potential has been undertaken. Granted, the 2016 studies (Wind Atlas [Koller and Humar, 2016] and Wind Cadastre [Oppliger et al., 2016]) are a noteworthy step in the right direction, but as the authors themselves admit, there is great uncertainty surrounding the resource estimates in the mountains [Koller and Humar, 2016]. With the emerging realization that terrain induced flows can form significant contributions to wind power supply [Draxl and Mayr, 2011], a more focused investigation of the wind power potential from mountainous terrain is imperative for a well informed discussion on the future direction of the Swiss power supply, if the latter is to include significant degrees of renewables. In this thesis the wind power potential in Switzerland is investigated, with a special focus on the complex terrain of the Alps.

**Chapter 2** An analysis of spatial correlation, persistent low wind power conditions and the diurnal and seasonal wind speed patterns over Switzerland is undertaken, based on data from two measurement networks across Switzerland. Spatial correlation is relevant for the smoothness of the overall power output when combining wind resources at different locations. Using extreme value theory, the likelihood of sustained low power production intervals is assessed, and related to spatial parameters (only elevation really). Finally diurnal and seasonal patterns are investigated and explained from terrain characteristics.

**Chapter 3** The Numerical Weather Prediction (NWP) model COSMO-1 is used to assess the potential for wind power in Switzerland. First, the model's performance in complex terrain is validated by comparing the modeled hourly wind speeds to measurement stations. Modeled wind speeds are then used to simulate power production and assess capacity factors. Next, the influence of turbines location on resulting system wide annual imports is assessed for scenarios of a fully renewable Switzerland with varying degrees of wind power generation. To this end, a model of the Swiss electricity system is deployed. Lastly, for annual wind power targets of 4, 6 and 12 TWh/a, the required number of turbines is calculated, and the dependence on elevation is assessed.

**Chapter 4** In order to investigate if the uncertainty of alpine wind power resource assessment can be further reduced, simulations with the Weather Research and Forecasting (WRF) model are undertaken on a powerful supercomputer. For two domains in the Swiss Alps, centered around existing wind turbines, a model set-up is derived that is validated against weather stations and the hub-height wind speed measurements. Comparing the simulation results against both the COSMO-2 and the COSMO-1 model, the relation between model resolution and the ability to represent terrain induced flows is investigated.



## 2 Potential contributions of wind power to a stable and highly renewable Swiss power supply

This chapter is a postprint version of the article previously published in *Applied Energy* 192 (2017) 1-11, doi: 10.1016/j.apenergy.2017.01.085, Bert Kruyt<sup>1,2</sup>, Michael Lehning<sup>1,2</sup>, Annelen Kahl<sup>1,2</sup>

**Candidate's contribution** *The candidate developed the research concept together with M.L. Furthermore, the candidate gathered the data, conducted the analysis and wrote the manuscript.*

### 2.1 Introduction

In 2011, following the Fukushima Daiichi nuclear disaster, the Swiss Federal council and Parliament decided on the phase out of Switzerland's five nuclear energy plants [Schweizerischen Eidgenossenschaft, 2018]. As nuclear energy is responsible for 37,9% of Switzerland's annual (2014) electricity supply [Bundesamt für Energie, 2015], this phase out implies a major overhaul of the Swiss electricity supply. To this end, the Federal council has developed the "Energy Strategy 2050" which - amongst others- encompasses an expansion of electricity production from renewable sources (wind, solar, hydro and geothermal).

Rapid expansion of weather dependent renewable electricity sources can however lead to undesired side effects. In Germany, where solar and wind power have seen a significant increase over the last decade, negative prices and high consumer costs are amongst such effects [Fanone et al., 2013, Ketterer, 2012]. With a high share of wind power (15% of total German electricity consumption in 2015) [Arbeitsgruppe Erneuerbare Energienstatistik, 2016], the ability to dampen fluctuations in production is also reduced. In extreme cases neighbouring countries are called upon to help smoothen out spikes in power production, as happened during a storm in March 2015, when the German TSO requested neighbouring countries

---

<sup>1</sup>Ecole Polytechnique Fédérale de Lausanne (EPFL), School of Architecture, Civil and Environmental Engineering (ENAC), Lausanne, Switzerland

<sup>2</sup>WSL Institute for snow- and avalanche research SLF Davos, Switzerland

## Chapter 2. Potential contributions of wind power to a stable and highly renewable Swiss power supply

---

to absorb German wind electricity in order to stabilise the German transmission grid [Rponline.de, 2015]. While in this case the neighbouring countries were able to assist, in a future, highly renewable Europe where all countries have a large share of weather dependent renewables, such balancing from neighbours cannot be guaranteed, since there is a strong correlation between wind speeds on those geographic scales [Giebel, 2000]. Recently, much research has therefore focussed on the integration of renewables into the grid (see for example [Brouwer et al., 2014, Lund et al., 2015, Ueckerdt et al., 2015]) and the associated costs [Brouwer et al., 2015, 2016]. Switzerland differs from the general European case due to the presence of large amounts of hydropower<sup>3</sup>, which has been shown to increase the market value of wind energy [Hirth, 2016], as hydropower allows for the compensation of short-term mismatches [Dujardin et al., 2017].

With current wind power penetration levels in Switzerland (0,14% of 2014 power production / 0.17% of consumption) [Prognos, 2012, Bundesamt für Energie, 2015] it appears most economical to locate the capacity based on maximum annual yield, ignoring the temporal generation profile, since the installed capacity is relatively small. Imports can be called upon when no wind power is delivered and demand is high. However as both Switzerland and the EU are expected to increase their wind capacity in the coming decade<sup>4</sup>, the temporal generation profiles and their correlation will become increasingly important. The case of Germany exemplifies that placing capacity based on maximum annual yield can become harmful to the system once penetration rates of renewables reach certain levels. Although it makes sense from an individual investor's perspective to locate capacity based on maximum annual yield (especially given current feed in tariffs), for the system as a whole it may be beneficial to consider other spatio-temporal statistics when allocating renewable sources.

The purpose of this work therefore is to explore those wind speed statistics over Switzerland that are relevant in case of high penetration rates of wind power. Specifically three elements are investigated: Firstly, we look into the correlation between wind speeds throughout the country, because this is related to the ability to smoothen overall wind power production. Secondly, using extreme value analysis, we examine the occurrence of long periods where wind speeds are outside the turbine's operating range (i.e. either too high or too low). Such a probabilistic assessment sheds light on the worst case scenarios that are to be expected. Lastly, we investigate the diurnal wind speed patterns across the country, and look into their seasonal variation. Given that demand for electricity is subject to significant diurnal and seasonal fluctuation, in a future Swiss power system with large shares of renewables, the temporal production patterns of non-dispatchable renewable sources are crucial to minimise mismatch between (residual) demand and supply. For all three aspects mentioned above, we try to assess the influence of the highly complex topography on the results. In so far as these themes

---

<sup>3</sup> 56,4% of annual (2014) electricity supply, 31.7% of which consists of storage hydropower [Bundesamt für Energie, 2015]

<sup>4</sup>The European Wind Energy Agency estimates installed wind capacity in the EU to reach between 251 and 391GW in 2030 (between 19 and 33% of the EU's 2030 demand) [Corbetta, 2015]. In Switzerland, wind power is projected to produce between 500 and 1700 GWh in 2035, when demand for electricity will be in the range of 55 to 60 TWh (0,8 to 3%) [Prognos, 2012]

have been researched, most studies have considered non-complex terrain. Given the profound influence of topography on meteorological parameters [Villanueva et al., 2011], there is little reason to assume the results of these studies could apply to complex terrain as well.

The correlation  $\rho$  between wind speeds as a function of distance  $d$  is typically related to a decay parameter  $D$ , which determines how fast the correlation decays with distance [Giebel, 2000]. Giebel [2000] finds a decay parameter of  $D=723$  km for correlation between wind stations across Europe. Holttinen [2005] finds a value of  $D=500$  km for Scandinavian countries, and Katzenstein et al. [2010] estimate  $D=350$  km for Texan wind power time series. Villanueva et al. [2011] describe a linear relation between correlation and distance, and compare correlations in both complex and non-complex terrain. They conclude that a linear relation between correlation and distance is a decent approximation in both cases. Reducing output variation therefore typically requires combining wind farms over distances in these orders of magnitude, where the relative variability of wind power decreases as the area considered as an interconnected system increases [Galanis, 2014]. However, the terrain in these studies is relatively flat. Given the aforementioned influence of topography on meteorological parameters, it is unlikely that the values found in these studies apply to more complex topography (such as that of Switzerland [Weber and Furger, 2001]). So far, no comparison between correlation of wind speeds in complex terrain with these existing studies has been made. With this study we aim to fill that gap.

Next, we examine the occurrence of long periods where wind speeds are outside of the turbine's operating range and consequently, no power can be produced. While short term fluctuations (in the order of minutes to hours) may be balanced by hydropower production [Dujardin et al., 2017], sustained periods with low wind speeds have a strong impact on power systems that are highly dependent on wind power production. Often, wind speed persistence is investigated using the autocorrelation function, conditional probability or speed duration curves [Cancino-Solórzano et al., 2010] [Koçak, 2002] [Koçak, 2008], but also runs analysis and intensity-duration analysis [Leahy and McKeogh, 2013]. Recently, Telesca et al. [2016] investigated the temporal structure of high frequency wind series in Switzerland, and found cyclic components of 24, 12, and sometimes 8 or 6 hours, that they relate to temperature and pressure variations. We will use extreme value analysis (EVA) to make inferences about long periods of low wind power conditions, because EVA allows for estimates beyond the length of the observed dataserie. Extreme value analysis is often used to describe extremes of processes in nature such as snowfall [Blanchet et al., 2009][Blanchet and Lehning, 2010][Blanchet and Davison, 2011], rainfall [Thibaud et al., 2013], and wind speeds [Simiu and Heckert, 1996], but also financial processes and value at risk [Smith, 2004]. Its basic premise is to separately model the tail of a distribution. Although the magnitude of extreme wind speeds in Switzerland and elsewhere has been investigated before [Ceppi and Appenzeller, 2008, Etienne et al., 2010, Laib and Kanevski, 2016, Palutikof et al., 1999], to our knowledge no effort has been undertaken to map the extremes of low-wind persistence in Switzerland, or relate these to power production.

Lastly, we examine the seasonal and diurnal evolution of wind speeds across Switzerland as

## **Chapter 2. Potential contributions of wind power to a stable and highly renewable Swiss power supply**

---

well as elevational trends. Given the varied and complex terrain found across the country, it is possible that the (evolution of) wind speeds will be affected by this. For example, Chow [2013] describes diurnal mountain wind systems or thermally driven winds: Due to the heating and cooling of the lower atmosphere, winds form that are driven by buoyancy. Mainly during stable summer weather, daytime heating in valleys will produce an up-valley flow. Nighttime cooling in its turn, will produce downwind flows, as cooler, heavier air flows down-slope. In section 2.3.4, we will investigate the evolution of the diurnal wind speed patterns over Switzerland, and infer implications for wind power production.

Apart from a diurnal evolution, there is also a seasonal pattern to the Swiss electricity demand that is mainly associated with an increase in lighting and heating in winter [Bartlett et al., 2015]. Combined with reduced hydropower production in winter due to the characteristics of the hydrological cycle, this leads to a power deficit in winter [Swissgrid, 2014]. We will therefore also investigate the seasonal evolution of diurnal cycles, and see to what extent wind power is able to meet this demand. This is especially relevant given the fact that solar power declines significantly in winter due to the earth's inclination, and as such is unable to complement hydropower in its seasonal cycle. Mean wind speeds in Europe, on the contrary, are reported to increase in winter [Heide et al., 2010]. We will investigate if this also holds for the complex terrain in the Alps.

The paper is structured as follows: In the next section we describe the two main datasets that were used as well as the data processing that was done and the methods to calculate correlation, return levels and diurnal patterns. Next, in section 2.3 we discuss the results. We analyse some of the sensitive parameters with regards to the calculation of return levels in section 2.4. In section 2.5 we present our conclusions.

## **2.2 Data and Methods**

### **2.2.1 Measurement stations**

The Swiss weather service MeteoSwiss deploys a network of roughly 160 automated measuring stations across Switzerland, called SwissMetNet (from here on SMN) [MeteoSchweiz, 2016]. We've manually selected the stations with long measurement series (minimum of 35 years) of hourly wind speeds, which gives us a dataset of 42 stations. These stations are located throughout Switzerland, at altitudes ranging from 273 (Lugano) to 3302 m.a.s.l. (Piz Corvatsch). A second dataset is formed by the IMIS station network [Lehning et al., 1999, SLF, 2016]. This network, consisting of 198 stations around the Alps and Jura mountains, is operated by the Swiss Institute for Snow and Avalanche Research SLF. These stations are located in pairs with a wind station at an exposed location and a snow station at a less exposed location, which is generally also at slightly lower elevation. All stations measure temperature, humidity and wind speed. Data are averaged over 30 minutes. For our purposes, we use the wind stations, and



only use the snow stations to interpolate missing data in the wind stations (see next section). These wind stations are located at elevations from 1936 (Amden - Mattstock) to 3345 (Zermatt - Platthorn) m.a.s.l. In total this gives us 62 of these stations, of which we use the 57 that have data sets longer than 5 years. Figure 2.1 shows both the IMIS and SMN stations in Switzerland.

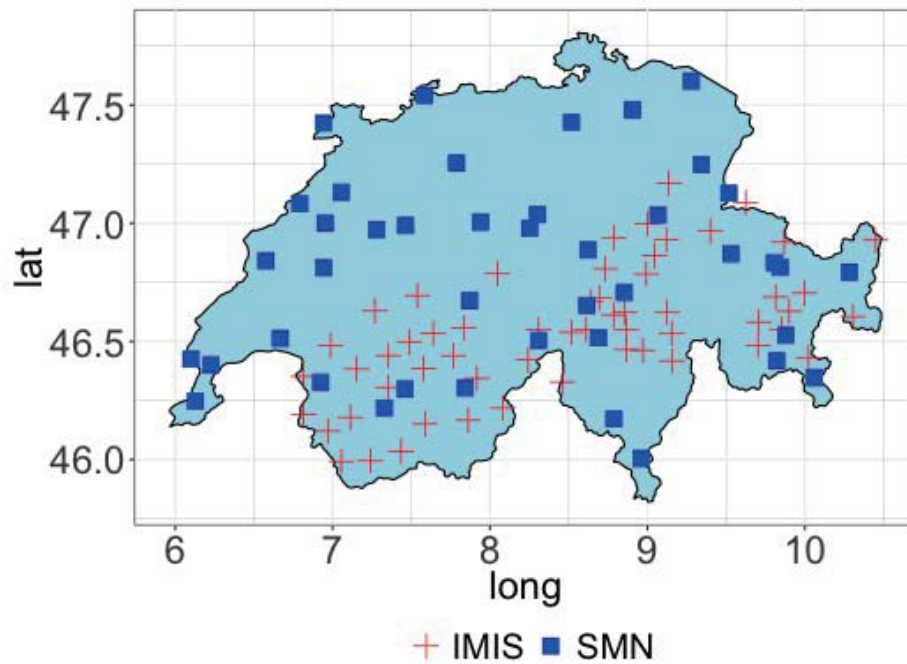


Figure 2.1 – Map with meteorological stations from the SMN and IMIS networks.

### 2.2.2 Missing Data

Most wind speed time series contain missing data, for example due to icing of the anemometers [Grünwald et al., 2012]. Since the continuity of the time series is important to infer results about persistence, we want to work with continuous data as much as possible. For the IMIS stations, the presence of a second station (snow station) close to the wind station provides a useful set to base our estimates of missing data on. Here, missing values are imputed with the Amelia package in R [Honaker et al., 2011][Honaker et al., 2015]. This package estimates missing values based on an Expectation-Maximization with Bootstrapping (EMB) algorithm. To this end, for each IMIS wind station, the overlapping periods with the IMIS snow station, as well as the neighbouring SMN station (based on smallest distance) are synchronised and fed into the Amelia algorithm to impute the missing values. As there are periods where both the corresponding snow station and the nearest SMN station are also without data, not all missing values have been resolved. Initially the average missing data per series was 8.9 % (with a median and max of 7.6% and 23.4% resp.). After imputation, these percentages are 0.4, 0.3 and

## Chapter 2. Potential contributions of wind power to a stable and highly renewable Swiss power supply

---

2.3% respectively. We then average the IMIS values over the hour, so that both datasets have hourly resolution and can be easily combined. For the calculation of correlation coefficients and the calculation of diurnal wind patterns, we use this dataset and ignore the entries with missing values. For the calculation of return levels, the remaining missing values are replaced with the mean, because leaving them as zero or missing would distort the calculation as they would be regarded as being below the cut-in speed, and this could falsely introduce long periods of no wind power.

### 2.2.3 Correlation

Cross-correlation between measurement stations describes the degree to which two time series change in the same direction and magnitude. It is usually quantified using Pearson's correlation coefficient. Several authors have fitted an exponentially decaying function to describe correlation between wind speeds as a function of distance [Giebel, 2000], [Holttinen, 2005], [Katzenstein et al., 2010]. These functions have mainly been of the form

$$\rho = e^{-d/D}, \quad (2.1)$$

where  $\rho$  is the correlation coefficient,  $d$  is the distance and  $D$  the decay parameter that describes how fast the correlation decreases with distance. The latter is usually determined by fitting equation 2.1 to the data.

### 2.2.4 Turbine choice

The power a wind turbine produces at a certain speed is described by a turbine's power curve, which is specific for each turbine. In this work, we use the Enercon E82 turbine with a capacity of 2MW, the cut-in speed at which the turbine starts to produce electricity, and the cut-out speed, at which the turbine is shut down to prevent damage. This turbine is widely used in Switzerland (a full list of current installations can be found on-line at [MeteoTest]). It has a relatively low cut in speed of 2.5 m/s, which is thought to be favourable in low(er) wind conditions such as Switzerland. Using the same turbine for all locations arguably leads to sub-optimal results, since a higher power yield could be achieved by optimising the turbine selection for the wind characteristics of each location. As the selection of a turbine for a specific site is not straightforward however, this is beyond the scope of the present work. Since the goal is to compare locations rather than find the optimal yields, using one turbine seems plausible.

### 2.2.5 Height transformation

The wind data is recorded at 10m, whereas most turbines are in the height range of 75-100 meters. Therefore a transformation has to be made to make these speeds comparable. The vertical wind profile is often represented as following a logarithmic or power law [DeMarrais, Gerard, 1958] [Emeis, 2005], the latter being given by

$$v_{hh} = v_{10} \left( \frac{hh}{10} \right)^\alpha \quad (2.2)$$

with  $v_{hh}$  the speed at hub height  $hh$ ,  $v_{10}$  the speed measured at a height of 10 meter and  $\alpha$  the wind shear coefficient. For neutral stability, a rule of thumb is to use a value of 0.143 or 1/7 for  $\alpha$ , although it is acknowledged that this may underestimate energy yield [Kubik et al., 2013] (and references therein), as  $\alpha$  is neither constant over height nor over time. Indeed, a range of (average) values for  $\alpha$  have been reported, from 0.1 in a mountain pass in Switzerland [Clifton et al., 2014] to 0.36 for a Mediterranean island [Farrugia, 2003]. When intra-annual values of  $\alpha$  are considered, it becomes clear that great variation during the year takes place. Kubik et al. [2013] finds values ranging from -0.5 to 0.5, with a mean of 0.119, as well as a clear diurnal pattern, where night time shear values are almost twice the daily values. Clifton et al. [2014] find negative values for south-easterly winds at a pass location, and Farrugia [2003] reports higher shear exponents during night-time and during winter. Furthermore, Bunse and Mellinghoff show that the distribution for  $\alpha$  is broader in flat terrain than it is in complex terrain, and concludes no general trend towards lower values of  $\alpha$  in complex terrain. Lastly, it has been noted by several authors that in complex terrain, the vertical wind profile does not always follow a logarithmic- or power law [Cattin et al., 2003] [Draxl and Mayr, 2009] and that this may lead to errors in power estimates of up to 50% [Firtin et al., 2011]. In absence of a clear parametrisation of  $\alpha$ , we stick to the common-yet-disputable value of 0.14. Rather than transforming the entire wind speed time series from 10 m to hub height, we transform the turbine's power curve (and thus the cut-in and cut-out speed) down to 10m, for an assumed hub height of 80m. This is done solely for computational purposes, as transforming these two is less time consuming than transforming all multi-year time series. This then gives us a direct translation from measured wind speeds at 10m to power output of a hypothetical wind turbine with a hub height of 80m.

### 2.2.6 Extreme Value Analysis

Extreme value analysis deals with the statistical behaviour of the extremes of a distribution of random variables [Haan and Ferreira, 2007]. For a sequence of independent and identically distributed random variables  $X_1, X_2, \dots, X_n$  the maximum is given by  $Z_n = \max(X_1, \dots, X_n)$ . Given that  $n$  is large enough, the probability that  $Z_n$  does not exceed a level  $z$  is given by the Generalised Extreme Value (GEV) distribution, whose cumulative distribution function is

## Chapter 2. Potential contributions of wind power to a stable and highly renewable Swiss power supply

---

given by

$$G(z; \mu, \sigma, \xi) = \begin{cases} \exp \left[ -\left(1 + \xi \frac{z-\mu}{\sigma}\right)^{-\frac{1}{\xi}} \right] & \text{for } 1 + \xi \frac{z-\mu}{\sigma} > 0 \\ 0 & \text{otherwise} \end{cases} \quad (2.3)$$

where  $\mu$ ,  $\sigma$  and  $\xi$  are the location, scale and shape parameter, respectively. The sign of the shape parameter  $\xi$  tells us whether the distribution is bounded ( $\xi < 0$ ), in which case the value of  $X$  is limited and theoretically no value above an upper bound can be observed. When the distribution is light tailed (i.e.  $\xi = 0$ ), extreme values are possible albeit not very likely. Lastly, in the case of a heavy tailed distribution ( $\xi > 0$ ), extreme values are more likely to occur. These three cases of the GEV distribution are also known as the Weibull-, the Gumbel and the Fréchet distribution respectively. For a visual representation of the GEV parameters, see [Blanchet and Lehning, 2010]. Two main methods exist for dealing with maxima. Traditionally, the data is separated into blocks (e.g. months) and the GEV distribution is fitted to the monthly maxima. Hence this method is referred to as the block maxima method. The obvious downside here is that a lot of extremal data is discarded. The so-called peaks-over-threshold (POT) method on the other hand, takes into account all values above a certain threshold  $u$ . Given that the threshold is sufficiently high, the distribution of threshold exceedances can either be described by a generalised Pareto distribution (GPD), or by a Poisson Point (PP) Process. The latter has the advantage that by rescaling the intensity function of the Poisson process, the parameters can be made identical to those of the GEV. (For details see [Coles, 2001] or [Coles and Davison, 2008]). This allows for the computation of the return level  $z_p$ , a value that is exceeded on average once every return period  $1/p$ . As such, a return level represents the  $(1 - p)$ th quantile of the GEV distribution. By inverting equation 2.3 we can obtain its value:

$$z_p = \begin{cases} \mu - \frac{\sigma}{\xi} \left[ 1 - \{-\log(1-p)\}^{-\xi} \right] & \text{for } \xi \neq 0 \\ \mu - \sigma \log - \log(1-p) & \text{for } \xi = 0 \end{cases} \quad (2.4)$$

Of relevance to power production are the periods when no power is produced because the wind speed is either below the cut-in speed, or because the wind speed is above cut out speed. To assess these, we record the length of the intervals where the wind speed is outside of the turbine's operating range (i.e. below cut-in or above cut-out). With the distribution of these interval lengths, a Poisson point process is fitted to the exceedances over a threshold, for which the 90th percentile is used. Since we are modelling the interval length rather than wind speed, these data are independent. An important issue is the role of declustering in these series. Is the end of a no-power interval defined by one hour of power production, or do we need several consecutive hours of power production before a no-power interval is over? The consequences for the power system of a single hour of power production in between large

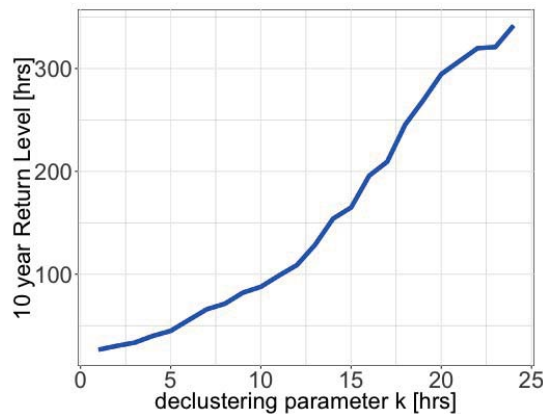


Figure 2.2 – The Return level (in hours) as a function of the declustering parameter  $k$ . Shown here for the location Chasseral, in the Bernese Jura region of Switzerland.

intervals of no power can be argued to be insignificant. Therefore the declustering is run with a declustering parameter [Süveges and Davison, 2010] of 3 hours. This means that wind speeds will have to be above the cut-in threshold (or below cut-out) for a minimum of 3 hours in order to separate no-power production intervals. Increasing this parameter leads to larger clusters of no-power events and as such will have a profound impact on the results. (see figure 2.2. The parameter choice is thus an important one, although there is no obvious choice. (For now we keep the declustering parameter  $k \ll$  threshold  $u$ ). No power production due to forced downtime is not considered here. The return periods for no production because of low or high winds are difficult to compare to production losses because of turbine service or material damages. However, most turbines require on the order of days of service time with a yearly return period [Hahn et al., 2007] but - more importantly - not all turbines of a farm will be off production at the same time. Therefore, we neglect the service and repair production losses in our analysis. Although it is acknowledged that in highly turbulent environments, fatigue loads may be higher [Brand et al., 2011], which could lead to shorter turbine life or increased downtime, the magnitude of such effects is highly site-specific.

### 2.2.7 Diurnal wind speed patterns

To investigate the diurnal wind patterns at different stations, data were processed as follows. Hourly time series for both station networks were averaged by hour of the day to produce annual averaged diurnal profiles. Secondly, the averaging was done per month and per hour of the day, so that intra-annual difference could be explored.

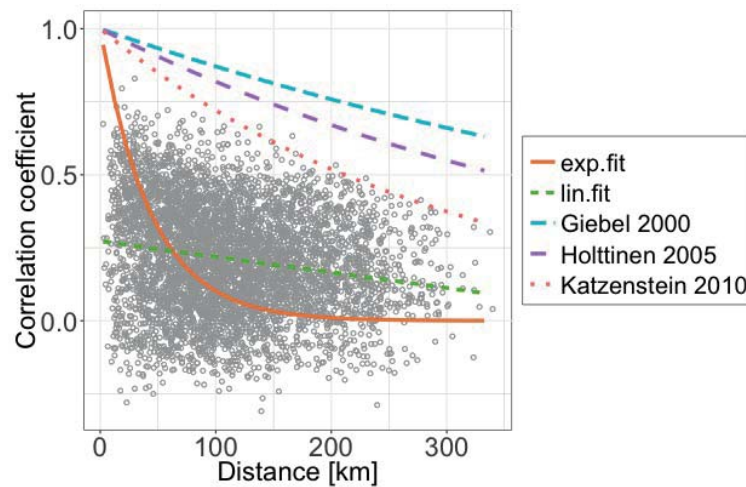


Figure 2.3 – Cross-correlation between wind speeds in Switzerland. Also shown are the fitted functions, as well as the other values found in literature describing this relation [Giebel, 2000, Holttinen, 2005, Katzenstein et al., 2010].

## 2.3 Results and Discussion

### 2.3.1 Correlation

Figure 2.3 shows the cross-correlation coefficients as a function of the distance for 99 wind measurement stations from both the IMIS and SMN network in Switzerland. Also shown are some of the functions found in literature describing the relation between wind speed (or power) correlation and distance as discussed in the introduction. Upon a first glance at the data in figure 2.3, fitting an exponential curve does not appear very obvious. And indeed, when we do, although we find a decay parameter  $D$  of 44km, the  $R^2$  value of -0.65 tells us this is a worse fit than a horizontal line. A linear fit is hardly better with an  $R^2$  of 0.04 . From a visual assessment we can conclude that the correlations between wind speeds as a function of distance are significantly lower in Switzerland when compared to the values found in literature. What is furthermore noteworthy, is the fact that a significant number of negative correlations are found, indicating anti-correlation. This finding is interesting in view of combining wind farms to reduce overall output variability. It should be noted that because of the non-linear relation between wind speed and power output, correlation between power production is not (exactly) the same as correlations amongst wind speeds. Generally, correlations between power are lower (in the case of Giebel [2000]  $D=723$  for speed and 641 for power). However, even with this remark, the above conclusion that correlations in Switzerland are lower still holds.

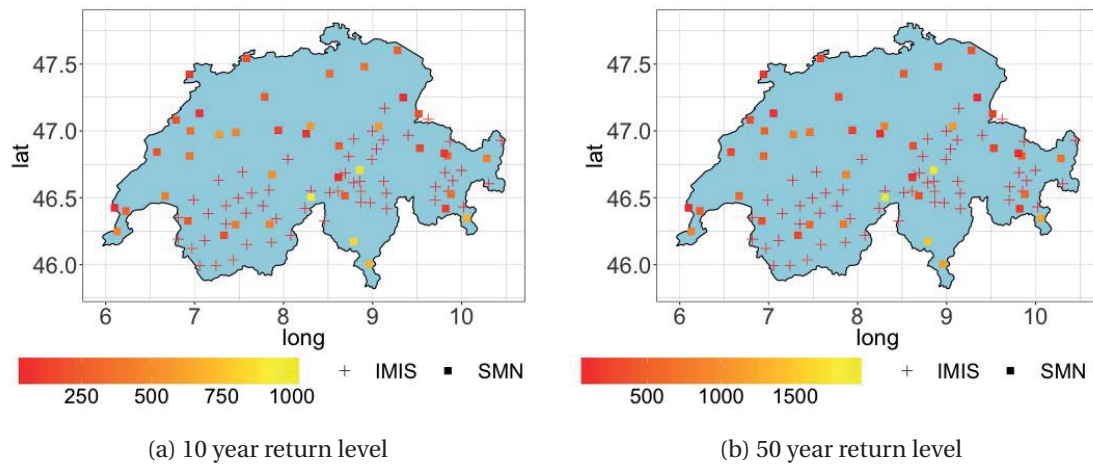


Figure 2.4 – Return levels (in hours) for no power intervals. These represent the no-power production intervals that are to be expected once every 10 (50) years.

### 2.3.2 Return levels

Figure 2.4 shows the return levels for return periods of 10 and 50 years, in hours of no power production. This can be interpreted as the level being exceeded once every 10 (50) years. It ranges from 29 to 1017 hours (roughly 6 weeks) for a return period of 10 years. For the return period of 50 years, the range spans from 34 hours to 1964 hours (figure 2.4). The highest 10 year return level is found in Disentis/Sedrun (1197 m.a.s.l.), in the central part of Switzerland, whereas the lowest return level was found at Sidelhorn, a summit close to the Grimsel pass on the border of the cantons of Bern and Valais. At a first glance, no clear spatial pattern seems apparent. An investigation into the relation between altitude and the parameters of the fitted Poisson Point process is shown in figure 2.6. It can be seen that there is a correlation between a station's elevation and the parameters of the fit, which leads to a correlation between the 10 year return level and elevation. We can also see that the majority of stations have an unbound distribution, indicated by the positive value of  $\xi$ . For a couple of stations the parameter  $\xi$  is negative, indicating a bound distribution. If we closer examine the 14 stations with a significant negative  $\xi$  parameter ( $\xi < 0.01$ ), we find that these are mainly stations above 2200 m.a.s.l, except for two stations in the (far) western part of Switzerland at lower elevations (the only two SMN stations in the lower right panel of figure 2.6). These two stations are both located at a hill with a long upwind fetch amidst relatively flat terrain, which may contribute to their above average wind speeds.

### 2.3.3 Seasonal decomposition

Switzerland's electricity consumption is higher in winter due to increased heating and lighting demand [Bartlett et al., 2015]. Combined with the characteristics of the hydrological cycle, this leads to a power deficit in winter [Swissgrid, 2014]. It is therefore insightful to look at the

## Chapter 2. Potential contributions of wind power to a stable and highly renewable Swiss power supply

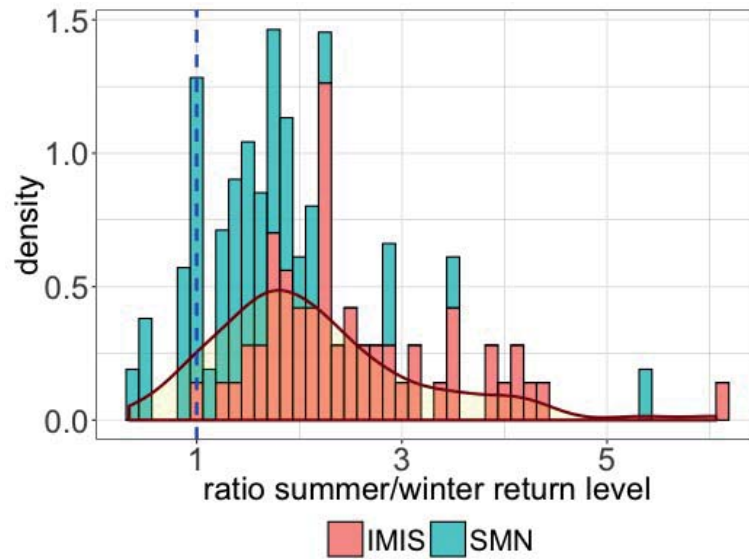


Figure 2.5 – Ratio of return levels in summer vs winter. A value above 1 indicates higher return levels in summer. The series were split into summer and winter, where summer was defined as consisting of the months May to October, and winter as November through April.

return levels for sustained no-power events in the summer and winter periods separately. To this end, the dataset is split into summer and winter. This creates yearly interruptions in the dataset, whereby the average interval length is shortened. As such, these results cannot be directly compared to the overall return levels, but only side by side. This is done in figure 2.5, where we see distinctly lower return levels during winter, when compared to the summer periods. This implies that no-power periods are -on average- shorter during the winter months.

### 2.3.4 Diurnal patterns

Figure 2.7 shows diurnal wind speed profiles for the stations in the SMN network (left) and IMIS network (right). There appear to be two distinct types of profiles, characterised either by an increase in wind speed during the afternoon, or a decrease. The majority of the stations belong to the latter, which can be explained by the diurnal evolution of the boundary layer. The other distinct pattern we see is wind speeds increasing during the afternoon. This occurs mainly at stations in the SMN network (compare fig a and b). In the IMIS network, only two stations display this behaviour. Both are situated at mountain ridges near the upper end of long valleys (Sidelhorn in the Rhone valley and Cho d'Valetta (Bever) at the Inn valley respectively). Long valleys are known to produce so called valley winds, when thermally induced pressure differences cause up-valley flows [Chow, 2013]. Specifically in the Inn valley, pressure differences of up to 5hPa have been reported [Vergeiner and Dreiseitl, 1987]. The SMN dataset includes more valley stations, and here the afternoon peak in speeds is more common (see fig



## 2.3. Results and Discussion

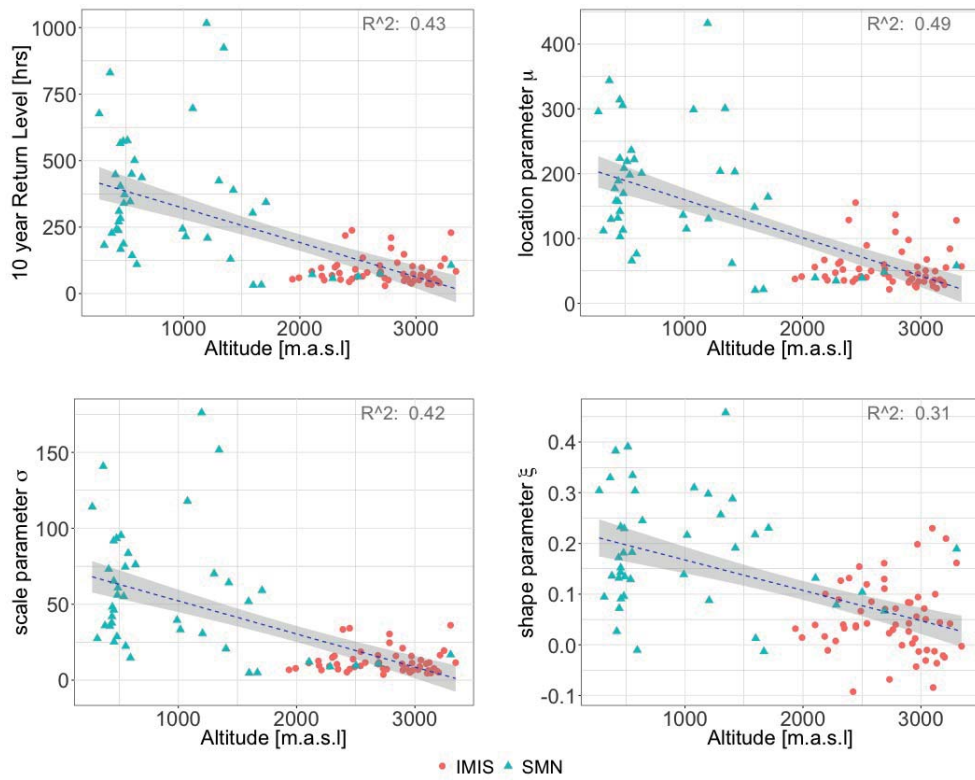


Figure 2.6 – The 10 year return level (upper left), and the parameters of the GEV distribution, plotted as a function of altitude.

## Chapter 2. Potential contributions of wind power to a stable and highly renewable Swiss power supply

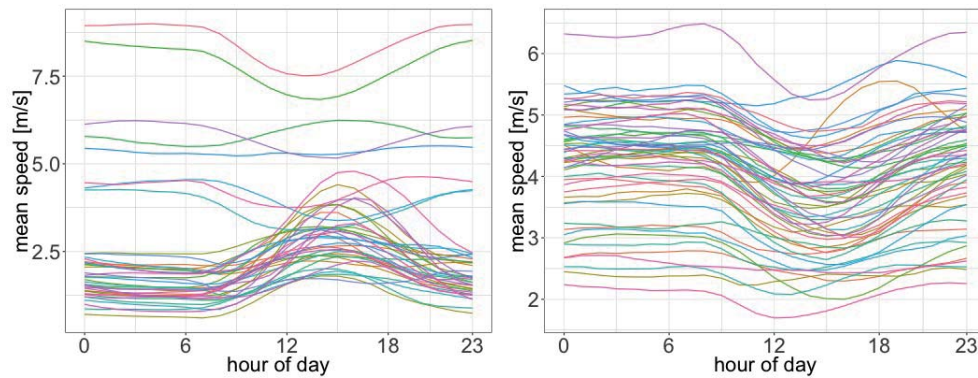


Figure 2.7 – Diurnal wind speed profiles for the a) SMN stations. b) the IMIS stations. The SMN dataset contains stations at lower elevations, and as such has more stations that display a typical valley wind pattern with wind speeds increasing in the afternoon. In The IMIS dataset with higher elevation stations this behaviour is less common. Times are in UTC (+1 hr for Swiss wintertime, +2 for summertime.)

2.7).

### Seasonal decomposition of diurnal patterns.

The majority of Switzerland's power comes from hydropower, which has a distinct annual cycle, with production peaking in mid-summer, although demand peaks in winter [Bartlett et al., 2015]. In a future renewable Swiss power system, high emphasis will be placed on compatibility with this annual hydropower cycle. Although photovoltaic power generation is assumed to play a big role in Switzerland's future electricity supply [Prognos, 2012], it also suffers from an annual cycle that is not complementary to that of hydro [Bartlett et al., 2015]. Wind power could provide a balancing component to the power supply. We therefore look at the monthly variations in diurnal patterns, by calculating the average diurnal cycle per month. Figure 2.8 displays such monthly decompositions for 6 selected stations. What is clear in all cases, is that there is significant variation from the annual average diurnal cycle, displayed by a dashed black line. Examining the stations at Gütsch, Bever, Chur and Visp, we see that the increase during the afternoon that is associated with a thermally induced valley wind, mainly occurs in the summer months when irradiance is high. During winter the peak is significantly less pronounced at these locations. Similarly for the stations without thermally driven winds (Chasseral, and Simplon) we also see a decrease in intra-daily variation during winter, as profiles become flatter.

### 2.3. Results and Discussion

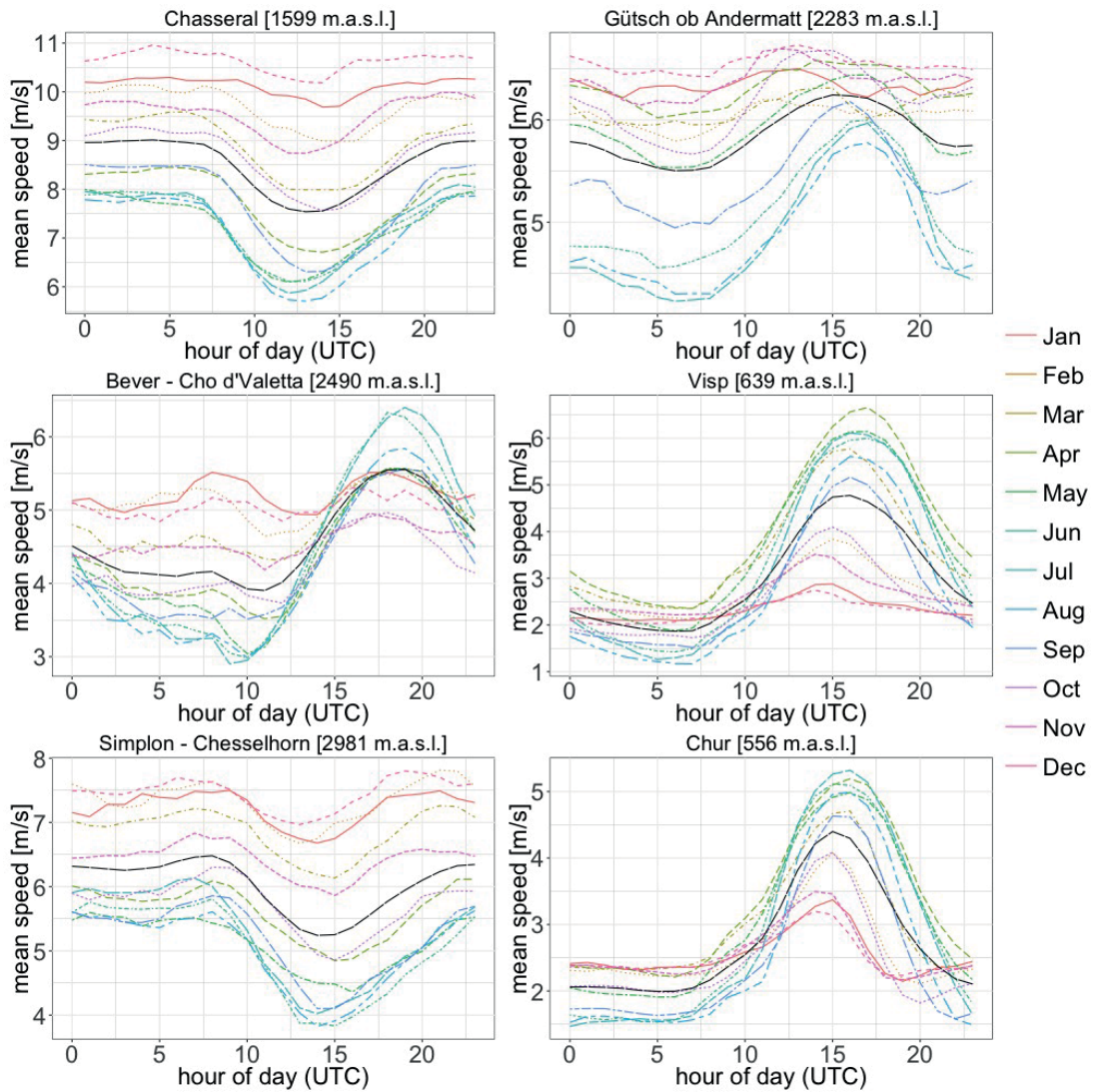


Figure 2.8 – Monthly diurnal patterns for the locations Chasseral, Gütsch, Bever Visp, Simplon and Chur. The black dashed line indicates the annual average, the coloured lines represent the months. Times are in UTC (+1 hr for Swiss wintertime, +2 for summertime.)

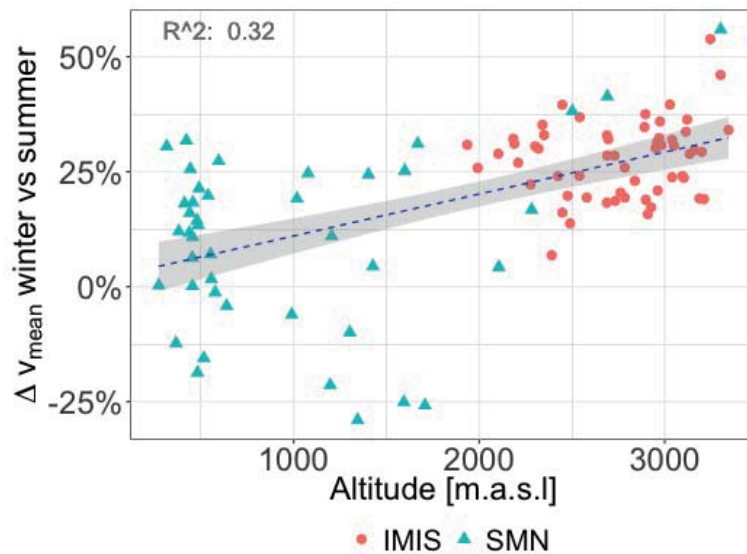


Figure 2.9 – Relative increase in mean speeds in winter compared to summer, as a function of elevation. Higher altitude locations seem -on average- to have relatively higher wind speeds in winter.

### 2.3.5 Elevation

Mean wind speeds in Europe are reported to be higher in winter [Heide et al., 2010], which based on our data we can confirm for Switzerland: On average, mean wind speeds in the winter months (November through April) are 20,2% higher than the mean speeds in summer. However, 11 out of the 99 locations do not have a higher mean speed in winter. These 'summer-high' stations all display a clear signature of thermally induced winds, which explains the high summer means. Plotting the relative difference in seasonal mean speed as a function of elevation, we see an interesting pattern depicted in figure 2.9. The relative increase in winter compared to summer increases with elevation.

Higher winter wind speeds could imply favourable conditions for wind farms at higher elevations, although at the same time air density decreases with elevation, leading to lower power output. To investigate this we have simulated the power production for each location, including a correction for reduced yield due to air density. The methodology is described in A. When we plot the power production (corrected for air density) as a function of elevation, we see that there is a clear increase in power production at higher elevations (figure 2.10). The negative effect that lower air density has on power production seems to be more than offset by higher wind speeds. Also included in this plot is a sensitivity analysis of the effect of the wind shear parameter  $\alpha$  on the results. The calculation was performed several times with values of  $\alpha$  between -0.07 and 0.42. The resulting spread in the results is indicated with vertical bars. The fit and R values are for an  $\alpha$  of 0.14.

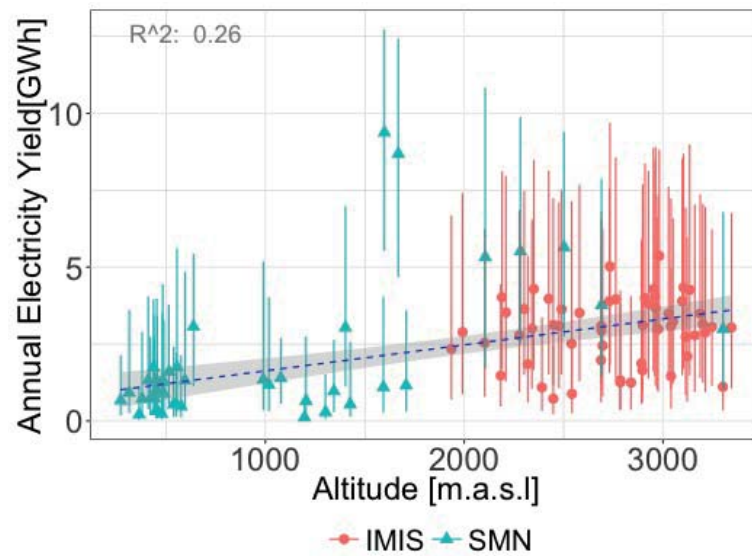


Figure 2.10 – Simulated electricity production as a function of elevation. Higher altitude locations seem -on average- to have relatively higher yield, despite lower air density.

## 2.4 Sensitivity and Outlook

In this section we investigate some of the assumptions and uncertainties that may influence the results. A large factor of uncertainty is introduced by the vertical translation of wind speeds. Although it is acknowledged that the value of the wind shear coefficient  $\alpha$  varies significantly (see section 2.2.5 and references therein), no suitable parametrisation has been found. Since the vertical translation is done for the cut-in and cut-out speeds of the turbine, the choice of  $\alpha$  will have a direct effect on the value of the (translated) cut-in speed and thus on the length of the intervals outside of the turbine's operating range (and hence the calculated return levels). Similarly, the cut-in and cut-out speeds themselves influence the interval length and return levels. The choice of turbine will therefore also have an effect on the results. Both effects can be captured by varying the cut-in speed and recording the effect on the 10 year return level of sustained no-power periods. The spread of the results is depicted in figure 2.11, where the most sensitive location (max) and the least sensitive location (min) are shown alongside the average effect. A similar graph (not shown) for the sensitivity to cut-out speeds showed very low sensitivity to cut-out speed variation.

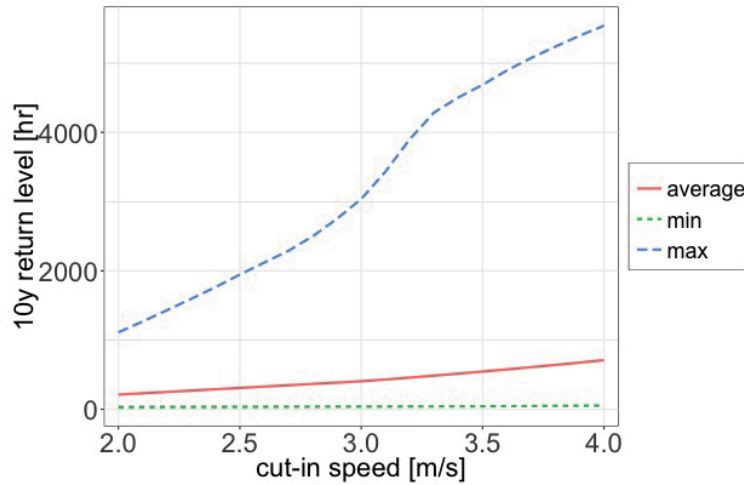


Figure 2.11 – Sensitivity of calculated return levels to cut in speeds

## 2.5 Conclusion

Using hourly wind speed data from two measurement networks across Switzerland, we have shown that cross-correlations as a function of distance between stations are significantly lower in Switzerland than values reported in literature for Europe and the US. The discrepancy with previously reported values can easily be understood from the complex terrain that makes up much of Switzerland's surface. This influences wind speed characteristics significantly, as can also be seen in other results. The implications for wind power production may however be positive: Smoothing the output from combinations of wind farms can in Switzerland be achieved over much shorter distances than those commonly reported in literature. This holds for any country with complex terrain influencing the wind climate. Furthermore, capacity credit -the ability to displace conventional generating capacity- increases with increased smoothing of the combined wind power output [Ensslin et al., 2008]. Because of this, the capacity credit of wind power will be higher with lower correlation.

We have analysed the length of periods where the wind speed is outside the operating range of the Enercon E82 turbine for 99 wind stations across Switzerland. An extreme value distribution was fitted to each of these length records, to allow for the calculation of return levels for return periods of 10 and 50 years. These return levels show great spatial variability, yet return levels clearly decrease as the elevation of the stations increases (figure 2.6), which implies that wind farms that are located at higher elevation are less likely to suffer long periods without power production. A decomposition of the return levels for summer and winter periods showed significantly lower return levels in winter, indicating that the likelihood of persistent periods where no wind power can be produced are lower for almost all locations in winter. This is beneficial for Switzerland, since it has an electricity deficit in winter, and a future renewables-based power system is likely to be under the greatest stress during the winter months, as is the current system.

We have confirmed that wind speeds are on average indeed higher in winter, although we have also been able to show that there are notable exceptions, with implications for wind power generation. While many of the measurement locations at mountain ridges are exposed to rather free tropospheric wind conditions during night and much of the day, the developing thermal up-slope and up-valley winds are able to create a local boundary layer. This boundary layer prevents the penetration of high wind speeds to ground level. Hence the majority of the measurement stations display a decrease in wind speed during the afternoon. Contrarily, long valleys experience rather low wind speeds during night time and most of the day. With strong solar irradiation however, thermally induced pressure differences can cause up-valley winds. As the temperature increases during the day, wind speeds increase with a peak between 3 p.m. and 8 p.m. These peaks are more pronounced during the summer months when solar irradiation is higher, whereas in winter they can be virtually non-existent. For the 88 of the 99 stations in our dataset, the mean wind speed is higher in winter. The few stations that have higher mean wind speed in summer are all found at the bottom of valleys, where the strong radiative heating in summer creates the afore-described increase in wind speed.

The usefulness of these valley stations for wind electricity production is limited since their pronounced peak mainly occurs during summer, when the demand for electricity is lower and hydropower is abundantly available. Moreover, as electricity production from PV is projected to increase both in Switzerland and in the neighbouring countries, in a future, highly renewable Europe there will likely be a surplus of power at daytime during summer.

For all but these few valley stations, not only is the mean wind speed higher in winter, but the relative difference between winter and summer is also more pronounced with increasing elevation (figure 2.9). Moreover, power production also appears to increase with elevation (figure 2.10), despite the negative effects of lower air density on electricity yield.

### 2.5.1 Implications and Outlook

Given Switzerland's power deficit in winter and its intended nuclear phase-out, electricity sources that are either dispatchable or have a seasonal pattern to complement this deficit are called for. However apart from biomass, all currently feasible dispatchable technologies are fossil based and as such are questionable in view of climate change. Amongst the currently mature renewable technologies, wind power has a highly favourable seasonal profile. We've been able to show that this seasonal pattern appears more pronounced at altitude, and that wind power in long valleys subject to thermally induced wind speed-up has an unfavourable seasonal profile. Annual average wind speeds can mask such important dynamics, which can become important as renewables penetrate the electricity market. Feed-in tariffs, which currently allow profitable power production from such valley wind farms will eventually be abolished as wind power reaches grid parity, at which point market prices reflecting demand will determine the profitability. Given our results it is highly debatable whether wind farms that mainly produce during periods of low (residual) demand should be subsidised in this way,

## **Chapter 2. Potential contributions of wind power to a stable and highly renewable Swiss power supply**

---

especially as we have shown that high elevation locations are able to provide power at times of high demand. In shaping Switzerland's energy transition, accounting for these dynamics may prevent costly mishaps. The results here underline the need for further research into seasonal-dependent feed-in tariffs for wind power.

There are still a lot of open questions however. For one, the wind climate in alpine terrain is extremely hard to map. Where in flat terrain correlations are relatively strong over long distances, facilitating extrapolation of measurements and models, in the complex terrain of the Alps this is challenging. Attaining an accurate overview of the wind climate in the Alps would require either a drastic (and possibly unrealistic) increase in measurement stations, or huge advances in computational power, as the resolution required to accurately model the flow in this terrain should be high enough to capture all relevant terrain features. Perhaps a hybrid approach, where high resolution modelling of specific locations can provide an estimate of the Alpine potential by extrapolation to similar features, is the first step to take.

Another aspect that has not been taken into consideration here is the performance of wind turbines in Alpine environments. Extreme temperatures can influence the material properties of various components [Battisti, 2015], while surface roughness has been linked to an increase in fatigue loads [Lee et al., 2012], and icing of the rotor blades can cause energy losses of ca 2% [Barber et al., 2011]. Although an algorithm to estimate icing frequencies in Switzerland has been developed, the authors acknowledge that model resolution is too low to capture local terrain features in the Alps that determine icing frequencies [Grünewald et al., 2012]. Combining all these elements to attain insight into the failure probabilities of wind turbines in alpine terrain, will therefore be an important next step on the road to extensive wind power deployment in the Swiss Alps.

## **2.6 Acknowledgements**

*This research is funded by the Swiss National Science foundation under the National Research Programme NRP 70 'Energy Turnaround'. We would further like to thank Christoph Marty and Michel Bovey for their help with data acquisition.*



# 3 Improvement of wind power assessment in complex terrain: The case of COSMO-1 in the Swiss Alps

Postprint version of the article previously published in *Frontiers in Energy Research Volume 6 (2018)*, doi: 10.1016/j.apenergy.2017.01.085, Bert Kruyt<sup>1,2</sup>, Jérôme Dujardin<sup>1</sup>, Michael Lehning<sup>1,2</sup>.

**Candidate's contribution** *The candidate developed the research concept together with both co-authors. The candidate gathered the data, conducted the analysis and wrote the manuscript. J.D. developed the model of the Swiss electricity system.*

## 3.1 Introduction

Switzerland has recently adopted a law to decommission its nuclear power plants at the end of their lifetime, and to significantly boost the production from renewables. In order to achieve these goals, it has developed the Energy Strategy 2050 [Federal Department of the Environment Transport Energy and Communications DETEC, 2018]. Large increases in power production from renewable sources such as wind and solar will have to be realised if they are to replace Switzerland's nuclear capacity, which currently produces 32,8% of Switzerland's annual (2016) electricity supply [Bundesamt für Energie (BFE), 2017]. Previous work has shown that wind energy has a favourable seasonal profile to complement hydropower and photovoltaics (PV) [Krüy et al., 2017, Dujardin et al., 2017], and as such is worth investigating further in view of the Energy Strategy 2050, which is the focus of this paper.

---

<sup>1</sup>Ecole Polytechnique Fédérale de Lausanne (EPFL), School of Architecture, Civil and Environmental Engineering (ENAC), Lausanne, Switzerland

<sup>2</sup>WSL Institute for snow- and avalanche research SLF, Davos, Switzerland

## Chapter 3. Improvement of wind power assessment in complex terrain: The case of COSMO-1 in the Swiss Alps

---

### 3.1.1 Wind resource assessment using NWP

Initial wind resource assessment is often based on numerical weather prediction (NWP) models. In relatively flat terrain, wind fields are rather uniform, which allows for relatively straightforward extrapolation of results. Similarly, NWP model resolution does not need to be very high for accurate assessment. In complex terrain such as the Alps however, the wind climate in the lower boundary layer is strongly influenced by the topography, which causes e.g. local speed up effects through gap flows and orography [Lewis et al., 2008, Mayr et al., 2007]. Hence accurate modelling of the wind climate in complex terrain requires spatial resolutions that capture these topographic features.

At the same time, long simulations or measurements are required so that seasonal and inter-annual variability can be assessed. The computational demands resulting from these two requirements (high spatial resolution and long simulations) make it unrealistic to simulate large areas such as the entire Swiss alpine domain for wind potential assessment.

Various methods have been developed in attempts to overcome these shortcomings by reducing computational demands. Most notably, diagnostic methods forego the time derivatives of the partial differential equations describing conservation of mass and momentum that govern NWP models, the so-called Navier-Stokes equations. The thus assumed steady state flow can be solved at lower computational expense. However, dynamic processes such as flow splitting, vortex shedding and thermally induced circulations cannot be accurately represented in such schemes [Truhetz, 2010]. Examples of such models include WindSim [WindSim, 2018] and 3DWind [Berge et al., 2006].

Other methods exist, that attempt to avoid the computational costs of solving the Navier Stokes equations at high resolution by using statistical relations instead. In such statistical models, (often linear) regression is used to interpolate relations between observations (synoptic scale wind fields, topography) and predictands: in this case near surface wind fields. As noted by Truhetz [2010] however, “Because of the terrain-induced decoupling effects between predictors and predictands these methods have conceptual shortcomings in the Alpine region”. (For a more detailed classification of wind resource modelling see Truhetz [2010] ).

### 3.1.2 Wind resource assessment in the Alps

Specifically for the alpine domain, a number of studies have attempted to assess the wind potential in sections of the Alps. Truhetz [2010] developed a hybrid method of using dynamic, diagnostic and statistical models to derive annual mean wind speeds and Weibull parameters for the Austrian Alps in a resolution of 100 x 100 m. This was then used to assess the wind potential in Austria [Truhetz et al., 2012, Winkelmeier et al., 2014]. Draxl and Mayr [2011] found the best locations in the Austrian Alps to be mountain ridges (with median wind speeds of 7 m/s and potential of 1600-2900 kWh/a/m<sup>2</sup>). In Switzerland, a statistical method was used to interpolate measurements onto a grid with a horizontal resolution of 100 x 100 m [Bundesamt

für Energie BFE, 2004a]. This method was expanded upon in the Alpine windharvest project [Schaffner and Remund, 2005]. More recently, a Swiss Wind Atlas was developed using the diagnostic model WindSim in combination with measurement series, where the latter were used to scale the model output to obtain mean annual wind speeds [Koller and Humar, 2016]. For the alpine domain, they report absolute differences (error) of 1.0 m/s (valley) to 1.5 m/s (mountains) in calculated mean annual wind speeds compared to long standing measurements. These mean annual wind speeds were combined with regional and national interests to produce a selection of areas that the federal government recommends suitable for wind power development. The document describing these areas is called the ‘Konzept Windenergie Schweiz’ (roughly translated here as Swiss Wind energy concept) [Bundesamt für Raumentwicklung, 2017, Bundesamt für Energie BFE, 2004b].

Other notable efforts to use statistical downscaling techniques specifically for Switzerland include the work of Helbig et al. [2017], who use sub-grid topography parametrization (the Laplacian of terrain elevations and mean square slope) to statistically downscale coarse-scale wind speeds from the ARPS model. Their results show large correlations with higher resolution wind speeds from the same model. Winstral et al. [2017] developed a statistical downscaling technique based on the exposure to / sheltering from wind based on high resolution (25 m) DEM data. They assess the performance of COSMO-2 (2.2 km resolution) and COSMO-7 (6.6 km resolution) forecasts and were able to reduce the biases in those forecasts with their downscaling technique.

Various efforts have also been undertaken to quantify the effect of increased horizontal resolution in NWP on wind speed prediction. Jafari et al. [2012] compare model resolutions for several areas including a domain within Switzerland, and conclude that in complex terrain the increase in horizontal resolution from 9 to 3 km leads to significant improvements in weekly-averaged wind speed predictions. Dierer et al. [2009] compare COSMO-7 (6.6 km resolution) to COSMO-2 (2.2 km resolution) wind speed forecasts for 5 locations in Switzerland and conclude that for all sites, the increase in resolution from COSMO-7 to COSMO-2 improves results.

#### 3.1.3 Outline and goals

The aim of this paper is to investigate the role of wind energy in the dynamics of highly renewable Swiss electricity scenarios. Specifically, since previous work indicates that wind power at higher elevations may have benefits in terms of the seasonal production profile [Kruyt et al., 2017], special attention is paid to the alpine domain. To this end we choose, contrary to previously described assessment methods, to not simplify the physics by using steady-state simplifications or statistical predictions. Rather, we opt to use a fully non-hydrostatic NWP with relatively high spatial resolution. The COSMO-1 model, described in more detail in section 3.2 below, has been running for roughly 2 years at a hourly time step. While this is arguably a rather brief period for wind resource assessment, we want to focus on improving the wind assessment in Alpine terrain, which can be judged from the new dataset. For this

## **Chapter 3. Improvement of wind power assessment in complex terrain: The case of COSMO-1 in the Swiss Alps**

---

terrain it is acknowledged that physical simplifications in the modelling approach have severe shortcomings. Therefore, the choice to compromise on the length of wind speed records rather than the physical representation of the phenomena is made.

This work aims to contribute to the understanding of wind power in complex terrain and thereby help the cost-efficient transition to a more sustainable electricity supply. Although the work is focussed on Switzerland, the methodology and results are applicable to any mountainous terrain. It is to our understanding the first time a mesoscale NWP model is coupled with model of the Swiss national power system to assess the influence of turbine siting on both required import and turbine capacity. To our knowledge, thus far all wind resource or potential assessments for Switzerland [Bundesamt für Energie BFE, 2004b, Schaffner and Remund, 2005, Koller and Humar, 2016] have to some extent been based on statistical methods, thereby foregoing the physics governing the actual flows. It is about time to see how a fully physical model compares.

This paper is structured as follows: Firstly, the performance of the COSMO-1 model is assessed by comparing the modelled wind speeds to weather stations across Switzerland. Next, we calculate power time series from the modelled wind speeds and use these in an existing energy model to investigate different wind turbine siting scenarios in Switzerland, where the constraints defined in the aforementioned policy document ‘Swiss wind energy concept’ are also investigated. Section 3.2, describes the models and calculations used throughout this work. Next, section 3.3 discusses the main results from the aforementioned calculations and finally we draw conclusions and provide an outlook in section 3.4.

### **3.2 Methods**

#### **3.2.1 COSMO-1**

The Consortium for small-scale modelling (COSMO) maintains the COSMO family of NWP models. These non-hydrostatic, mesoscale NWP models are used by research institutes and meteorological services around the world [Consortium for Small-scale Modeling, 2017]. In this work, we use the output of the COSMO-1 model, which has a horizontal resolution of  $0.01^\circ$ , which corresponds to 1.11 km N-S and 0.74 to 0.78 km E-W. Vertically, it features 80 levels with smooth level vertical (SLEVE) terrain following coordinates. The SLEVE scheme allows for smaller terrain features to decay faster than larger ones, thus reducing computational errors and allowing for a smooth transition to the upper homogeneous levels [Schär et al., 2002, Leuenberger et al., 2010]. This version of the COSMO model has been operational at the Swiss national weather service since the end of 2015, providing us with a little more than two years of hourly (reanalysis) data. The 10 m wind speeds are used for verification against the measurement stations, while interpolating between the two nearest vertical levels gives the wind speed at 100 m above the surface for scenario analysis. With the exclusion of lakes, the number of  $0.01^\circ$  pixels within Switzerland amounts to 48657.

### 3.2.2 IMIS network

The IMIS station network [Lehning et al., 1999, SLF, 2016], consisting of 198 stations around the Alps and Jura mountains, is operated by the Swiss institute for snow and avalanche research SLF. These stations are located in pairs with a wind station at a wind-exposed location and a snow station at a wind-sheltered location, which is generally also at slightly lower elevation. In addition, a small number of reference stations exist. All stations measure temperature, humidity and wind speed. Data are averaged over 30 minutes. The wind stations are located at elevations from 1936 (Amden - Mattstock) to 3345 (Zermatt - Platthorn) m.a.s.l. While the snow stations range from 1513 to 2914 m.a.s.l. In total there are 177 stations within Switzerland that have more than one year of data within the period that COSMO-1 has been operational. A map with the locations of the stations is shown in Figure 3.1. The other, well known network of weather stations in Switzerland is the SwissMetNet. However the data from these stations are assimilated in the COSMO models and can therefore not be used for validation.

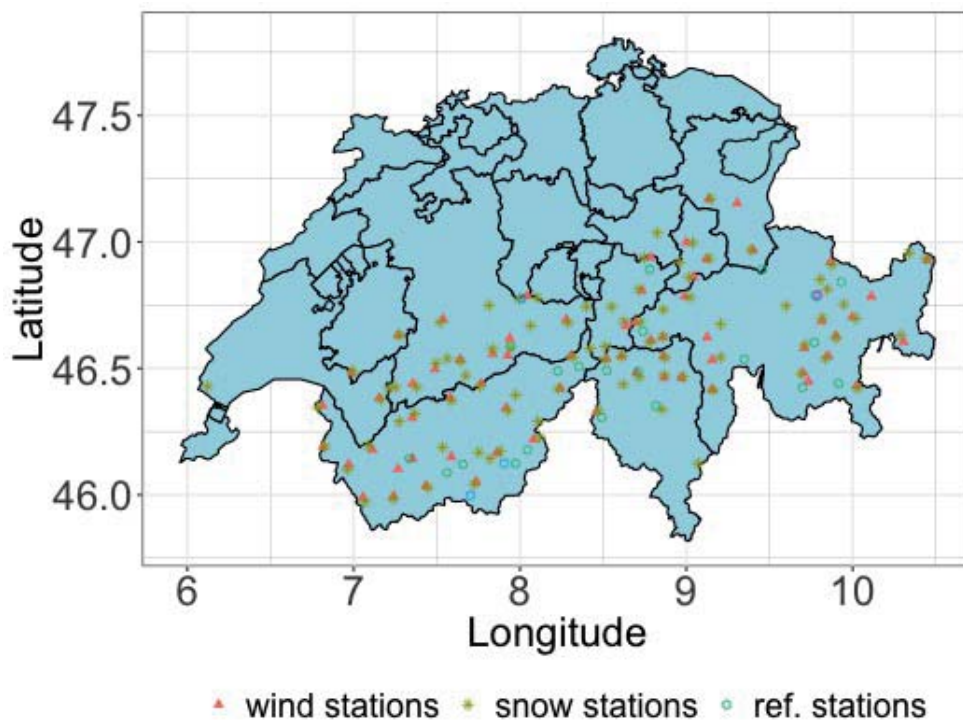


Figure 3.1 – The IMIS stations.

### 3.2.3 Validation of COSMO-1

The performance of the COSMO-1 model in complex terrain is assessed by comparing the modelled wind speeds against the IMIS stations described above. Since IMIS stations record their data on 30 minute intervals, their data is averaged over hourly intervals so it can be

### **Chapter 3. Improvement of wind power assessment in complex terrain: The case of COSMO-1 in the Swiss Alps**

---

compared against COSMO-1's hourly output. We then assess correlation for pairwise-complete observations, as well as root mean square error (RMSE) and mean bias error (MBE).

#### **3.2.4 Power transformation**

The wind speed time series of each COSMO-1 pixel are transformed to power output by applying a power curve. To this end we use the power curve of a wind turbine commonly found in Switzerland, the Enercon E82. Although site-specific wind turbine selection can arguably increase local wind power production, this is a rather complex matter and therefore refrained from. See Kruyt et al. [2017] for a discussion on wind turbine sensitivity for Switzerland, as well as a more detailed description of the methodology. We use the wind speeds at 100 meter above the surface for the analysis. Using the Enercon's power curve, we then calculate 1 MW power time series for each pixel. In subsequent modelling steps, we can then easily scale the production in each pixel to achieve various targets. Analogous to Kruyt et al. [2017] the power production is corrected to account for reduced air density at higher elevations.

#### **3.2.5 Wind energy potential**

It is worthwhile to distinguish between various types of wind energy potential. Loosely based on Hoogwijk and Graus [2008], Hoogwijk et al. [2004], we can distinguish:

- The theoretical potential, which relates to the power that can be extracted from the wind (limited by Betz' law).
- The technical potential is the theoretical potential reduced by the conversion efficiencies of the turbines, losses due to maintenance etc.
- The geographical potential is the technical potential reduced by land-use constraints. As this inherently also involves political choices, we have dubbed it geographical/political potential.
- The economical potential is that part of the above which is feasible at current competitive cost levels.
- The market potential is the amount of wind energy that can be integrated into the market given constraints on demand and supply patterns, institutional barriers and subsidies.

These various forms of energy potential have been schematically represented in Figure 3.2 . The work in this paper is mainly concerned with the technical potential, although comparisons are made to the Swiss wind energy concept [Bundesamt für Raumentwicklung, 2017, Bundesamt für Energie BFE, 2004b], which describes areas deemed suited for wind power development by the federal government, and as such touches onto the geographical potential.

Seen from the perspective of a wind developer at a potentially profitable location, the modelling presented in this paper is only a first step in the wind resource assessment process. For the development of an actual wind farm, such modelling is usually followed by on-site measurements, modelling of turbulence intensities to select an appropriate turbine and micro-siting, and, in case of a multi-turbine wind farm, the modelling of wind turbine interactions such as wake effects [ADB, 2014, Sharma et al., 2018]

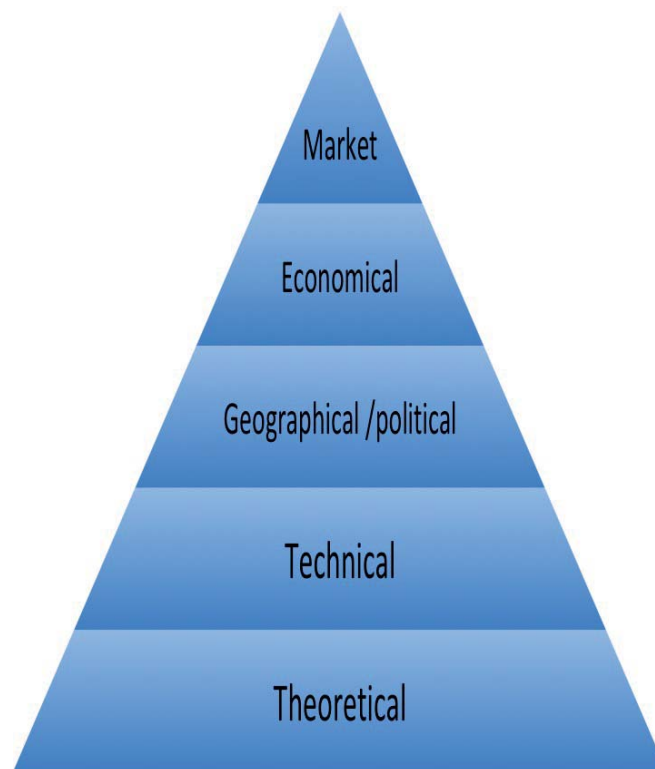


Figure 3.2 – The various definitions of wind energy potential, described in more detail in 3.2.5.

#### 3.2.6 Modelling Switzerland's power supply

The Swiss power system is simulated to investigate the effect of different turbine locations on the dynamics of the power system. We deploy a model that is described in detail in Dujardin et al. [2017], with simulations run for the period of 01-01-2016 through 31-12-2017, two full years. This model uses the time series of Switzerland's electricity production and consumption to compute the amount of energy that can not be generated indigenously. In this work we simulate a fully renewable Swiss power supply, where all current nuclear capacity is replaced by

### Chapter 3. Improvement of wind power assessment in complex terrain: The case of COSMO-1 in the Swiss Alps

---

renewables. This implies that 47% of the current demand<sup>3</sup> will be covered by new renewables (PV, wind, geothermal). In our model, 4.4 TWh/a will come from geothermal energy as a constant base load, and the remaining 49.38 TWh for the 2-year simulation period come from a combination of PV and wind energy. We investigate various wind targets of 8, 12 and 24 TWh for the 2 simulation years. In each of these cases, the remainder of this 49.38 TWh comes from PV. The PV time series are generated from satellite data while we model production from panels located in urban areas. Panels are located following population density, representing the idea that mainly rooftops will be used. Recently insights have emerged [Kahl et al., 2018] that this is far from optimal in terms of both cost and winter yield. However, for simplicity's sake we adhere to this simple and plausible scenario. The remaining 53% of the demand in our generation portfolio is met by the current Swiss hydropower installations. For the run-of-river plants, we directly use the production time series for the given period (33 TWh for the two years). For the storage hydropower plants, we use the time series of production and reservoir levels to compute the energy equivalent inflow into the system (33 TWh). We also use the plants' and reservoirs' characteristics to get a nationally aggregated capacity for storing and releasing the aforementioned energy inflow. The model's behaviour can be summarized by these 3 steps: 1. From the national demand time series, compute the residual demand by subtracting the non-dispatchable sources (run-of-river, PV, wind, geothermal); 2. Compensate for the mismatch using short-term storage (pumped hydropower) within its capacity; 3. Use the flexibility of storage-hydropower to compensate for the remaining mismatch, within its capacity. Finally, the sum of what could not be alleviated by storage hydropower corresponds to the amount of energy that could not be transferred from the summer period to the winter period. This winter energy deficit is referred to as required import. For more detailed information about this power and energy balance model, we refer to Dujardin et al. [2017].

As mentioned, total production from PV and wind amounts to 49.38 TWh over the two years in order to reach bi-annual self sufficiency and a fully renewable power system. We investigate bi-annual wind power targets of 8, 12, and 24 TWh, where the remainder of the bi-annual 49.38 TWh 'new-renewables' target is met by PV in all scenarios. While a potential of 4 TWh/a in 2050 is often mentioned [Prognos, 2012, VSE, 2014, Hirschberg et al., 2005, Abhari et al., 2012, Brugger et al., 2009, Bauer et al., 2017], this number appears to stem from reports dating back 14 years [Hirschberg et al., 2005, Bundesamt für Energie BFE, 2004b]. In the mean time, global wind power development has continuously surpassed expectations, driving down prices [Ayuso and Kjaer, 2016] and rotor diameters have increased. Furthermore, increases in model resolution have shown the potential in complex terrain and at elevation to be significant [Kruyt et al., 2017, Draxl and Mayr, 2011, Truhetz et al., 2012]. Because of these reasons, we feel a higher production target is most likely attainable. Also, previous work [Kruyt et al., 2017, Dujardin et al., 2017] has shown that wind power can have a beneficial effect on system stability and required import. Moreover, comparing several targets allows us to show the dynamics of the system.

---

<sup>3</sup>Current Swiss electricity demand is about 62 TWh/a. [Bundesamt für Energie (BFE), 2017]



The results and targets will from here on be presented as annual results and targets, rather than bi-annual. Although strictly not the same, this is done to increase the readability of the text and allow for quicker, intuitive comparison to other studies and targets. The main differences are that we do not enforce the production of any wind power target in one year, but allow for compensation between the two years. Similarly, national demand and supply are required to be balanced on a bi-annual basis instead of on an annual one.

### 3.2.7 Required number of wind turbines

An important question is how many turbines are required to achieve a certain amount of annual wind energy production, and how this depends on the siting of those turbines. Specifically, as previous work has indicated that high elevation wind power may offer higher yields [Kruyt et al., 2017], we want to investigate the effect that locating turbines at higher elevations has on production and thereby, the required amount of turbines. In order to investigate this, we deploy a methodology where the maximum elevation at which turbines can be placed is varied iteratively, and look at the resulting amount of turbines required to reach the annual production target (4, 6, or 12 TWh/a). One methodological challenge is the fact that there are more locations (pixels) below 4000 m.a.s.l than there are below 2000 m.a.s.l. In order to make a 'fair' comparison between scenarios, we take random subsets of a fixed size from the all locations below each maximum elevation cap, so that each scenario is based on the same amount of initial candidates. As this random process introduces an element of chance, we repeat this random draw 10 times for each elevation cap, in order to increase the robustness of the results. The size of this random subset will obviously have an influence on the results. The smaller this subset, the fewer locations with high capacity factors will be included, and thus more pixels (and thus turbines) are needed to reach the national production target. For too large a subset, insufficient pixels will be available below a low elevation threshold. As there is no 'right' amount, we use the arbitrary amount of roughly 22000 (out of the total of 48657). To represent the fact that turbines require space, the amount of turbines that can be placed in one (0.01°) pixel is limited to 6 MW, corresponding to 3 2 MW turbines [Denholm et al., 2009, Meyers and Meneveau, 2012].

The resulting algorithm can thus be summarized in the following steps: 1. A random subset of fixed size is drawn from all pixels below the maximum allowed elevation for that iteration; 2. Capacity (6 MW max per pixel) is assigned to the pixel with the highest capacity factor, then the second highest and so on, until the annual production target is met; 3. The resulting nationally aggregated wind power time series is then used to run the electricity model described in the previous paragraph to assess its effects on the Swiss power system. 4. The steps above are repeated 10 times, after which the process starts for the next elevation maximum.

Due to the seasonality of hydropower production and electricity demand, the mismatch between supply and demand is highest in winter [Dujardin et al., 2017]. To see if it would be worthwhile to place wind turbines focussed specifically at alleviating this 'winter gap',

## Chapter 3. Improvement of wind power assessment in complex terrain: The case of COSMO-1 in the Swiss Alps

we conduct the same calculation but this time sorting the COSMO-1 grid cells based on the capacity factor in the winter months (November through April). Hence the locations with best winter production are picked first, and not necessarily the locations producing the most throughout the year. It goes without saying that this second method will require more capacity to meet a similar target, since the targets are (bi-)annual ones.

### 3.3 Results and Discussion

#### 3.3.1 Validation of COSMO-1 against IMIS weather stations

Figures 3.3 through 3.5 show the results of the model validation comparing the hourly wind speeds of the model with the IMIS stations. Overall, it can be seen that the COSMO-1 model performs significantly better for wind-exposed stations than it does for wind-sheltered stations: From Figure 3.3 we can see that the RMSE is lower for the wind-exposed stations and has a smaller spread. Similarly, the correlation is higher for the wind-exposed stations and has a smaller spread (Figure 3.5). Lastly the MBE is almost zero for the wind-exposed stations, whereas it is 1.78 m/s for the wind-sheltered stations (Figure 3.4). Winstral et al. [2017] find a positive bias for sheltered locations when compared to COSMO-2 forecasts, while they find a negative bias for wind-exposed stations. It should be noted that their definition of sheltered and exposed is different from ours, as we take the IMIS station types (i.e. ‘snow’ or ‘wind’ stations, see Section 3.2), and Winstral et al. [2017] use the topographic position index (TPI), a measure of the station’s location relative to the mean elevation in a 2km radius surrounding the station.

Table 3.1 summarizes these same data. We could not discern a significant relation between any of the error measures (MBE, RMSE) and the station’s elevation (not shown). RMSE increased slightly with elevation for both wind ( $R^2 = 0.01$ ) and snow stations ( $R^2 = 0.17$ ), as did MBE ( $R^2_{wind} = 0.07$ ,  $R^2_{snow} = 0.11$ ) but these  $R^2$  values prevent any strong conclusions. Similarly, correlation decreased slightly with elevation for the wind-sheltered stations ( $R^2 = 0.02$ ), and no relation was found for the wind-exposed stations.

	type	mean.RMSE	RMSE.sd	mean.MBE	MBE.sd	mean.cor	cor.sd	MAE.of.bi.annual.mean
1	wind	2.87	0.52	0.03	1.08	0.51	0.12	0.83
2	snow	3.03	0.97	1.78	1.03	0.45	0.15	1.77
3	ref	2.48	0.57	1.19	0.80	0.46	0.16	1.22

Table 3.1 – COSMO-1 validation against IMIS stations, for wind-exposed ‘wind’ stations, wind-sheltered ‘snow’ stations and reference stations. Means and standard deviations of RMSE, MBE, and correlation for hourly wind speeds. The last column gives the mean average error (MAE) for the bi-annual mean speeds.

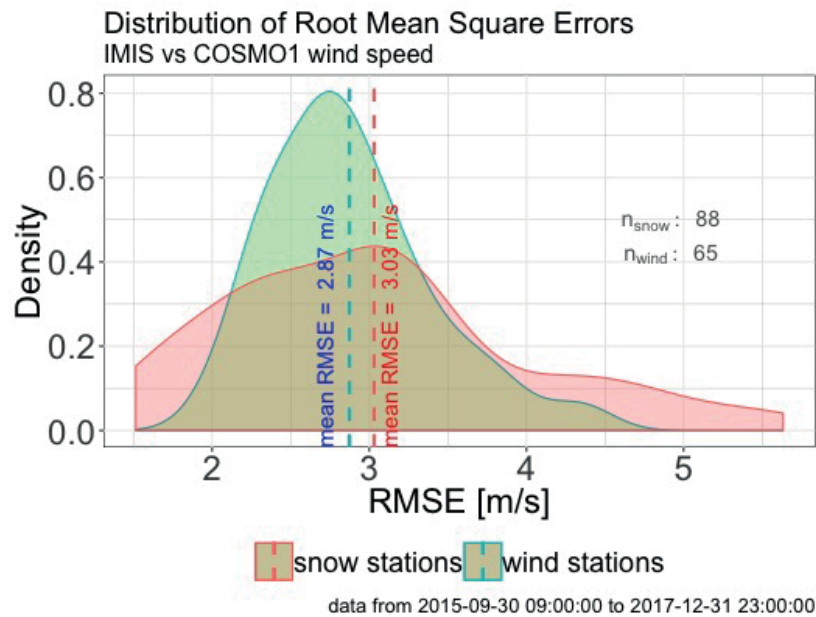


Figure 3.3 – Root Mean Square Error (RMSE) between IMIS and COSMO-1 wind speeds. The plot shows the distribution of the individual RMSE's, that were calculated as the RMSE between each station's observed (measured) time series and the time series of the corresponding COSMO-1 grid cell.

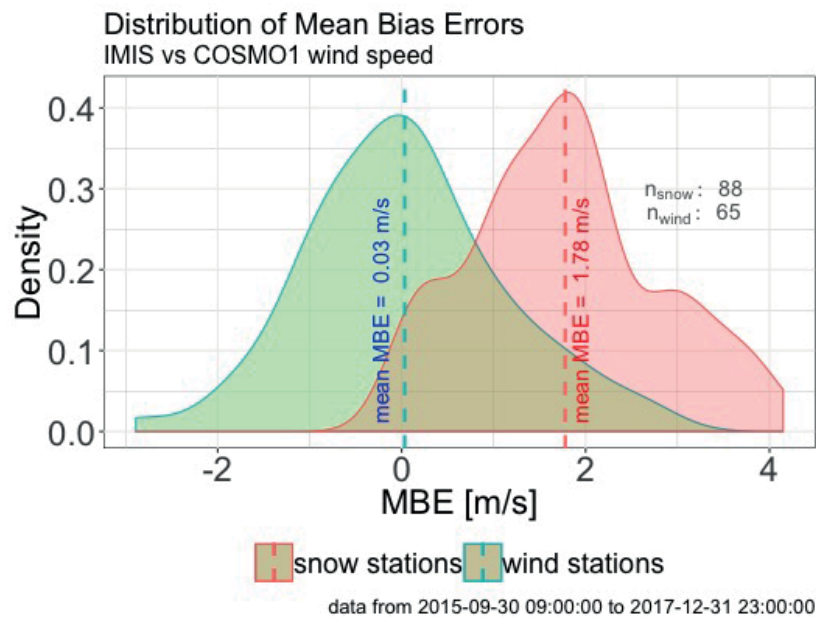


Figure 3.4 – Mean Bias Error (MBE) between IMIS and COSMO-1 wind speeds. The plot shows the distribution of the individual MBE's, that were calculated as the MBE between each station's observed (measured) time series and the time series of the corresponding COSMO-1 grid cell.

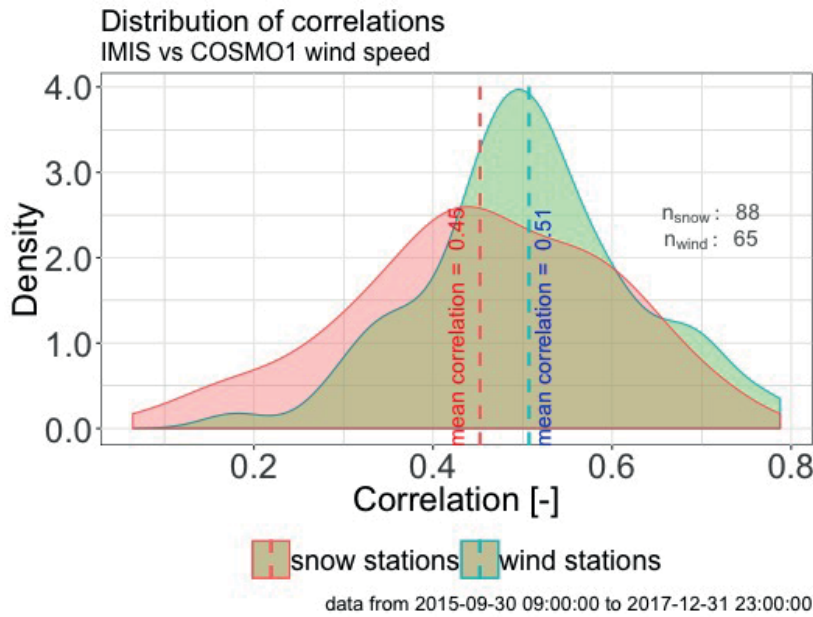


Figure 3.5 – Correlations between IMIS and COSMO-1 wind speeds, for both wind- and snow stations. Correlation coefficients were calculated between the wind speed timeseries of each station and the wind speed timeseries of the corresponding COSMO-1 grid cell.

### 3.3.2 Comparison with Wind Atlas

In the analysis for the official Swiss wind atlas (windatlas.ch), Koller and Humar [2016] reported an absolute error of 1.0 m/s for valleys and 1.5 m/s for mountains in mean annual wind speeds. Comparing the bi-annual means of the COSMO-1 wind speed to the station data, we find a mean average error of 0.83 m/s for the wind-exposed stations. As these are the type of locations that are interesting from a perspective of wind power development, as opposed to the wind-sheltered stations, this is a significant improvement when compared to the Swiss wind atlas. Although it is unclear if the absolute error reported in Koller and Humar [2016] is based on one or all seven of their validation points<sup>4</sup>, the fact that our calculations are based on 65 wind-exposed stations makes them significantly more robust.

### 3.3.3 Capacity factor

We calculated capacity factors for each COSMO-1 pixel, defined as the actual production versus the theoretical (i.e. rated) production. We account for forced outage and maintenance by assuming an availability factor of 96% [Williams, 2014]. Although arguably in alpine environments there are additional factors to consider such as icing [Grünewald et al., 2012], at the same time losses due to icing reported from a Swiss test site are minimal [Barber et al.,

<sup>4</sup>Koller and Humar [2016] write they report the error of a ‘representative location’ for a landscape type (i.e. mountain, valley etc.)

2011] and with current blade heating technologies may be reduced to near zero<sup>5</sup>. Although one could incorporate a correction factor into the capacity factor calculation that accounts for additional downtime at higher elevations, the lack of reliable spatially distributed data would make this a rather arbitrary undertaking, and introduce more uncertainty than it resolves.

The calculated capacity factors are shown in Figure 3.6 and range from 0.01 to 0.42. If the capacity factor is calculated over just the winter months (November through April), the range increases from 0.01 up to 0.49.

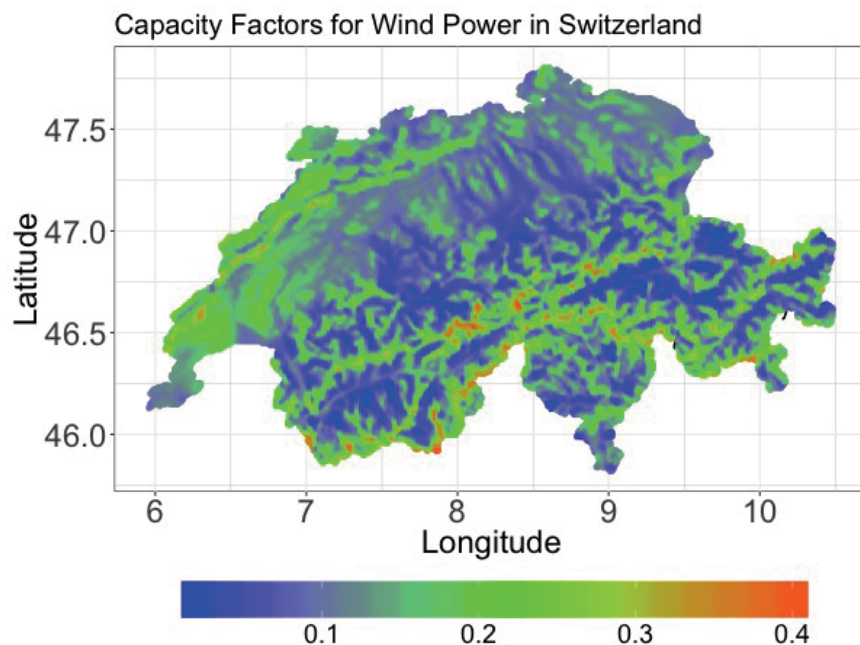


Figure 3.6 – Capacity Factors, defined as the ratio of produced power vs rated power, with a correction for down time due to maintenance or other purposes.

#### 3.3.4 Potential import reduction due to turbine siting

To assess the influence of wind siting scenarios on the resulting import for a renewable Swiss power supply, we run a set of simulations where we produce the entire wind power target from the time series of one COSMO-1 pixel. This is obviously an unrealistic scenario, however it does provide us with a range of influence on the power system. In other words, what is the influence wind power can have on overall system performance?

For annual wind targets of 4, 6, and 12 TWh/a, the unit power time series from each pixel is scaled to reach the desired target. The electricity model is then run to provide the required import, which we can display in the same pixel, thus creating a map that tells us how much import is needed should the entire wind target be produced from locations with such char-

<sup>5</sup>personal communication with major Swiss wind power developer

### Chapter 3. Improvement of wind power assessment in complex terrain: The case of COSMO-1 in the Swiss Alps

---

acteristics. This theoretical scenario provides some valuable insights. Producing 4 TWh/a of wind power from the characteristic wind time series from a single location can lead to a (bi-)annually self sufficient system with as little as 9 TWh/a of imports, whereas the ‘worst’ locations can lead to an increase of 26.2% (11.4 TWh/a). For higher annual wind power targets of 6 or 12 TWh/a the range of required import to balance the system increases. Imports to balance a power system producing 6 TWh/a range from 8.1 to 11.7 TWh/a, and a power system with 12 TWh/a of wind power requires at least 6 TWh/a and at most 13.3 TWh/a. The resulting maps are shown on the left hand side of Figure 3.7. What these results tell us is twofold: one, there is great disparity in the wind potential across Switzerland, and two; As the amount of wind power in the system increases (from 4 TWh/a to 12 TWh/a), the range of required imports increases. This means that accurate wind turbine siting becomes more important as the installed capacity is increased. But also, as the share of wind power in the electricity mix increases, it becomes possible to make the system (bi-)annually self-sufficient with less imports.

We can look at these results in another way by plotting the resulting import as a function of the share of total production that is produced in the winter months. In the right side of Figure 3.7 this is done for the 3 wind targets of 4, 6 and 12 TWh/a. From these figures it becomes clear that the best producing wind locations (in terms of capacity factor) do not reduce import the most. Those locations that contribute most to low imports are the ones that produce most of their annual power during the winter months. In other words: in order to reduce the import the winter production needs to be as high as possible, relative to the total annual production (a high winter capacity factor relative to the annual capacity factor). Those locations that exhibit this behaviour (the lower right corner of Figures 3.7 D through F) unfortunately have low overall capacity factors, making them unattractive for wind power development. The feasible locations, i.e. the ones with high capacity factors, are the orange to red points. For increasing annual wind power targets from 4 TWh/a to 12 TWh/a, the resulting imports associated with these points goes down (compare the red points in Figure 3.7 D with those in Figure 3.7 F), showing that high shares of wind power in a renewable Swiss electricity supply lead to self-sufficiency with lower imports. This is in line with the findings in Dujardin et al. [2017].

One caveat should be placed however: In this section we have disregarded the capacity required to reach a wind power target. Therefore, in order to minimise imports, wind locations that produce high shares of their production in winter are favoured, even if their total annual production is low, because we scale the production until the annual target is met. In reality, wind locations producing high absolute amounts of power will be the economically viable ones. Therefore, economically viable options that also reduce imports will be the ones producing both a high absolute amount of power as well as a large part of this in winter. Obviously, in a future electricity market without subsidies per kWh and with high amounts of PV, it remains to be seen what the market value of summer electricity will be, compared to that of winter electricity. In the next section, we will look at the required capacity to reach a certain target.

### 3.3. Results and Discussion

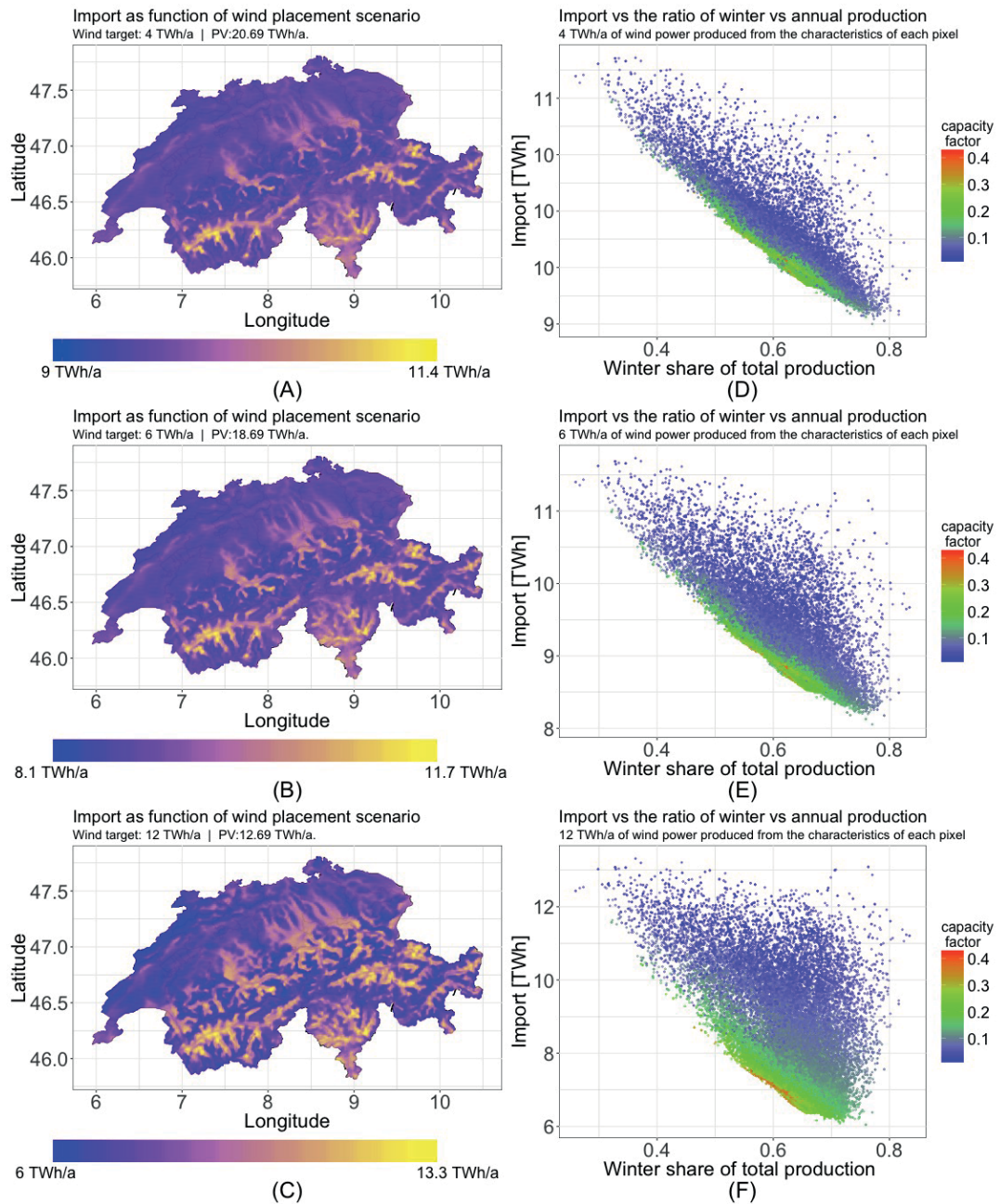


Figure 3.7 – **Left (A) through (C)**: Producing various annual wind power targets (4, 6 or 12 TWh/a) from the characteristic time series of each COSMO-1 pixel. The Import required to balance the system is plotted in each pixel. We can see a clear relation to the topography.

**Right (D) through (F)**: The relation between import and the share of total production that is produced in winter, for the same data as on the left. The highest capacity factors are found around the 60% winter production range. Each point in the plot represents the time series from a 0.01° pixel in the COSMO-1 dataset, scaled to produce 4, 8, or 12 TWh/a. Winter is defined as November through April.

### **3.3.5 Required number of turbines**

In this section we investigate the optimal placement of turbines across Switzerland, with the goal of minimising the capacity required to produce a certain annual wind power target. In order to assess the influence of turbine siting on the required turbine capacity, the production of a bi-annual national production target from turbines with increasing elevation limits is simulated. Initially, the capacity to produce an annual wind power target of 6 TWh/a is assessed, while in a later section, higher and lower targets are explored. To improve robustness, the simulation is repeated 10 times for each elevation cap, as it involves a random selection of a pixel subset. Two cases are simulated. First, from this random subset, turbine locations are selected based on the highest annual capacity factor. Secondly, we have selected candidate locations based on the highest capacity factor in the winter months. The results are shown in Figure 3.8, where the capacity in MW required to produce 6 TWh of annual wind power is plotted as a function of the mean elevation of the locations used for wind power production in each scenario. Clearly visible is a downward trend in the required capacity with increasing mean elevation. This holds for both the cases where locations are selected based on annual capacity factor, as when they are selected based on winter capacity factor. An annual production target of 6 TWh/a could be achieved with as little as 1914 MW when turbines are located at a mean elevation of 2967 m.a.s.l.. However when we restrict the elevation, the required capacity increases as the maximum elevation at which we allow turbines to be sited decreases, up to 2454 MW for a maximum elevation of 1400 m.a.s.l. Obviously selecting the pixels with highest annual capacity factor (and thus production) will lead to the lowest capacity required to reach a certain annual target. However when we look at the resulting import, we see that selecting turbine locations based on winter capacity factor leads to a small but significant reduction in the resulting imports for the system. This becomes more clear when we plot the same data as a function of import (Figure 3.9). Apparently reducing imports (through wind turbine siting) comes at a cost of increased capacity if the same annual target is to be met. This is however partly a result of the separate PV and wind power targets. Reducing imports under a combined renewables target might lead to more wind power at the expense of PV, as we have seen in section 3.3.4 , as well as in Dujardin et al. [2017].

### **3.3.6 Swiss wind Energy Concept**

We have also investigated the capacity required to produce 6 TWh/a when the potential turbine locations are constrained according to the Swiss Wind Energy Concept Bundesamt für Raumentwicklung [2017]. Plotted in Figures 3.8 and 3.9 is the siting scenario constrained by this policy document. From the locations described in the Swiss Wind Energy Concept, the best pixels (based on the annual capacity factor) have been selected and filled with 6 MW per pixel until the bi-annual target of 12 TWh (6 TWh/a) was reached. 2508 MW is required to reach this target. This can be compared to the unconstrained scenario, where the best pixels from the whole of Switzerland are selected without any limitations on elevation or number of candidate locations. This gives a theoretical best attainable solution of 1824 MW. It should be



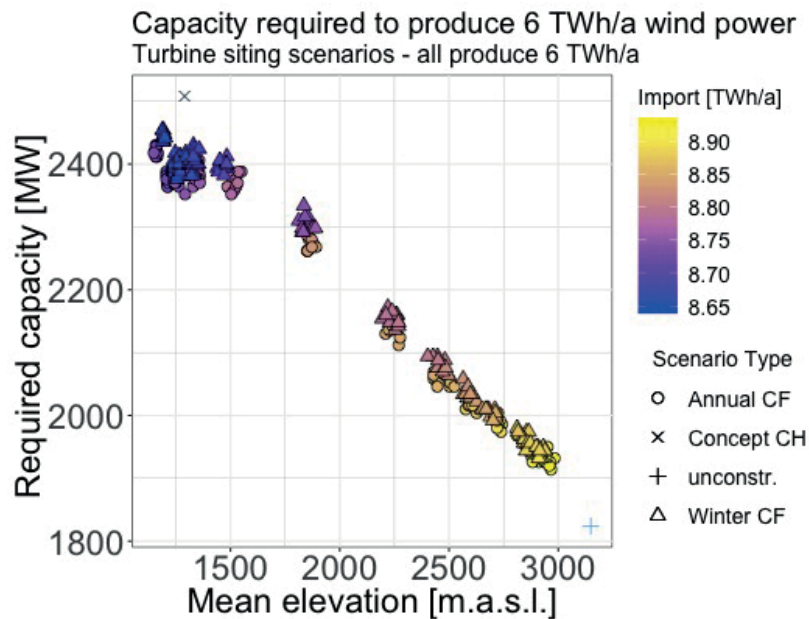


Figure 3.8 – The required capacity as function of the mean elevation of the locations where turbines are located in each scenario. Also included in this figure are a scenario based on the Swiss Wind Energy Concept Bundesamt für Raumentwicklung [2017], 'Concept CH', as well as a scenario without constraints on elevation or locations ('unconstr').

noted that all practical and logistic constraints are neglected in this latter case, as well as in the elevation dependent scenarios. Therefore a direct comparison with the Swiss Wind Energy Concept scenarios does not hold.

### 3.3.7 Capacity as function of annual wind power production

Although the dynamics are relatively similar for wind targets other than 6 TWh/a, in Figure 3.10 the capacities that are required for 4 and 12 TWh/a are also plotted, again as a function of mean turbine elevation. Where in Section 3.3.4 we speculated that for higher wind power targets it might be possible to achieve lower overall imports to balance the energy system on an annual basis, we can see in Figure 3.10 that this is indeed the case. What we however can also see, is that increasingly more capacity is required to produce additional wind energy. This can be explained from the fact that the best locations get used first, and increasingly less productive locations are used to produce additional output. As an example, the lowest capacity we found to produce 4 TWh/a is 1230 MW, whereas 6 TWh/a requires at least 1914 MW, which is more than a 150% increase.

Chapter 3. Improvement of wind power assessment in complex terrain: The case of COSMO-1 in the Swiss Alps

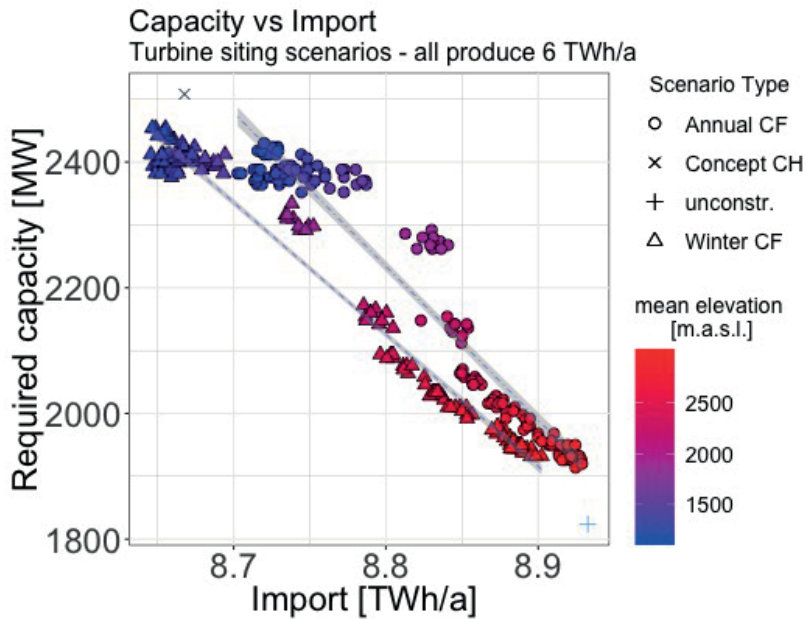


Figure 3.9 – Various random subsets of the COSMO-1 pixels to reach 6 TWh/a wind power production. Also included in this Figure are a scenario based on the Swiss Wind Energy Concept Bundesamt für Raumentwicklung [2017], 'Concept CH', as well as a scenario without constraints on elevation or locations ('unconstr'). Two regression lines are shown, one for the elevation-dependent winter capacity factor scenario-set and one for the elevation-dependent annual capacity factor scenario-set.

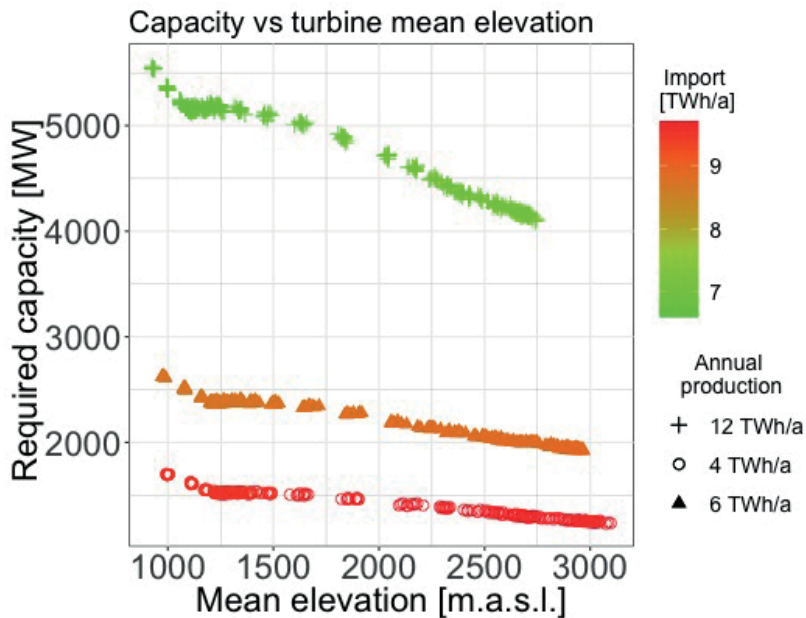


Figure 3.10 – The required capacity as function of the mean elevation of the locations where turbines are located in each scenario, with scenarios for the 3 production targets of 4, 6, and 12 TWh/a.

#### 3.3.8 Sensitivity to wind speed errors

In this work, as in any modelling exercise, we have had to make a number of assumptions and simplifications that have an impact on the results. For one, the selection of an optimal wind turbine for a specific location can arguably increase the yield, something we have not incorporated in our approach. However the uncertainty in wind speeds is arguably more significant and has the highest influence on the results. To grasp the effects this may have, we have assessed how this translates to power output as follows: Since the power curve of a wind turbine is not a linear function of the wind speed, translating errors in wind speed measurement to power output is not straightforward. The power curve can be divided into four important sections: Below cut-in speed no power is produced, while between the cut-in speed and the rated speed the power output increases nonlinearly with the wind speed. Finally between rated and cut-out speed the power output is constant, until there is no power produced when wind speeds exceed the cut-out speed. In Figure 3.11 we have plotted the MBE for the COSMO-1 wind speeds in these three important operating ranges of the turbine used in this work, the Enercon E82, where we have translated the cut-in, rated, and cut-out speeds to the 10m level via the log law, as described in Kruyt et al. [2017]. We can see that in the nonlinear part of the power curve, between cut-in and rated speed, the bias is small with  $-0.4$  m/s. For the speeds below cut-in, we have a positive bias of  $1.65$  m/s. This tells us that on average, our model set up will produce small amounts of power at low wind speeds that a turbine at that location would not produce. However, since this will be at the bottom of the nonlinear part of the power curve, these effects can be expected to be small. Finally at the top end of the power curve is where we see a large negative bias of  $-2.74$  m/s. This tells us that our modelled power output will on average (over all stations) be lower than in reality.

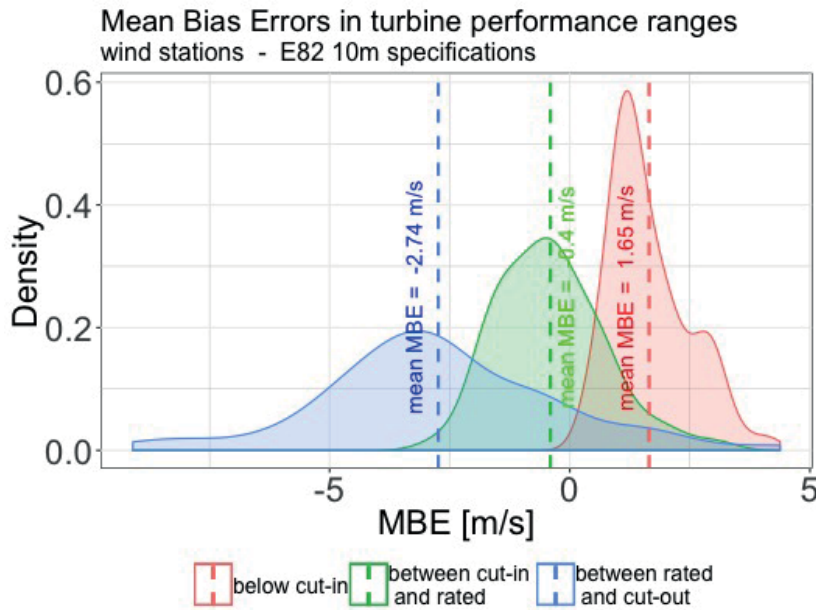


Figure 3.11 – MBE for turbine performance ranges.

### 3.4 Conclusions

#### 3.4.1 Wind resource assessment with COSMO-1

In this paper a series of calculations have been presented investigating the dynamics of a highly renewable Swiss power system with a focus on the role of wind energy. We have used the COSMO-1 model to this end, after assessing its performance in complex terrain with regards to hourly wind speeds. Although the RMSE for wind exposed locations in the Swiss Alps is still significant with a RMSE of 2.87 m/s, the MAE of (bi-)annual mean speeds is lower than previous works (at 0.83 m/s compared to 1.5 m/s reported in the wind atlas [Koller and Humar, 2016]), as well as more robust given the high number of stations used in our validation. Moreover, to our knowledge it is the first time wind resource assessment for the complex terrain of the Swiss Alps is based on a fully physical model, rather than using statistics to correlate static wind fields to topography. COSMO-1 systematically overestimates wind speeds at sheltered stations of the IMIS network, but since these locations are chosen to be relatively sheltered, this bias may be more due to the location and not representative of the entire  $0.01^\circ$  grid cell. For wind exposed stations, bias is almost zero. Analysing the bias for the ranges of speeds that correspond to the different linear and non-linear sections of the turbine's power curve, we estimate that the error in the wind speed likely leads to a slight underestimation of overall power simulations. However we also ignore forced outage due to maintenance and icing, which likely overestimates results.

### 3.4.2 Import reduction & wind power

Next, the wind speeds from the COSMO-1 model were used to produce time series for wind power production. We then used these power time series in a spatially aggregated model of the Swiss electricity system to investigate the influence of wind turbine locations on the power system. We have conducted a series of simulations where increasing amounts of wind power were produced from the characteristic wind time series of single locations in Switzerland. We've used the resulting power time series in a model of the Swiss electricity system where we simulate a renewable Swiss power supply. This has shown us that for a hypothetical, fully renewable Swiss power system, the higher the share of wind power in the renewable electricity mix, the lower the resulting imports can be. This crucially depends on the turbine's locations however, since there are large differences in wind climate across Switzerland. The turbine locations that contribute most to import reduction are those with high production during the winter months. This shows that wind power has to be a key element in a future renewable Swiss power supply, if a heavy dependence on imports is to be avoided.

### 3.4.3 Required capacity

We have investigated the capacity that is required to reach a certain annual wind target, and how the siting scenarios influence overall system parameters such as the import required to balance the system. As with any modelling exercise of complex real world phenomena, there are a number of simplifications and assumptions that call for somewhat cautious interpretation of the exact values. However, since the focus of this work has been on the dynamics of the energy system, the following conclusions can be drawn from our results:

For an annual wind power production of 6 TWh/a, the theoretical minimum amount of capacity required to produce this target is 1824 MW. This neglects all practical and political restraints on turbine siting, and should be seen as a rather theoretical limit more than a practical goal. However, it does give a sense of scale to the rest of the results. Because for further simulations, turbines have been located at different elevations to achieve an annual target. Here we found a strong relation between the mean elevation of the turbine locations and the required capacity to reach that goal. Increasing the mean elevation of turbine locations from 1189 m.a.s.l. to 2967 m.a.s.l. leads to a 28.2 % reduction in the capacity that is required to produce 6 TWh/a of wind power. For the often mentioned Swiss wind power target of 4 TWh/a in 2050, we calculate the minimal capacity to reach this to be 1230 MW. But also here, this requires turbines to be built at high elevations.

These results call for a focus on high elevation wind power in the planning and development of wind power capacity. Transitioning away from nuclear power towards a renewable electricity supply will prove a daunting task, and as such it is imperative to do so in the most space- and cost efficient manner. Our results show that high-elevation wind power can form a crucial element in achieving the Energy Strategy 2050 wind power target with minimal capacity. In Switzerland, public opposition against wind turbines in mountains appears significant.

### **Chapter 3. Improvement of wind power assessment in complex terrain: The case of COSMO-1 in the Swiss Alps**

---

However, the 'Energy Strategy 2050' was accepted in a 2017 referendum [Bundesrat, 2017] and previous research shows that generally, Swiss people are accepting of wind energy [Jegen, 2015]. That same research however also cites the multi-level decentralisation, sectoral policies with diverging objectives and high population density as reasons for the slow increase in wind power capacity in Switzerland. As land-use conflicts as well as population density are arguably fewer at high elevations, focussing efforts on high elevation wind power may also minimize conflicts in these domains.

Our modelling approach has been focussed on minimising the capacity to reach an annual goal, and as such not well suited for other optimisation goals. However, scenarios where capacity was located based on highest winter capacity factor rather than the annual capacity factor did achieve a slight decrease in overall imports required to balance the system.

#### **3.4.4 Outlook**

Although we have managed to qualitatively assess the effects that uncertainties in wind speed may have on power estimates, reducing the RMSE in the modelled wind speeds would be an important step forward. Given the scales of the topography, this most likely implies an increase in horizontal modelling resolution. Given the increase in computational burden this entails, it is more feasible to simulate small areas of interest than the whole of Switzerland. Such areas should be pre-selected based on lack of spatial planning conflicts, logistic feasibility and initial potential assessments. As is the case with any wind farm development project, after initial site identification which may be based on the work in this paper, various steps such as those described in section 3.2.5 will need to be undertaken at the individual site level before a wind farm may actually be developed.

Further integration of resource and electricity models may allow for more complex optimisation problems. We have now looked at turbine locations and their effects on the capacity required to reach a certain target, but it may be more insightful to analyse the combined optimal siting of both PV and wind, with the objectives of minimising both required capacity and resulting system imports. Our current set up with separate targets for wind and PV production does not allow for this. Also, recent insights have emerged that allow for a shift of part of the summer PV production to the winter months without reducing overall yield [Kahl et al., 2018]. Combining such strategies with optimal wind siting strategies in a power flow model will be the next step towards a better understanding of a fully renewable and efficient Swiss power system.

All land-use and spatial planning concerns that may limit areas for wind turbines to be build have been ignored in this study, except for the scenario based on the Swiss Wind Energy concept, which by definition includes such considerations. Caution should therefore be taken in comparing these numbers directly to our idealised scenarios. We have also ignored all logistical limitations of building wind turbines at high elevations. It may very well be technically near impossible, or at least very costly, to build turbines at some of the high

elevation locations we used in this study. A study into the economical wind potential for Switzerland could include such effects, possibly by incorporating a cost function based on the inverse distance to roads or other infrastructure to take into account the additional cost of high elevation wind power in remote locations. The downside of economic potential assessment is that it is heavily dependent on current prices and subsidies of not only the technology in question, but also those of competing ones, making the relevance of the results very short-lived. Moving the current work forward towards a geographical/political potential assessment (see section 3.2.5) will be a complex task, given the decentralized and layered structure of Swiss governance. While federal considerations have been accounted for in the ‘Swiss wind energy concept’ [Bundesamt für Raumentwicklung, 2017], at the cantonal and municipality level there is little information available. We hope that this work will at least lead to better awareness of the potential, and prompt a structured mapping of other land-use and political interests at various political levels, which will be the next step in moving a national wind energy potential assessment forward.

### 3.5 Acknowledgements

This research is funded by the Swiss National Science Foundation under the National Research Programme NRP 70 ‘Energy Turnaround’, and Innosuisse (SCCER-SoE). It would not have been possible without the cooperation and excellent infrastructure from both MeteoSwiss and the Swiss National Supercomputing Centre CSCS. We would further like to thank Christoph Marty, Benoit Gherardi and Michel Bovey for their help with the data acquisition, and Annelen Kahl for supplying irradiance data and PV modelling methodology.





# 4 Downscaling surface wind speeds over very complex terrain for wind potential identification

## 4.1 Introduction

With the rapid increase in wind power capacity over the last decades, wind turbines are increasingly being built in complex terrain. This is in part due to evolving insights that potential from terrain induced flows can be very significant [Kruyt et al., 2017, Draxl and Mayr, 2011]. However it brings about various challenges that do not arise in homogeneous or less complex terrain. For one, potential assessment is difficult, as the correlation as function of distance is low [Kruyt et al., 2017]. This implies that point measurements cannot be extrapolated to nearby locations easily. At the same time, due to the ongoing increase in computational power the possibilities to simulate flows over complex terrain have also increased. There are still quite a few pitfalls and limitations however. Because wind flow in complex terrain is heavily influenced by the topography [Chow, 2013, Jimenez et al., 2016], accurate modeling requires proper representation of that topography. This implies the use of model grid scales that capture (at the very least) the main terrain features, or account for it by parameterizing the sub-grid scale (SGS) topography [Jiménez and Dudhia, 2012, Lee et al., 2015]. However high horizontal resolutions very quickly lead to high computational costs, which limits the applicability for wind power assessment, as this typically requires long standing records or simulations. Attempts to lessen the computational demand by linearizing the equations governing the flow not only have methodological shortcomings in complex terrain [Truhetz, 2010], but have also been shown to be unable to reproduce the flows in complex terrain [Palma et al., 2008, Cattin et al., 2003].

At the same time computational capacity continues to increase, and fully physical Numerical Weather Prediction (NWP) models have been using higher resolutions for their regional assessment [Bauer et al., 2015] and mesoscale NWP models are nowadays pushing into the

#### **Chapter 4. Downscaling surface wind speeds over very complex terrain for wind potential identification**

---

sub km scale. Arguably at the forefront of these developments is the Weather Research and Forecasting (WRF) model [Skamarock et al., 2008], the world's most widely used NWP model maintained by the scientific community [Powers et al., 2017]. WRF has been used extensively for the modeling of wind speeds in complex terrain. Gómez-Navarro et al. [2015] use WRF to simulate various storms over Switzerland, and conclude that the increase in horizontal resolution from 6 to 2 km significantly improves model performance. Unresolved topography leads to a general overestimation of surface wind speeds. Specifically, the 2 km resolution is not able to reproduce channeling effects in e.g. valleys. Jiménez et al. [2010] analyzed the daily-mean surface wind variability over a region of complex terrain in the Iberian peninsula. Downscaling to a 2 km resolution, they were able to reproduce the wind speed variability for several subregions 'reasonably well'. Jiménez et al. [2013] also use WRF at 2 km resolution to see how well it simulates the wind fields from typical synoptic wind patterns. As with the previous study the evaluation is based on daily averages. The same group also investigated the models' ability to reproduce the surface wind direction, and found higher errors for more complex terrain, that decrease with the magnitude of the wind speeds [Jiménez and Dudhia, 2013].

With regards to boundary layer parameterizations, it has been noted that there is no single best boundary layer parameterization that performs best under all weather conditions and at all locations: Siuta et al. [2017] assess the sensitivity of hub height wind speed forecasts at 4 and 12 km resolution, and conclude that the best-performing model configuration in terms of grid length and PBL scheme varies by location and season. Averaged over all locations and the whole year however, the ACM2 scheme performed best. Fernández-González et al. [2017] investigate the performance of physical schemes in the WRF model under varying atmospheric stabilities at 1 km resolution. They find increasing accuracy in wind speed hindcasts with increasing elevation. Furthermore, the MYNN PBL scheme systematically underestimates wind speeds, which was partially corrected using the YSU scheme. WRF performed better under unstable atmospheric conditions, although wind speeds were underestimated during neutral and stable conditions. Draxl et al. [2014] investigate the effect of PBL parameterization on wind shear in complex terrain under varying atmospheric conditions, and find different schemes perform better under different atmospheric stabilities. They note that 10 m wind speeds are not sufficient to verify NWP model performance for wind energy applications, since accurate 10 m wind speeds do not imply accurate hub height simulations. Because local topography, roughness length and obstacles influence near-surface wind speeds measurements significantly, their representativeness is low. For complex terrain, it is therefore questionable to compare mesoscale wind output with observations below 40 m. On the other hand, Gómez-Navarro et al. [2015] concluded that the YSU scheme combined with the previously mentioned correction term for unresolved orography [Jiménez and Dudhia, 2012] performed better than other PBL schemes in storms over Switzerland. Hari Prasad et al. [2017] found the YSU PBL scheme to best reproduce slope wind flows from a selection of PBL schemes.

With the studies mentioned above, it appears that most of them use horizontal resolutions of several to one km. One can debate if this is sufficient to simulate the highly complex terrain

such as that found in the Alps. Although computational power nowadays allows for higher resolutions, by increasing the resolution of mesoscale models to the sub-km scale we enter what has been dubbed the 'terra incognita' [Wyngaard, 2004, Mazzaro et al., 2017], or 'grey zone' [Shin and Dudhia, 2016], a range in between where what the mesoscale and microscale (with fully or partially resolved turbulence) models were designed for. This increase in model resolution can lead to poorer results, as grid-dependent convection can occur [Zhou et al., 2014].

Other methodological problems that arise with mesoscale modeling of complex terrain are related to numerical errors introduced by grid skewness and high aspect ratios. The commonly used terrain following coordinates lead to skewed grid cells near steep terrain, which is known to cause numerical errors, as do high aspect ratios ( $\Delta x/\Delta z$ ) [Daniels et al., 2016]. One way to resolve these numerical problems currently being developed is the immersed boundary method (IBM) [Wiersema et al., 2016], where the model grid continues under the surface and boundary conditions are imposed along this surface. The skewness around steep slopes is thereby avoided. However, the computational demands of WRF-IBM are significantly higher than the standard WRF, and coupling with non-IBM boundary conditions is challenging [Arthur et al., 2018].

Switzerland has recently adopted an ambitious new energy strategy, in which it aims to shut down its existing nuclear capacity and replace it with predominantly indigenous renewables [Swiss Federal Office of Energy SFOE, 2018]. Wind power is assumed to replace part of the nuclear capacity, yet the potential for wind power development is still largely unclear. Because large parts of the country are made up of rugged mountainous terrain, all the challenges described above apply when assessing the resource. In recent years, significant steps have been made towards understanding the resource potential in Switzerland [Koller and Humar, 2016, Oppliger et al., 2016, Kruyt et al., 2017, 2018], yet errors in the alpine remain high [Koller and Humar, 2016]. It was shown that these errors can be reduced significantly with a fully physical numerical weather prediction model at a 1 km horizontal resolution [Kruyt et al., 2018]. However, this resolution is still relatively low in comparison to the scale of the topographic features. A logical question therefore is, if better resolved topography due to increases in model resolution is able to improve wind speed, and thereby resource estimates. This is supported by studies that report terrain-induced speed up effects in the Alps [Clifton et al., 2014, Draxl and Mayr, 2011].

This work therefore aims to explore the use of a sub-km resolution mesoscale model for the initial identification of wind power potential. The area of study is the Swiss Alps, but the methodology can be applied to any area of complex terrain. We will use the latest version of the WRF model to downscale analysis data from the COSMO-2 model, a model chain previously explored by Gerber et al. [2018] for the analysis of precipitation patterns in the Swiss Alps. The first step consists in finding a model setup that balances reasonable computational demands with appropriate results. With such a model set-up, we can then assess if these increased resolutions also show indications of higher wind resource estimates than the COSMO-2

## Chapter 4. Downscaling surface wind speeds over very complex terrain for wind potential identification

---

boundary conditions, or other models with lower resolutions.

This paper is structured as follows: Section 4.2 describes the setup for the WRF model, the boundary conditions and the other models used to compare the results against. We also introduce the two domains around operational wind turbines, and their data that we use for validation. Section 4.3 Describes and discusses the main findings: the performance of both the WRF model as well as two models from the COSMO family, and the difference in representing terrain and terrain-induced flows. Conclusions and an outlook are given in Section 4.4.

## 4.2 Methods

### 4.2.1 Simulated domains

Simulations are run over two domains in the Swiss Alps, depicted in Figure 4.1. These two domains are centered around existing wind turbines, whose data will be used to validate model performance.

#### Gütsch ob Andermatt

The first domain is centered around the alpine wind farm at Gütsch ob Andermatt (from here on Andermatt), in the central Swiss mountains and has an extend of 77 by 78 km. The terrain is characterized by steep mountains with elevations ranging from 459 to 3402 m.a.s.l.<sup>1</sup>, and can therefore be described as highly complex. Prevalent wind directions are north and south. The wind farm consists of 4 wind turbines at a ridge, with hub heights between 49 and 55 meters and rotor diameters of 40 to 44 meters. This wind farm has been the subject of many studies on alpine wind turbine performance and potential, e.g. Schaffner and Gravidahl [2003], Cattin et al. [2003, 2009], Barber et al. [2011]. We compare our simulations against the 3rd turbine, a 900 kW Enercon E44 with 55m hub height, located at an elevation of 2340 m.a.s.l. We chose this particular turbine because it does not have an upwind fetch towards the north, as does turbine nr.1. Cattin et al. [2002] showed that at the Andermatt location, the absence of an upwind fetch leads to a near constant vertical wind profile.

#### Chur

The second domain is centered around a 119 meter hub-high turbine located at the small village of Haldenstein, near the city of Chur, Grisons, and has an extent of 55 km (east-west) by 89 km (north-south). This wind park consists of a single Vestas V112 turbine with a rotor diameter of 112 m and a capacity of 3 MW. Its hub height is 119 m. It is situated at an elevation of 540 m.a.s.l., in a long north-south aligned valley that is approximately 2.5 km wide. This valley experiences strong Foehn winds in case of synoptic currents with a southerly component.

---

<sup>1</sup>after smoothing of the terrain.

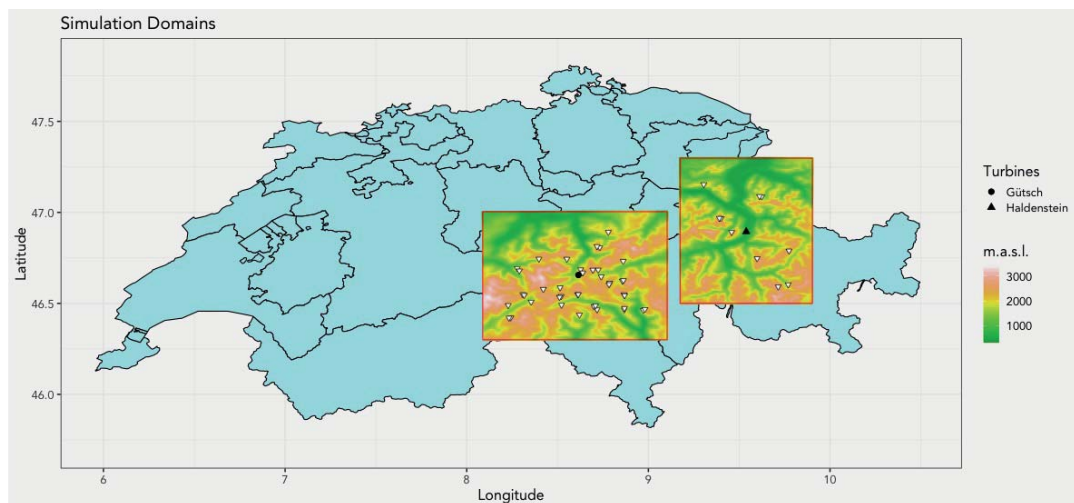


Figure 4.1 – The simulated domains, with black icons indicating the wind turbine location, and white triangles indicating IMIS stations within the domain.

Although elevations in the domain range from 400 m.a.s.l. up to 3127 m.a.s.l., they are generally lower than in the domain around Andermatt, especially in the center of the domain. The terrain is also complex, but at the site of the turbine it is significantly less complex than the turbine location in the Andermatt domain.

For the turbines in both domains, hub height wind speed data was made available at sub-hourly resolutions. This will be used to validate the model performance. Power production data is also supplied, and will be used to assess simulated power production.

#### 4.2.2 The WRF model setup

Simulations were conducted with version 4.0 of the Weather Research and Forecasting (WRF) model [Wang et al., 2016, 2018, Skamarock et al., 2008], run on the supercomputer 'Piz Daint' at the Swiss National Supercomputing Centre<sup>2</sup>. WRF version 4.0 offers various improvements over previous versions, amongst which the most notable for the application in complex terrain is the inclusion of a hybrid sigma-pressure vertical coordinate scheme.

Initial work consisted of finding optimal model settings for our purposes that strike a balance between results and computational demand. Since boundary conditions were available at a relatively high resolution of 2.2 km, no downscaling with successive nests was conducted, which would have also increased the computation time. We use a horizontal resolution of 450 m. The number of vertical levels was 80, with a model top at 50 mb. With the hybrid sigma-pressure vertical coordinate scheme, we used vertical levels of 10 m thickness at the bottom (dzbot). With increasing height the vertical resolution increased to a maximum of 1200 m thickness.

<sup>2</sup>[www.cscs.ch](http://www.cscs.ch)

## **Chapter 4. Downscaling surface wind speeds over very complex terrain for wind potential identification**

---

All domains were run with a boundary layer (BL) parameterization scheme. The main scheme used is the Yonsei University (YSU) scheme. Specifically for this scheme, Jiménez and Dudhia [2012] developed a parameterization for the subgrid-scale orography, to represent the unresolved terrain features. For both domains however we also ran simulations with the MYNN3 scheme to assess the influence of BL parameterization on the results. The results for the YSU scheme were significantly better. Tests with nested domains up to 250 or 150 m resolution in LES mode provided unsatisfactory results, as well as longer running times.

Topography is taken from the Aster Global Digital Elevation Model V002 with a resolution of one arc-second [METI/NASA, 2009]. As touched upon in section 4.1, steep terrain can lead to numerical instabilities [Daniels et al., 2016]. To prevent this, terrain was smoothed to keep the slope angles below 35 degrees. Steeper slope angles led to a rapid decline of the results. Between 3 (Chur) and 5 (Andermatt) cycles of the WRF 1–2–1 smoothing (i.e. a moving window filter with a window length of 3 and weights of 1:2:1 for the grid points  $i-1$ ,  $i$  and  $i+1$ ) were applied. At the border of the domain, transitional smoothing is applied in order to facilitate the transition from the boundary conditions to the finer topography. Land use data is taken from the Corine dataset European Environmental Agency [2006] and translated to the USGS conventions [Arnold et al., 2010, Pineda et al., 2004]. For more details on the data preparation, we refer to the excellent document by Gerber and Sharma [2018]

In order to keep computational demand low, certain options that were not deemed to have a big influence on wind speeds were turned off. As such we did not include any micro-physics scheme, cumulus parameterization or surface physics, except for the simulations in July, where we investigate how well the model reproduces thermally induced flows by including a simple surface physics scheme. For most other settings, we followed those described by Gerber et al. [2018]. The time step deployed is small ( 0.2 - 0.3 sec), which is required to keep the model numerically stable. Experiments using the adaptive time step function of WRF showed mixed results, where gains in computational time were offset by numerical instabilities.

### **Boundary conditions**

Boundary conditions are provided by analysis data from the COSMO-2 model, which has a horizontal resolution of 2.2 km [Consortium for Small-scale Modeling, 2017]. The coupling of WRF and COSMO2 is relatively new, and was first explored in the context of snow precipitation in complex terrain by Gerber et al. [2018]. As the process of coupling the two models is quite laborious, we refrain from listing all the steps but refer to the technical description of the coupling in [Gerber and Sharma, 2018].

### **Simulated periods**

Typically, long records or simulations are required for wind power assessment. With the computational demands of the setup described here this is not possible. We therefore opt to

simulate a handful of days representing common weather patterns. Similar approaches of decomposing time series into representative patterns or snapshots have proven successful in the case of snow drift simulations [Raderschall et al., 2008, Lehning et al., 2008]. As we are not attempting to assess the exact potential but rather identify areas of interest, this approach appears justified. We simulate two periods in winter, motivated by the importance of wind power during winter in Switzerland, as outlined in Kruyt et al. [2018], Dujardin et al. [2017], as well as one period in summer. The first winter period from 26 to 31 January 2016 is characterized by an initially weak westerly synoptic wind and high pressure. Towards the end of the simulation period however, roughly from the end of the 29th, a stronger west to northwestern current causes increased wind speeds. The second winter period is from 1 to 9 March 2016, and is characterized by an strong initial forcing from the west, with strong synoptic winds over both domains. From March 7th onwards, winds subside and more gentle, stable high pressure dominates. Lastly we also simulate a period of stable, high pressure weather in July 2016 (17/7 till 22/7) with the aim of assessing WRF's capabilities in representing thermally induced flows. For the simulations in this period, we therefore employ a basic 5-layer thermal diffusion surface physics scheme in WRF. Notable shortcomings of methods mentioned in Section 4.1 are their inability to reproduce thermal flows. If WRF can reproduce these this would make an appealing case for more physically based wind potential assessments in the mountains.

The selection of simulation periods was partially based on the weather classification scheme from MeteoSwiss, which classifies weather into clusters based on various schemes. A dataset with these classifications at the SwissMetNet Station Rheinwaldhorn was used to this purpose [Weusthoff, 2011]. Clustering weather into regimes is a popular method to assess weather variability, even for wind power applications [Grams et al., 2017]. We are however not attempting to capture the whole range of wind speed variability over these domains. Rather, the goal is to show how the WRF model performs for a selection of typical weather patterns. Thus we refrain from a detailed discussion of weather classification and clustering, and its many pitfalls.

### 4.2.3 Validation

#### Validation against IMIS stations

The IMIS station network [Lehning et al., 1999, SLF, 2016] is a network of 198 weather stations around the Alps and Jura mountains. These stations are located in pairs with a wind station at a wind-exposed location and one or two snow station(s) at a wind-sheltered location, which is generally also at a lower elevation. All stations measure temperature, humidity and wind speed. Data are averaged over 30 minutes. Wind speed is measured at 6 m above the surface. Apart from the validation of our simulations at hub height against the turbines in the simulation domains, we compare our simulations against the IMIS stations in each of the domains. To account for boundary effects, we ignore stations that are within 10 km from the WRF domain border. Similarly, the first 10 hours of the WRF run are discarded as we consider

## **Chapter 4. Downscaling surface wind speeds over very complex terrain for wind potential identification**

---

the model needs some spin-up time to reach a physical valid state [Ulmer and Balss, 2016], which is especially important for higher resolution local models to initialize local small-scale effects [Siuta et al., 2017]. WRF simulation data are averaged to 30 minutes to allow proper comparison, and for each station we compare the data to the simulated output for the nearest grid cell. No horizontal interpolation was done. We did however interpolate between the nearest vertical model levels to find the appropriate wind speed, as it is known that the vertical profile in complex terrain is not exponential [Draxl and Mayr, 2011, Clifton et al., 2014], and changes with speed and direction [Cattin et al., 2003] depending as well on the presence of an upwind fetch [Cattin et al., 2002]. We analyze Root Mean Square Error (RMSE) and Mean Bias Error (MBE) when comparing against the IMIS stations.

### **Validation against wind turbines**

Similar to the IMIS stations, we compare the measured (hub height) wind speed to the wind speed in the nearest grid cell. We interpolate modeled wind speeds in the vertical direction to the turbine's hub height. RMSE, MBE and Mean Average Error (MAE) are then compared for various model set ups. As with the the IMIS comparison, we allow for a 10 hour spin-up time in the case of WRF.

#### **4.2.4 Comparison with COSMO-1 and COSMO-2**

The non-hydrostatic COSMO family of NWP models are widely used by research institutes and meteorological services, and are maintained by the consortium for small-scale modeling (COSMO) [Consortium for Small-scale Modeling, 2017]. We use the COSMO-2 model for the boundary conditions of our WRF simulations, similar to Gerber et al. [2018], who established this to be a very useful modeling chain for simulating precipitation and snow deposition in the complex terrain of the Alps. The COSMO-2 model has a horizontal resolution of approximately 2.2 km. Analysis model output was extracted from the supercomputer Piz Daint, and re-gridded to standard coordinates with the use of the COSMO toolbox Fieldextra [Bettems, 2017]. The fact that this is analysis data implies that it includes assimilated observations, amongst others from weather stations. The IMIS stations are however not used for data assimilation, and as such provide a useful tool for model validation. Since we do not use any data assimilation in our WRF simulations, the comparison is not completely fair, as WRF simulations are allowed to deviate from the initial observations in the boundary conditions, whereas both sets of COSMO data cannot. We compare our results to the COSMO-2 output to assess the improvement WRF can bring. We also compare our results against analysis data from the latest version of the COSMO model; COSMO-1. This version of the COSMO model has been operational at the Swiss national weather service since the end of 2015, and has a horizontal resolution of  $0.01^\circ$ , corresponding to 1.11 km N-S and 0.74 to 0.78 km E-S. Vertically, it features 80 levels with smooth level vertical (SLEVE) terrain following coordinates. The SLEVE scheme allows for smaller terrain features to decay faster than larger ones, thus reducing computational errors and allowing for a smooth transition to the upper



homogeneous levels [Schär et al., 2002, Leuenberger et al., 2010]. We use the 10 m wind speeds for verification against the measurement stations, and interpolate between model layers to find speeds at the turbine hub heights.

After the model set up has been validated, we assess to what extent the simulated wind resource is influenced by the increased model resolution. This is done by comparing the mean wind fields from the WRF simulations to those of the COSMO-2 model. The difference in horizontal mean wind speed between WRF and COSMO-2 is calculated, and projected onto the terrain using NCAR's VAPOR<sup>3</sup> visualization suite [Clyne et al., 2007]. This will show if the increase in resolution leads to better resolved wind fields, and how this depends on the topography. Using a very rudimentary power production model, the power production for these turbines is simulated, and compared against measured power output for the same periods. To this end, the power curves of the respective turbines are used to transform the hub height wind speeds to power output, which we correct for air density at the turbine's height analogous to [Kruyt et al., 2017], because power production strongly depends on air density [Wagenaar and Eecen, 2011].

### 4.3 Results and discussion

#### 4.3.1 Model performance and validation

##### Andermatt

Figure 4.2 shows the root-mean-square errors (RMSE) for the simulations at Andermatt. The boxplots display the spread in RMSE for the simulated near-surface wind speeds compared to the IMIS stations. In these box plots, the lower and upper hinges correspond to the first and third quartiles (the 25th and 75th percentiles). The first thing that catches the eye is the apparent performance of COSMO-2 in reproducing near-surface wind speeds. Separating the results for wind- and snow stations (Figure 4.3), the low near-surface RMSE scores from COSMO-2 appear to stem predominantly from the wind sheltered snow stations, where COSMO-2 RMSE is significantly lower than the other two models. If we look at the mean bias error (Figure 4.4 and Table 4.1), it becomes clear that COSMO-2 has a low bias, underestimating wind speeds. As a consequence COSMO-2 strongly underestimates wind speeds at windy locations, and is performs relatively well at sheltered locations. It is relevant to note here that the terrain characteristics that cause these snow stations to be sheltered from the wind have typical length scales that cannot be represented in the resolution of COSMO-2. Thus the -at first glance- impressive performance of COSMO-2 at these stations is more likely to stem from the overall low bias of the model. The combined RMSE for both wind and snow stations is therefore significantly lower than that of the other two models. Both COSMO-1 and WRF tend more to the opposite, i.e. overestimating wind speeds at sheltered locations, while showing relatively good agreement (little bias) at wind exposed stations. This shows the limitations

---

<sup>3</sup>[www.vapor.ucar.edu](http://www.vapor.ucar.edu)

## Chapter 4. Downscaling surface wind speeds over very complex terrain for wind potential identification

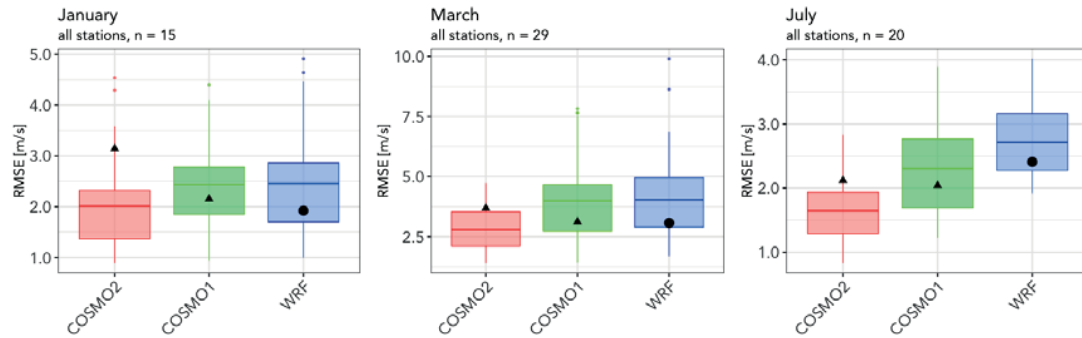


Figure 4.2 – Root Mean Square Errors (RMSE) of the WRF and COSMO models for the domain around Andermatt. Plots for the simulation periods in January 2016 (L) and March 2016 (C) and July (R). Validation against IMIS stations (boxplots) and turbine hub height (points). The line inside the box shows the mean.

of the applied metrics: the RMSE and MBE alone need careful interpretation to assess their values. In the context of wind speed development, one may argue that the model performance at wind exposed stations is more important than the performance at wind sheltered locations.

Nevertheless, there are additional factors that may contribute to the lower agreement of the WRF model with near-surface wind speed measurements. The first is the absence of a land surface parameterization scheme for the simulations in January and March. This was motivated by a desire to keep the model set-up as simple as possible while still being able to accurately reproduce hub height wind speeds. Secondly, the COSMO simulations displayed here are from analysis data, that uses assimilated ground measurements to reproduce the best possible state of the atmosphere. Our WRF simulations do not incorporate any data assimilation, nor nudging to force the model to stay true to observations or boundary conditions. Therefore the WRF model has more freedom to deviate from initial conditions.

The WRF model's performance with regards to simulating near-surface wind speeds is counterbalanced by a significantly better agreement in hub height wind speeds. The points in Figures 4.2 through 4.4 represent the model performance at the turbine's hub height. For the simulations in January and March the WRF model clearly outperforms both COSMO models, although the difference with COSMO-1 is small. (The simulation in July will be discussed separately below.) For both these runs, a clear improvement is visible with increasing model resolution, both in terms of RMSE (Figure 4.2) as well as MBE (Figure 4.4). At hub height, WRF has almost zero bias, and clearly lower RMSE.

For the simulations in January and March, Figure 4.5 shows both COSMO models clearly underestimating the peaks in wind speed. Seeing that this behavior is not present in the simulations for the domain around Chur at hub height (Figure 4.7, discussed in more detail in the section below), another explanation could be that the lack of an upwind fetch at the Andermatt turbine site is not accurately represented in the coarse COSMO-2 resolution, i.e. in the COSMO-2 model terrain is not as steep, leading to more drag and different wind shear.

### 4.3. Results and discussion

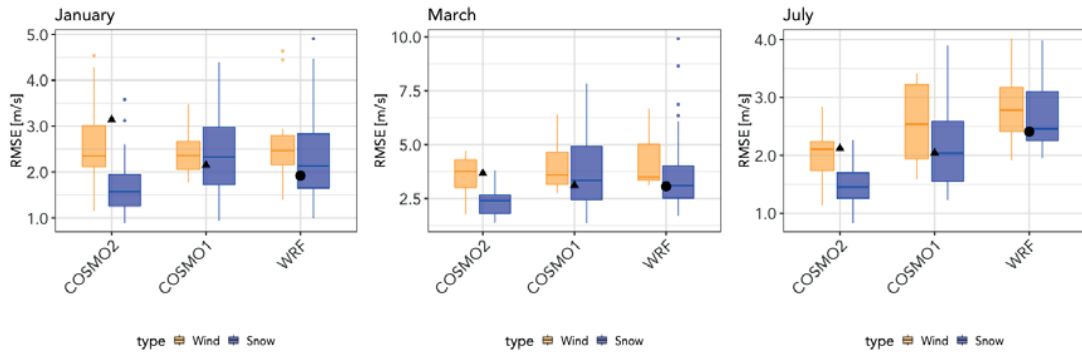


Figure 4.3 – Root Mean Square Errors (RMSE) of the WRF and COSMO models versus IMIS stations, for the domain around Andermatt. Separated boxes are shown for wind and snow stations, where the width represents the number of stations, and the line inside the box shows the median value. Plots for the simulation periods in January 2016 (L), March 2016 (C) and July 2106 (R).

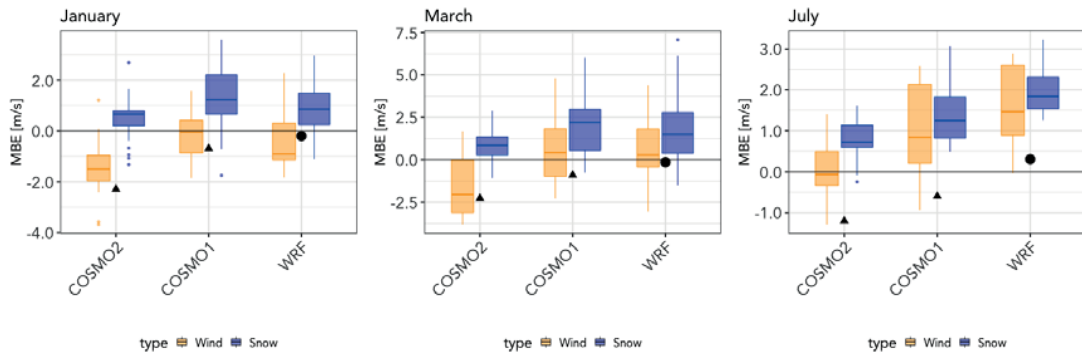


Figure 4.4 – Mean Bias Error (MBE) of the WRF and COSMO models at Andermatt, for the simulation periods in January 2016 (L) and March 2016 (C) and July 2016 (R). Validation against IMIS stations. Separate boxes are shown for wind exposed 'wind' stations and wind sheltered 'snow' stations. The width of the boxes represents the number of stations.

## Chapter 4. Downscaling surface wind speeds over very complex terrain for wind potential identification

---

A remark about the simulation for July should be made. The model run displayed for this time period is not the best available result for this period in terms of the statistical indicators presented here. Without a land surface scheme, model results for this period were actually better in terms of RMSE and MBE. However as this failed to reproduce the thermally induced flows during the afternoons of July 19th and 20, it was decided to include a run with a land surface physics scheme for this time period. This illustrates the shortcomings of the applied indicators for model performance. As useful as these statistical indicators may be, certain dynamics are better assessed from a visual comparison of the time series. Specifically for the model run in July, the bottom plot in Figure 4.5 shows that the WRF model does reproduce the thermal flows that occur during the second half of the first four days. In absence of a land-surface physics scheme, these flows could not be reproduced. However, with the current, arguably simple scheme, these thermal flows are overrepresented in WRF, which leads to excessive wind speeds. A possible explanation for this is the relatively basic surface physics scheme that was used. Little effort was spent on fine-tuning or comparing different surface physics parameterization schemes to produce accurate results. Similarly, an assessment of roughness length parameterization, especially in combination with a more sophisticated land-surface physics scheme, may improve results for these types of conditions.

### Chur

For the simulations of the domain around Chur, the RMSE are depicted in Figure 4.6. With regards to the near-surface wind speeds, a similar trend as for the domain around Andermatt can be observed with COSMO-2 having relatively low RMSE scores. Again this can partially be explained from the low bias that COSMO-2 has for near-surface speeds (see Table 4.2 ). At turbine hub height, a clear improvement is seen for models with increasing resolution (i.e. COSMO-2 to COSMO-1 to WRF), except for the simulation in January. Here, WRF is outperformed by COSMO-1. This is intriguing as the model set-up is the roughly same, indicating that the optimal settings may differ for various weather types. A finding in line with Siuta et al. [2017] and Fernández-González et al. [2017].

Where in the domain around Andermatt, the COSMO-2 model systematically underestimated wind speeds at hub height (Table 4.2 and Figure 4.5 ), in Chur this low bias at hub height has largely disappeared. In fact all three models tend to have a slightly positive bias for this model domain at hub height.

A very good representation of the thermal flows during the second half of the day is observed in the simulation in July (bottom figure in Figure 4.7). During the first four days, a distinct peak in wind speeds is observed, that is very well represented in the WRF model. From running the same simulation without the surface physics we know that these are thermally induced flows. While in the domain around Andermatt these thermal flows are overrepresented in the WRF simulation, in the domain around Chur this is not the case and the WRF model follows the hub height measurement quite accurately (bottom figure in Figure 4.7). In both simulations for the July period we can observe rather unstable behavior for the WRF model towards the

### 4.3. Results and discussion

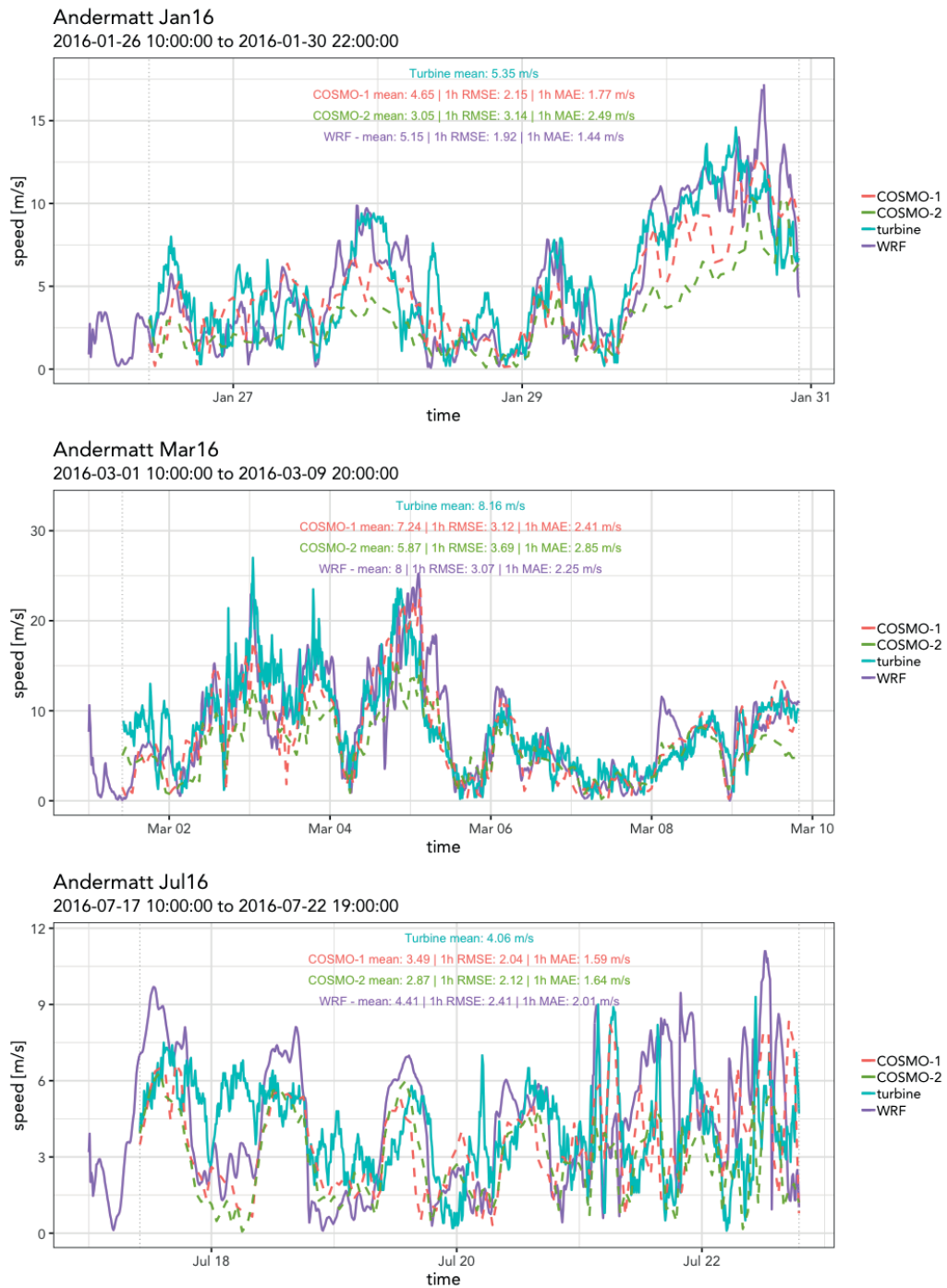


Figure 4.5 – Comparison of WRF runs at Andermatt. Simulated wind speeds for three periods of the year 2016

## Chapter 4. Downscaling surface wind speeds over very complex terrain for wind potential identification

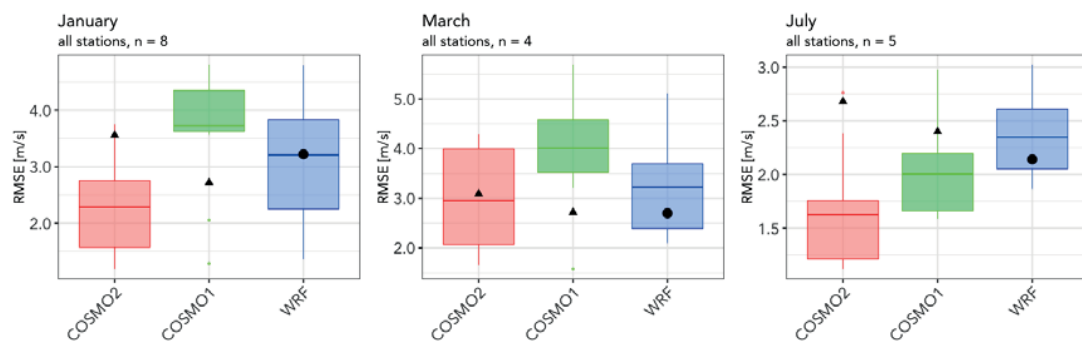


Figure 4.6 – Root Mean Square Errors (RMSE) of the WRF and COSMO models for the domain around Chur. Plots for the simulation periods in January 2016 (L) and March 2016 (C) and July 2016 (R). Validation against IMIS stations (boxplots) and turbine hub height (points).

end of the simulation period.

### 4.3. Results and discussion

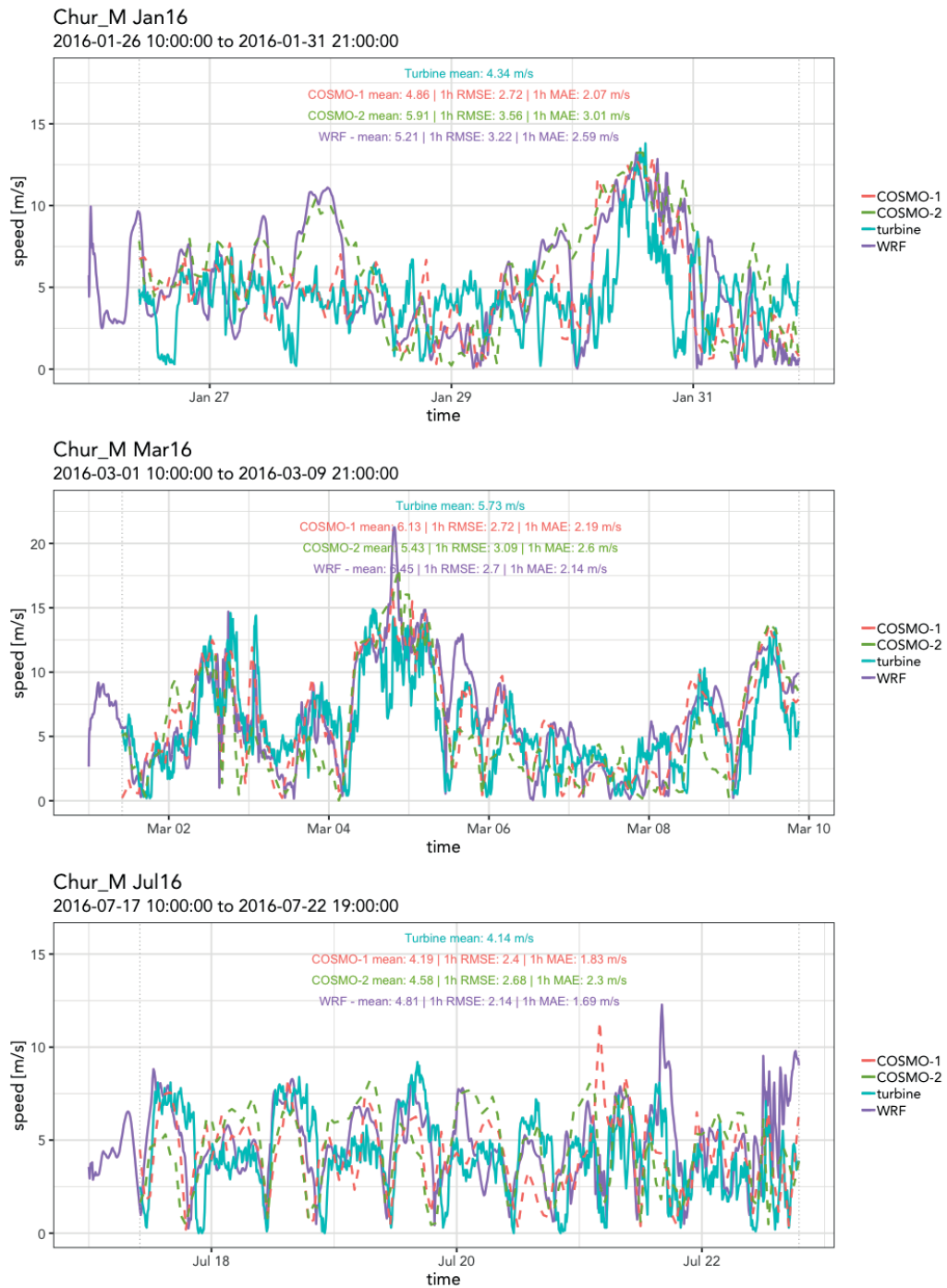


Figure 4.7 – Comparison of WRF runs at Chur.

## Chapter 4. Downscaling surface wind speeds over very complex terrain for wind potential identification

Table 4.1 – Model comparison for near-surface wind speeds: comparison to IMIS stations. Results per model run.

<i>domain</i>	<i>model</i>	<i>RMSE</i>	<i>RMSE_wind</i>	<i>RMSE_snow</i>	<i>MBE</i>	<i>MBE_wind</i>	<i>MBE_snow</i>
<b>Andermatt Jan16</b>	COSMO2	2.01	2.59	1.70	-0.22	-1.44	0.44
	COSMO1	2.44	2.40	2.46	0.80	-0.12	1.30
	WRF	2.45	2.61	2.37	0.38	-0.39	0.79
<b>Andermatt Mar16</b>	COSMO2	2.80	3.53	2.43	0.00	-1.55	0.78
	COSMO1	3.99	4.04	3.96	1.78	0.86	2.24
	WRF	4.03	4.33	3.88	1.47	0.78	1.81
<b>Andermatt Jul16</b>	COSMO2	1.65	2.00	1.46	0.52	0.05	0.77
	COSMO1	2.31	2.52	2.19	1.29	1.07	1.41
	WRF	2.71	2.83	2.65	1.89	1.63	2.02
<b>Chur Jan16</b>	COSMO2	2.29	3.05	1.96	-0.19	-1.98	0.58
	COSMO1	3.73	3.58	3.79	1.85	-0.14	2.71
	WRF	3.21	3.29	3.17	1.32	-0.62	2.15
<b>Chur Mar16</b>	COSMO2	2.96	3.38	2.78	0.28	-1.22	0.92
	COSMO1	4.01	3.83	4.09	1.96	0.08	2.76
	WRF	3.22	3.21	3.23	1.18	0.00	1.69
<b>Chur Jul16</b>	COSMO2	1.63	2.18	1.39	0.02	-1.00	0.46
	COSMO1	2.00	2.21	1.92	0.72	-0.52	1.25
	WRF	2.35	2.33	2.35	1.37	0.31	1.82



Table 4.2 – Model comparison for hub-height wind speeds: Results per model run.

<i>domain</i>	<i>model</i>	<i>RMSE</i>	<i>MBE</i>	<i>MAE</i>
<b>Andermatt Jan16</b>	COSMO2	3.14	-2.289	2.49
	COSMO1	2.15	-0.687	1.77
	WRF	1.92	-0.196	1.44
<b>Andermatt Mar16</b>	COSMO2	3.68	-2.271	2.84
	COSMO1	3.12	-0.897	2.42
	WRF	3.07	-0.146	2.26
<b>Andermatt Jul16</b>	COSMO2	2.12	-1.200	1.64
	COSMO1	2.04	-0.598	1.59
	WRF	2.41	0.306	2.01
<b>Chur Jan16</b>	COSMO2	3.56	1.567	3.01
	COSMO1	2.72	0.511	2.07
	WRF	3.22	0.863	2.59
<b>Chur Mar16</b>	COSMO2	3.09	-0.335	2.59
	COSMO1	2.72	0.383	2.19
	WRF	2.68	0.693	2.12
<b>Chur Jul16</b>	COSMO2	2.68	0.4437	2.30
	COSMO1	2.40	0.0502	1.83
	WRF	2.14	0.6714	1.69

## Chapter 4. Downscaling surface wind speeds over very complex terrain for wind potential identification

---

### 4.3.2 Potential indication

From the above it is clear that the increase in resolution has a positive effect on the simulated wind speeds at hub height. Terrain and therefore terrain induced flows are better resolved, which becomes clear from looking at Figure 4.8, showing the effect of the increased resolution on the wind speed simulations. To further explore the effect that the increase in resolution has, we average the COSMO-2 and WRF wind fields over the simulated period, and calculate the difference between the WRF and COSMO-2 mean speeds for each grid point. To this end the COSMO-2 mean speeds are remapped onto the WRF grid, after which a gridded difference is calculated. This difference is then plotted on the terrain using NCAR's VAPOR software suite.

Figure 4.9 shows this difference in time-averaged speeds for the Andermatt domain for the simulations in January and March 2016. The differences in mean speeds at model levels closest to 100 m above the surface are shown. It is instantly clear that wind speeds are not uniformly higher over the whole domain, but that terrain plays a decisive role with regards to the magnitude and sign of the difference. But equally important, for different simulation periods, the main differences in mean speeds vary, underlining the fact that it is imperative to account for different weather patterns and periods. A more systematic comparison of these results is presented in Figure 4.10, which shows histogram of the difference in mean speeds between WRF and COSMO-2. For both domains, we can see relatively similar behavior. The simulations in July show a sharp, narrow peak, with a positive mean, indicating that WRF mean speeds are only slightly higher, but for almost all pixels. The simulations in March show distinctly more spread, and means around zero, although slight positive skew can be observed in the Andermatt domain.

### 4.3.3 Power production

In an attempt to illustrate the effects on power production, we simulate the production from the wind turbines in the two domains based on COSMO-2 and WRF wind speeds. Table 4.3 shows the relative difference with actual power output for both models. The effect of higher speeds from the WRF model is exaggerated by the non-linear behavior of the power curve. Especially for the domain around Andermatt, we see significant improvements from WRF, apart from the simulation in July, which -as explained before in section 4.3.1 - overestimates thermally induced flows. This leads to a significant overestimation of power production. At Chur, both models overestimate power production for all simulated periods, although the degree to which differs per model run. As the simulations are idealized cases, and no influence of turbulence, shear or conversion losses on the turbine is accounted for, a slight overestimation is to be expected. With that in mind the WRF model seems to be better capable at estimating realistic power output, especially in the very complex terrain of the Andermatt domain.

### 4.3. Results and discussion

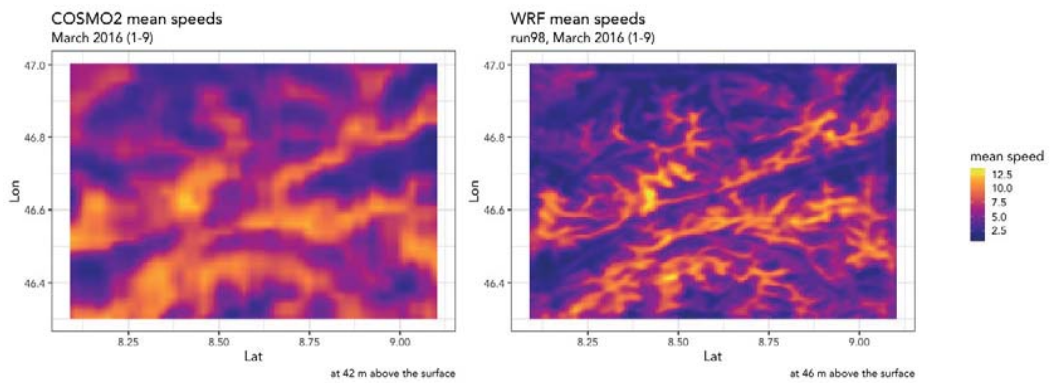


Figure 4.8 – Comparison of COSMO-2 and WRF wind speeds for the domain around Andermatt, for the simulation in March 2016.

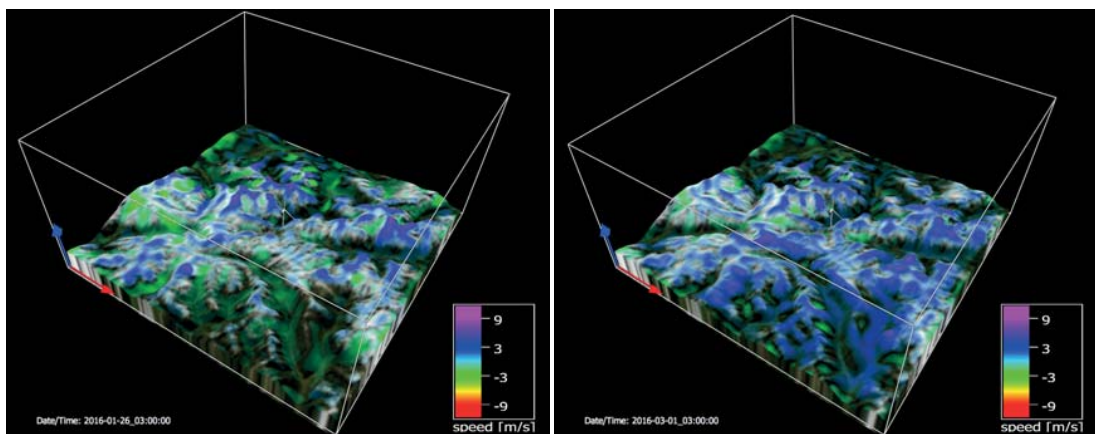


Figure 4.9 – Difference between WRF and COSMO2 mean wind speeds for the domain around Andermatt at approximately 100 m above the surface, for the model runs in January (L) and March (R). Positive differences indicate that WRF mean speeds are higher. For differences close to zero, the color has been made almost totally opaque, to aid visibility.

## Chapter 4. Downscaling surface wind speeds over very complex terrain for wind potential identification

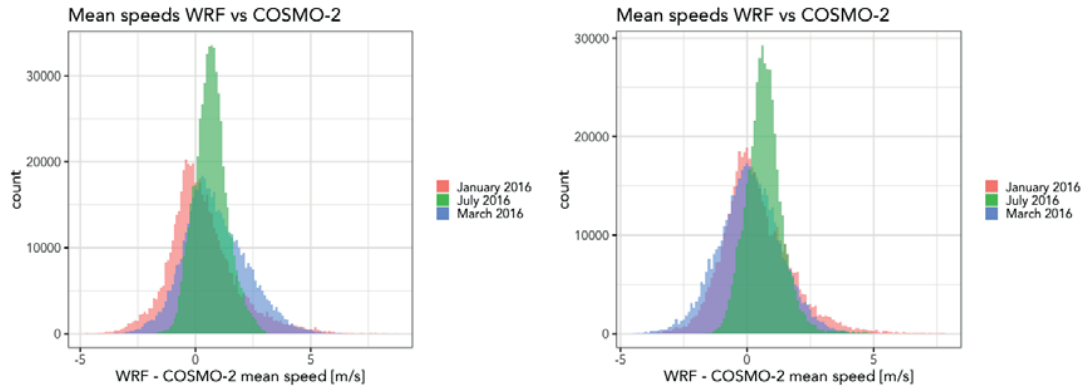


Figure 4.10 – Frequency distributions of the differences between WRF and COSMO2 mean wind speeds for the domain around Andermatt (L) and Chur (R) at 100 m above the surface, (Positive differences indicate that WRF mean speeds are higher).

Table 4.3 – Simulated power production as deviation from actual wind turbine production

domain	model	power (%)
<b>Andermatt Jan16</b>	COSMO2	-80
	WRF	-15
<b>Andermatt Mar16</b>	COSMO2	-29
	WRF	22
<b>Andermatt Jul16</b>	COSMO2	-57
	WRF	71
<b>Chur Jan16</b>	COSMO2	217
	WRF	156
<b>Chur Mar16</b>	COSMO2	13
	WRF	44
<b>Chur Jul16</b>	COSMO2	35
	WRF	45

## 4.4 Conclusions

In this work we have investigated wind flow representation in complex terrain. By deploying models with increasing resolutions, we have attempted to improve our insights into the role that terrain representation plays in simulating wind speeds over terrain of varying complexity. For two domains in the Swiss Alps with varying degrees of terrain complexity, simulations with the WRF 4.0 model at a horizontal resolution of 450 m were compared to analysis data from the COSMO-1 and the COSMO-2 models, with respective horizontal resolutions of 1.1 km and 2.2 km. The latter model also supplies the boundary conditions to the WRF simulations, thus offering a good measure of improvement from downscaling. We compared simulations of all three models to measurements from both wind turbines as well as meteorological stations closer to the ground. We were able to show that in most cases, WRF outperforms both COSMO models in reproducing wind speeds at turbine hub heights. This can be attributed to the higher resolution of the WRF model, which allows topographical features to be better represented, which in turn has an effect on the flows that are heavily influenced by the terrain. This is in agreement with Siuta et al. [2017], who conclude that terrain-flow interactions are most influenced by horizontal resolution. RMSE are lower for all but two simulations, where in one case WRF is outperformed by COSMO-1 (Chur January) and in the other case by both COSMO models (Andermatt July). In the latter case this appears to be related to inaccurate land surface physics interactions, where an inclusion of a land-surface model leads to an over-representation of thermal flows. Apart from the statistical indicators discussed here, visual comparison of the time series in 4.5 and 4.7 shows that the WRF model follows the observations better than either of the COSMO models.

By comparing the modeled speeds to meteorological measurement stations, the models' abilities in reproducing near-surface winds has also been assessed. Based purely on the statistical indicators presented here, it appears that the WRF model is not able to improve upon the COSMO-2 model. Average root mean square errors are higher for WRF than for either of the COSMO models. At wind exposed locations however, the difference is smaller. COSMO-2 has a low bias that leads to an underrepresentation of wind speeds at wind exposed stations and unrealistic low errors at wind sheltered stations. Because the horizontal resolution of the COSMO-2 model is too low to reproduce the terrain characteristics that lead to the wind sheltered stations being sheltered, the high agreement that the COSMO-2 model shows with measurements can only be explained from the overall negative bias the model has. WRF on the other hand, has a much smaller bias for wind exposed locations, whereas it overestimates wind speeds at sheltered stations, as does COSMO-1. Since the wind stations are -by definition- more likely to be exposed to the terrain induced flows that we are interested in, the model performance at these stations can be considered more important than the performance at the sheltered snow stations. For wind resource assessment purposes the main points of interest are exactly those wind exposed locations, and the performance at those stations can be said to be of higher importance than the accurate representation at wind sheltered locations. However, near-surface wind measurements are argued to be too heavily influenced by land-surface

## Chapter 4. Downscaling surface wind speeds over very complex terrain for wind potential identification

---

interactions to form a trustworthy source for model validation, especially in the context of wind energy applications [Draxl et al., 2014]. Given their abundant availability relative to hub height measurements, it is nevertheless understandable that they are extensively used. Our results can be interpreted to confirm these claims, as the models performing better at reproducing near-surface measurements typically perform worst at hub height and vice-versa.

Having asserted that WRF provides the most accurate representation of wind speeds at typical hub heights, we calculated the difference in mean wind speeds compared to the lower resolution COSMO-2 model. We showed that terrain is a determining factor, because mean wind speeds are not higher at all grid points, but rather, the variability appears highly terrain dependent (see e.g. Figure 4.9). Furthermore, the difference between high resolution and low resolution simulation of wind speeds not only depends on the topography, but shows significant variability for different periods of the year with different weather patterns. This is in line with other studies that show varying accuracy in WRF's ability to reproduce wind speeds depending on atmospheric stability and PBL parameterization. Lastly, a simplified power production calculation showed that especially in the highly complex terrain around Andermatt, power estimated based on the WRF model are in better agreement with the operational data from the turbine than estimates based on COSMO-2.

### 4.5 Outlook

The coupled COSMO-WRF model chain is a promising instrument for wind resource assessment given its ability to represent flows in complex terrain. There are however certain simplifications that have been made in this assessment that could be addressed to improve future resource assessments. We have not included the possible effects that turbulence and stability may have on the wind power output. Both turbulence intensity and atmospheric stability have been shown to affect the power production differently for different regimes of a turbine's power curve [St. Martin et al., 2016]. Our power model is a very simple one, used only for illustrative purposes. Proper inclusion of turbulence and stability effects would surely improve it, but will require more data for model validation. We have only considered wind speeds at hub height, whereas especially for large turbines such as the one at Chur, the wind shear across the rotor span is relevant for mechanical wear on the axle. As such it may limit the potential locations, or turbine size.

Siuta et al. [2017], based on literature research, note that none of the PBL physics parameterization schemes available in WRF have been derived from data taken over complex terrain, but rather, have all been based on field data over flat terrain, with a heavy focus on improving precipitation forecasts. An obvious improvement of WRF for complex terrain would therefore be to development of complex terrain-specific PBL schemes. On that same topic, we are excited about the promises that immersed boundary methods (IBM) bring. For the terrain under study in this work, these method(s) could provide significant improvements in numerical stability and accuracy. In the current work terrain smoothing arguably distorts the terrain steepness, such that very local phenomena cannot be accurately represented. IBM may offer

significant improvements in steep terrain and its developments should therefore be closely monitored.

Simulating extended periods of time for reliable resource assessment is computationally taxing with the current set up. A possible work-around would be to apply clustering algorithms and divide the weather over the Alps in representative patterns. Then, given likelihoods of these patterns, simulations of typical forcings could be recombined to an accurate description of the wind resource. However, pitfalls loom with such approaches. Care should be taken to include all possible (and relevant) weather patterns for wind power production. Dividing the weather based solely on synoptic pressure gradients may miss valuable local effects. And given the importance of seasonal and diurnal patterns for the electricity supply of the country Dujardin et al. [2017], Kruyt et al. [2018], representing the wind resource solely as an annual mean does not provide sufficient information from an power optimization perspective.





# 5 Conclusions

## 5.1 Conclusions

With the impending changes to the Swiss electricity supply, the wind potential of the country is an urgent topic. Although current studies have yielded fairly accurate assessments of the resources in the lower regions of the country, the potential from the complex terrain of the Alps remains largely unclear. Switzerland has an excellent network of meteorological measuring stations, that has been explored in the second chapter of this thesis to shed light on some dynamics of wind patterns in the Alps. However, for resource assessment, it is not sufficient to only rely on point measurements. Not only is the spatial coverage too low, but vertical extrapolation is challenging as current methods break down in complex terrain. The commonly used log law is known to be invalid in absence of long upwind fetches, something that is encountered often in the complex terrain of the Alps. This has not stopped many potential studies from using it, mainly for lack of a better alternative.

Atmospheric models may offer a solution to some of these shortcomings, but come at large computational demands, making it challenging to run them at high spatial resolutions for extended periods of time. And even the most complex model will still be a simplified version of reality, with its many parameterizations and discretization, and unavoidable errors. These models need to be validated against observations if we are to place any trust in them. It seems that the best way to tackle questions such as those presented in this thesis is therefore to make use of both measurements and models to come to the most robust findings. Which is why in this thesis, various measurement networks and several NWP models have been applied to to further the insights into the dynamics of the wind resource in terrain of high complexity. Although the focus of this thesis has been the Swiss Alps, there is no reason why the methods and findings would not be applicable to other areas with similarly complex terrain.

**The dynamics of the Swiss wind resource** were investigated using point-measurements from the country-wide SwissMetNet (SMN) and mountain-centered IMIS meteorological measurement networks. Pair-wise spatial correlations were investigated, and found to have very little relation to distance, whereas studies focusing on larger scales found exponentially decaying

correlations with distance. This absence of a strong relation to distance can be attributed to the influence of the topography, which is responsible for decoupling the local flow from the synoptic one. This is an important finding, for it implies that the smoothing of the overall wind power output that has thus far been shown possible only on large spatial scales, can be achieved on a much smaller scale in complex terrain such as that in the Alps. It implies that large fluctuations in wind power output for high shares wind power in the grid can potentially be avoided, if such considerations are taken into account in the planning of wind power locations. Further integrated grid and wind-resource modeling and economical analysis should be conducted to investigate if trade-offs in this regard are worthwhile, i.e. if increased smoothness of the cumulative wind power output signal can be achieved with minimal reduction in cumulative production. The optimal combination of PV and wind power is also important to consider here, as they are able to partially balance each other in the Swiss context [Dujardin et al., 2017].

An assessment of the likelihood of long durations with wind speeds below turbine cut-in speeds was conducted using extreme value statistics. Here, the results showed great disparity, while no distinct spatial pattern could be distilled that could account for the spread in outcomes, other than a relation to the elevation of the stations. With increasing altitude, the return levels for no-power production decreased, indicating more stable wind power production at higher elevations. The influence of the topography on the wind patterns was further exemplified by analyzing seasonal and diurnal wind speed patterns for a selection of stations with very different topographies. The major differences could be explained by the topography, thereby strengthening the notion that the terrain is the dominant influence on wind flows at the local scale. The notion that wind speeds are generally higher in winter in northern Europe was confirmed for Switzerland, and it was shown that the relative increase in wind speed in winter with regards to summer increases with elevation. This elevation dependence of both the likelihood of sustained low wind periods, as well as increased winter wind speeds can be considered the second important conclusion of this chapter, and warrants further research into high alpine wind power. Since it is however apparent that station based analysis alone cannot cover the wide variability of topography and wind flow encountered in steep Alpine terrain, in the following chapter, the focus was shifted towards numerical modeling.

**Wind power assessment in complex terrain using a Numerical Weather Prediction (NWP) model** was investigated in chapter 3. As discussed in chapter 1, linearized and statistical assessment methods have methodological shortcomings in complex terrain. This formed the motivation to use a model that accounts for the dominant features in terrain induced flows by simulating the underlying physics. Analysis data from the latest generation of the COSMO models, COSMO-1, was the source of hourly wind speed data. Validation of the model's performance against 177 meteorological stations showed mean RMSE to be 2.87 m/s, mean MBE 0.03 m/s and mean correlation 0.51. For the wind-sheltered stations, model performance is slightly worse. However, when comparing the errors in mean annual wind speeds to those of the Swiss wind atlas, an improvement of 45% (0.83 m/s compared to 1.5 m/s) is achieved for mountainous terrain. This is significant, and a slightly higher improvement than that

reported by Oppliger et al. [2016] using a hybrid CFD/statistical method for a small part of Switzerland. Furthermore, the fact that this error is based on a large number of stations (177) makes it statistically relevant, especially when compared to the wind atlas. The first major conclusion from this chapter is therefore that a numerical weather prediction model with reasonable high resolution is able to produce better wind resource estimates for complex mountainous terrain than previous attempts with hybrid statistical/CFD methods. It thus appears justified to investigate the Swiss wind power potential based on these simulated wind speeds. When combined with a rudimentary wind turbine model to calculate power production, capacity factors up to 0.42 are found. In comparison to average capacity factors for Europe, reported to be 0.24 for onshore and 0.37 to 0.41 for offshore wind farms [European Wind Energy Association, 2013, Wind Europe, 2017], these numbers are quite promising.

Next, simulated power time series are combined with a model of the Swiss electricity system to assess what high wind penetration may imply for crucial power system parameters, and how the location of wind turbines has an effect on this. This model-based scenario analysis assumes a fully renewable Swiss power supply that is self-sufficient at an annual basis. As explained in Chapter 1, owing to the seasonal production profile of hydropower, it is not possible for Switzerland to be fully (i.e. on an (sub-) hourly basis) self-sufficient without excess production (i.e becoming a net exporter) or fossil power. One way of assessing the effectiveness of this annual self-sufficiency is by looking at the annual electricity imports that are required to balance the system. Investigating annual wind power targets of 4,6, and 12 TWh it is shown that required imports can range from 6 TWh/a to 13.3 TWh/a, but most crucially, are lower for high wind power scenarios, confirming the findings in [Dujardin et al., 2017].

Since the work in Chapter 2 revealed that elevation is a crucial parameter in the wind resource across the country, a logical question is if this can be exploited to benefit an efficient wind power supply. To this end the same model chain was used with various wind power targets. Because the notion of wind power potential is highly subjective and context dependent, as is explained in Chapter 1, for this analysis the reasoning is reversed, and we instead asked the question what would be required to produce a certain amount of electricity with wind power. By allowing turbines to be located in different elevation ranges, and subsequently picking those allowed locations with the highest capacity factors until the annual production target is met, it could be shown that significantly fewer turbines are required to produce the same amount of wind power when they are allowed to be located at high elevations, than when the turbines are restricted to lower elevations. This is a highly relevant finding in the context of the impending Swiss energy transition, for it shows that for a cost-efficient, and arguably socially acceptable energy transition, wind power development at high elevations could, and should play an important role.

**High resolution simulations of wind flows over very complex terrain** were conducted in Chapter 4. While the work in the previous chapter yielded positive results, a lingering question remained if the potential from complex terrain could still be underrepresented by the relatively coarse resolution of the applied model. To investigate if increases in model resolution lead

to better wind resource estimates, simulations at 450 m resolution were conducted for two domains in the Alps. The latest version of the Weather Research and Forecasting model was used to downscale boundary conditions provided by COSMO-2, and results were compared to wind turbine hub height measurements, as well as near-surface measurements from weather stations. Because of the computational demands associated with these resolutions, 3 distinct periods in 2016 were simulated, each approximately one week in duration. For both domains significant improvements in simulated wind speeds at hub height were achieved for the majority of the simulated periods, in comparison to analysis data from both the COSMO-2 as well as the higher resolution COSMO-1 model. This can be attributed to the better resolved terrain. For the simulation that did not show significant improvements, the insufficiently explored parameterization of the land surface physics could explain the performance. While an attempt was made to find one model set-up that performs well for all periods and domains, one of the conclusions of this work is that different weather patterns and flow regimes require different parameterizations to yield the best results, a finding that is in line with other studies on PBL parameterization for the WRF model [Siuta et al., 2017, Fernández-González et al., 2017, Draxl et al., 2014].

A comparison of near-surface wind speed simulations with measurements from weather stations in the domain showed significantly poorer results for the WRF model when compared to those from COSMO-2. This can be explained by the partial absence of the parameterization of land-surface interactions in our WRF set-up. However, it is more likely that near-surface measurements do not provide the best validation set for hub height wind speeds, as has been suggested by Draxl et al. [2014].

Finally in this chapter, it was investigated what increased spatial resolution implies for the wind resource. The main findings from this comparison are that the increased resolution shows higher wind speeds, but not only due to slight differences in near-surface bias. Rather, the increases in mean speeds are highly terrain dependent, and moreover, are not similar under all weather patterns. This conclusion is important for wind resource assessment, for it implies that when using a small sample of observed weather to assess long-term characteristics, care should be taken that all possible patterns are accurately presented. It furthermore implies that high resolutions that capture the terrain variability are required in the assessment of wind resources in terrain as complex as the Alps.

Summarizing the main findings in this thesis, it can be concluded that the wind resource in the Swiss Alps has several characteristics that are favorable for wind power development, such as the low correlations in wind speeds between nearby locations and the increase in potential with elevation. It was shown that exploiting this relation to elevation can significantly reduce the capacity that is required to produce large amounts of wind power. Lastly, more precise assessments of the wind resource in the very complex terrain of the Alps are possible when deploying NWP models with high resolution, as these are able to produce thermal speed up effects and better resolve the topography that influences the flow patterns. From the results here it appears that the potential in such complex terrain could be higher than thus

far assumed based on lower resolution models. However the optimal parameterization of the high resolution model has shown to be dependent on weather and terrain, and thus an accurate assessment based on a highly resolved model such as WRF requires careful weather type assessment and parameterization to acquire accurate and representative results.

## 5.2 Outlook

Although this thesis has yielded many interesting conclusions, as with any scientific endeavor, many new questions have appeared. It was shown that the correlation between wind speeds over distance is significantly lower in Switzerland compared to other studies. The implication that it is possible to smooth the overall wind power output does however not mean that this is an economically optimal strategy. Firstly, optimizing the wind power output with regards to the variability in the combined output would require coordinated nation-wide planning, something that is unlikely in today's liberalized electricity markets. The important question is if exploiting the temporal and spatial anti-correlations between potential wind farm locations will not yield significant trade offs in cumulative output. And if so, who will provide the economic incentive to overcome such losses. This depends on many factors, amongst which the relative pricing of future electricity sources, as well as their intra-day and seasonal variability. Answering such questions will require a holistic modeling approach of the European electricity market combined with detailed wind power modeling for Switzerland. Given the proposed transformation of the Swiss electricity system, this is a worthwhile undertaking. Care should however be taken to ensure that the uncertainties introduced in the various steps of such a complex modeling exercise do not outweigh the significance of the final results

This thesis has also provided compelling arguments in favor of wind power at high elevations. Deliberately, no attention has been paid to the logistical and technical aspects of developing wind power at remote and challenging locations. Logistical limitations relate to the access and infrastructure required to erect wind turbines and associated transmission capacity. For certain sites with favorable wind conditions the logistical challenges and thus, the associated cost may be very high, making such projects unattractive from an economical perspective. The next modeling steps towards realistic scenarios for high Alpine wind power development should therefore include an assessment of infrastructural constraints. For instance, relating areas with high capacity factors from Chapter 2 to the existing distribution grid, as well as access roads seems a step forward. Similarly, an assessment of the additional costs of wind power development at rugged locations compared to the costs at more conventional locations may be informative. The disadvantage here, and the very reason such factors have not been included in this work, is the fact that such economical parameters can change rapidly, as a function of market- and learning effects.

With regards to the accurate assessment of wind resources in complex terrain, it is clear that many opportunities for improvement exist. Although developments in computational power

## Chapter 5. Conclusions

---

are happening fast, the possibility of quickly simulating the atmosphere with a NWP model over a country the size of Switzerland for several years at resolutions in the order of hundreds of meters is still out of reach. Until then, several options exist that may be able to improve upon the results presented here. One option that has been touched upon in Chapter 4 is to simulate a limited amount of typical weather patterns, and relate those to long standing weather statistics in order to assess the wind resource taking into account intra-annual variability.

Increasing the horizontal resolution of simulations in very complex terrain is another step that should be taken. Although the scales presented here are a step forward, properly resolving the influential topographic features will likely yield even more accurate results. This will imply resolving at least part of the turbulence explicitly. During this work, experiments with LES modeling have been conducted but yielded unsatisfactory results. Gerber et al. [2018] also found very high wind speeds using a COSMO-WRF coupling down to LES scales. Clearly there is room for improvement here. The development of boundary layer parameterizations specifically for complex terrain may also offer much needed improvements, as it is shown to be of major influence to the simulated wind speed, yet the currently available, flat-terrain based schemes have been shown to be unsatisfactory for complex terrain has been found [Siuta et al., 2017, Fernández-González et al., 2017, Draxl et al., 2014]. Lastly, the advances in Immersed Boundary Methods (IBM) for NWP's should be closely monitored, for these methods have the potential to bring vast improvements to the modeling in complex terrain. Current terrain-following coordinates require the terrain to be smoothed in order to keep the model numerically stable. IBM is not held to this limitation, thereby opening the door to more realistic representations of very steep terrain and its effects of wind patterns.

It is often claimed that the acceptance of wind power in Switzerland is too low for large shares of wind power to be incorporated into the electricity supply. Apart from the question whether such claims hold any truth, rejecting lines of inquiry based on speculations seems like a flawed approach to scientific problems. Public opinion is a transient thing, and it could well be that in a few years time, as the severity of the changing climate is more broadly realized in society, public opinion and political willingness will shift drastically. And even if that is not to happen, at least the debate should be held based on facts, not assumptions. Hopefully this work is able to make a small contribution to a well-informed and fact-based debate on the future of the Swiss electricity system.

## A Air density and altitude

With increasing altitude, air density decreases and as such, the momentum that can be extracted from the air by a turbine is lower. The energy produced at similar wind speeds is therefore lower at altitude, and for a country such as Switzerland, this could be significant. To investigate this effect on power production, we calculate a correction factor to account for the differences in air density at a certain altitude.

The power that can be extracted from the wind is given by

$$P = \frac{1}{2} \rho A v^3 \quad (\text{A.1})$$

where  $\rho$  is the air density,  $A$  is the rotor swept area, and  $v$  the wind speed. The air density  $\rho$  in its turn is a function of pressure  $p$ , Temperature  $T$  (and humidity):

$$\rho = \frac{pM}{RT} \quad (\text{A.2})$$

with  $M$  the molar mass and  $R$  the ideal gas constant. Both pressure and temperature can be expressed as a function of altitude  $h$  NASA [1976]

$$p = p_0 \left(1 - \frac{Lh}{T_0}\right)^{\frac{gM}{RL}} \quad (\text{A.3})$$

$$T = T_0 - Lh \quad (\text{A.4})$$

where  $p_0, T_0$  are the pressure and temperature at sea level, respectively;  $L$  is an average

## Appendix A. Air density and altitude

---

constant representing the temperature lapse rate ( 0.0065 K/m), and  $g$ , the gravitational constant (9.80665  $m/s^2$ ). Combining A.5, A.3 and A.4 we obtain an approximate correction factor for the power production at altitude  $h$  compared to sea level:

$$\frac{\rho(h)}{\rho_0} = \left(1 - \frac{Lh}{T_0}\right)^{\frac{gM}{RL} - 1} \quad (\text{A.5})$$

As temperature varies during the course of the day, the air density is not constant Rehman and Al-Abbadi [2005]. However, here we neglect diurnal fluctuations in air density.



## **A** WRF Namelist

```

&time_control
run_days           = 3,
run_hours          = 12,
run_minutes        = 0,
run_seconds        = 0,
start_year         = 2016, 2015, 2015, 2015,
start_month        = 03, 10, 10, 10,
start_day          = 01, 01, 02, 02,
start_hour         = 00, 00, 03, 03,
start_minute       = 00, 00, 00, 00,
start_second       = 00, 00, 00, 00,
end_year           = 2016, 2015, 2015, 2015,
end_month          = 03, 10, 10, 10,
end_day            = 09, 05, 05, 05,
end_hour           = 23, 23, 23, 23,
end_minute         = 00, 00, 00, 00,
end_second         = 00, 00, 00, 00,
interval_seconds   = 3600,
input_from_file    = .true., .true., .true., .true.,
fine_input_stream  = 0, 2, 2, 2,
history_interval   = 3, 5, 2, 2,
frames_per_outfile = 20, 12, 30, 30,
restart            = .false.,
restart_interval   = 60,
io_form_history    = 2,
io_form_restart    = 2,
io_form_input      = 2,
io_form_boundary   = 2,
io_form_auxinput2  = 2,
debug_level        = 0,
/

```

```

&domains
time_step          = 0,
time_step_fract_num = 1,
time_step_fract_den = 5,
use_adaptive_time_step = .false.,
step_to_output_time = .true.,
target_cfl         = 0.5,
target_hcfl        = 0.5,
starting_time_step = -1,
max_time_step      = 5,
min_time_step      = 1,
min_time_step_den  = 3,
adaptation_domain  = 1,
max_dom            = 1,
!s_we              = 1, 1,
e_we               = 124, 241, 451, 451,
!s_sn              = 1, 1,
e_sn               = 199, 316, 451, 451,
!s_vert            = 1, 1,
e_vert             = 80, 40, 60, 80, 80,
vert_refine_method = 0,0,0,0,2,2,

```

```

max_dz                = 1200.,      ! maximum level
thickness allowed (m)
  auto_levels_opt     = 2,          ! new default (also set
dzstretch_s, dzstretch_u, dzbot, max_dz)
  dzbot               = 10,        ! thickness of lowest
layer (m) for auto_levels_opt=2
  dzstretch_s         = 1.1,      ! surface stretch factor
for auto_levels_opt=2
  dzstretch_u         = 1.3,      ! upper stretch factor
for auto_levels_opt=2

```

```

p_top_requested       = 15000,
num_metgrid_levels   = 39,
num_metgrid_soil_levels = 6,
dx                   = 450, 150, 50, 50,
dy                   = 450, 150, 50, 50,
grid_id              = 1, 2, 3, 4,
parent_id            = 1, 1, 2, 2,
i_parent_start       = 1, 80, 100, 350,
j_parent_start       = 1, 105, 270, 160,
parent_grid_ratio    = 1, 3, 3, 3,
parent_time_step_ratio = 1, 3, 3, 3,
feedback             = 1,
smooth_option        = 1,
sfcp_to_sfcp        = .true.,

```

/

```

&physics
mp_physics           = 0, 0, 0, 0,
ra_lw_physics        = 1, 1, 0, 0,
ra_sw_physics        = 1, 1, 0, 0,
slope_rad            = 1, 1, 0, 0,
topo_shading         = 1, 1, 0, 0,
radt                 = 5, 5, 5, 5,
sf_sfclay_physics    = 1, 1, 1, 2,
sf_surface_physics   = 0, 0, 0, 0,
bl_pbl_physics       = 1, 0, 0, 0,
bldt                 = 0, 0, 0, 0,
cu_physics           = 0, 0, 0, 0,
cudt                 = 0, 0, 0, 0,
isfflx               = 0,
ifsnow               = 1,
icloud               = 1,
surface_input_source = 1,
num_soil_layers       = 4,
num_land_cat         = 24,
sf_urban_physics     = 0, 0, 0, 0,
topo_wind            = 1,

```

/

```

&fdda

```

```

/

&dynamics
rk_ord           = 3,
diff_opt         = 2,
km_opt           = 2,
diff_6th_opt     = 2, 0, 0, 0,
diff_6th_factor  = 0.12
damp_opt         = 3,
zdamp            = 5000., 5000., 5000., 5000.,
dampcoef         = 0.2, 0.2, 0.2, 0.2,
w_damping        = 0,
khdif            = 0, 0, 0, 0,
kvdif            = 0, 0, 0, 0,
non_hydrostatic = .true., .true., .true., .true.,
moist_adv_opt    = 1, 1, 1, 1,
scalar_adv_opt   = 1, 1, 1, 1,
epssm            = 1, 1, 5., 5.,
mix_isotropic    = 1,
/

&bdy_control
!open_xs         = .true.,
!open_xe         = .true.,
!open_ys         = .true.,
!open_ye         = .true.,
!periodic_x      = .true.,
!periodic_y      = .true.,
specified        = .true., .false., .false., .false.,
spec_bdy_width   = 5,
spec_zone        = 1,
relax_zone       = 4,
nested           = .false., .true., .true., .true.,
/

&grib2
/

&namelist_quilt
nio_tasks_per_group = 0,
nio_groups           = 1,
/

```

# Bibliography

Reza Abhari, Göran Andersson, Silvia Banfi, Bruno Bébié, Konstantinos Boulouchos, Lucas Bretschger, Ulrich Bundi, Paolo Burlando, Rudolf Dinger, Christof Duthaler, Daniel Favrat, Klaus Fröhlich, Werner Graber, Maxi Grebe, Lino Guzzella, Matthias Gysler, Peter de Haan, Walter Hauenstein, Sandra Hermle, Michael Höckel, Peter Houzer, Peter Jansohn, Eberhard Jochem, Klaus Jorde, Tony Kaiser, Wolfgang Kröger, Kurt Küffer, Filippo Leuchthaler, Marco Mazzotti, Anton Meier, Martin Michel, Rudolf Minder, Peter Molinari, Andrew Neville, Stefan Nowak, Hans Pauli, Michel Piot, Christian Plüss, Horst-Michael Prasser, Reto Rigassi, Christian Schaffner, Anton Schleiss, Ulrich Schmocker, Hans-Jörg Schötzau, Renate Schubert, Ralf Schulz, Heinrich Schwendener, Gunter Siddiqi, Michael Siegrist, Aldo Steinfeld, Samuel Stucki, Bernadette Sütterlin, Renato Tami, Jakob Vollenweider, Marcel Wickart, Alexander Wokaun, Hansruedi Zeller, Niklaus Zepf, and Pieter Zuidema. *Zukunft Stromversorgung Schweiz*. Technical report, Akademien der Wissenschaften Schweiz, Bern, 2012.

Asian Development Bank ADB. *Guidelines for Wind Resource Assessment Best Practices for Countries Initiating Wind Development*. pages 1–49, 2014. URL <https://www.adb.org/sites/default/files/publication/42032/guidelines-wind-resource-assessment.pdf>.

Arbeitsgruppe Erneuerbare Energienstatistik. *Zeitreihen zur Entwicklung der erneuerbaren Energien in Deutschland*. 2016.

Cristina L. Archer and Mark Z. Jacobson. Evaluation of global wind power. *Journal of Geophysical Research D: Atmospheres*, 110(12):1–20, 2005. ISSN 01480227. doi: 10.1029/2004JD005462.

Cristina L. Archer and Mark Z. Jacobson. Supplying baseload power and reducing transmission requirements by interconnecting wind farms. *Journal of Applied Meteorology and Climatology*, 46(11):1701–1717, 2007. ISSN 15588424. doi: 10.1175/2007JAMC1538.1.

Cristina L. Archer and Mark Z. Jacobson. Geographical and seasonal variability of the global "practical" wind resources. *Applied Geography*, 45:119–130, 2013. ISSN 01436228. doi: 10.1016/j.apgeog.2013.07.006. URL <http://dx.doi.org/10.1016/j.apgeog.2013.07.006>.

Delia Arnold, Irene Schicker, and Petra Seibert. *High-Resolution Atmospheric Modelling in Complex Terrain for Future Climate Simulations (HiRmod) Report 2010*.

## Bibliography

---

- pages 1–8, 2010. URL [http://www.vsc.ac.at/fileadmin/user{}\\_upload/vsc/reports/BOKU-p70075-Schicker-Report.pdf](http://www.vsc.ac.at/fileadmin/user{}_upload/vsc/reports/BOKU-p70075-Schicker-Report.pdf).
- Robert S. Arthur, Katherine A. Lundquist, Jeffrey D. Mirocha, and Fotini K. Chow. Topographic effects on radiation in the WRF model with the immersed boundary method: implementation, validation, and application to complex terrain. *Monthly Weather Review*, pages MWR–D–18–0108.1, 2018. ISSN 0027-0644. doi: 10.1175/MWR-D-18-0108.1. URL <http://journals.ametsoc.org/doi/10.1175/MWR-D-18-0108.1>.
- Maria Ayuso and Christian Kjaer. World Energy Resources Wind | 2016. *World Energy Council*, page 71, 2016.
- Sarah Barber, Ndaona Chokani, and Reza S. Abhari. Assessment of Wind Turbine Performance in Alpine Environments. *Wind Engineering*, 35:313–328, 2011. ISSN 0309-524X. doi: 10.1260/0309-524X.35.3.313.
- Franziska Barmettler, Nick Beglinger, and Christian Zeyer. Cleantech Energiestrategie. Technical Report 3.1, swisscleantech, Zurich, 2013.
- S Bartlett, B Kruyt, A Kahl, and M Lehning. Risks and Reliability in a Fully Renewable Switzerland. *Esrel*, pages 4251–4256, 2015.
- Lorenzo Battisti. *Wind Turbines in Cold Climates: Icing Impacts and Mitigation Systems*. Springer, Trento, 2015. ISBN 9783319051901.
- C Bauer, S Hirschberg, Y Bäuerle, S Biollaz, A Calbry-Muzyka, B Cox, T Heck, M Lehnert, A Meier, H-M Prasser, W Schenler, K Treyer, F Vogel, HC Wieckert, X Zhang, M Zimmermann, V Burg, G Bowman, M Erni, M Saar, and M Q Tran. Potentials, costs and environmental assessment of electricity generation technologies. Technical report, Bundesamt für Energie BFE Sektion Energieversorgung und Monitoring Potentials,, Bern, 2017. URL <https://www.psi.ch/ta/HomeEN/Final-Report-BFE-Project.pdf>.
- Peter Bauer, Alan Thorpe, and Gilbert Brunet. The quiet revolution of numerical weather prediction. *Nature*, 2015. doi: 10.1038/nature14956.
- S. Becker, R. A. Rodriguez, G. B. Andresen, S. Schramm, and M. Greiner. Transmission grid extensions during the build-up of a fully renewable pan-European electricity supply. *Energy*, 64:404–418, 2014. ISSN 03605442. doi: 10.1016/j.energy.2013.10.010. URL <http://dx.doi.org/10.1016/j.energy.2013.10.010>.
- Erik Berge, Arne Gravdahl, Jan Schelling, Lars Tallhaug, and Ove Undheim. Wind in complex terrain. A comparison of WAsP and two CFD-models. In *Proceedings from European Wind Energy Conference and Exhibition 2006*, volume 2, pages 1569–1577, Athens, Greece, 2006. ISBN 9781622764679. URL [http://www.windsim.com/documentation/papers{}\\_presentations/0602{}\\_ewec/ewec{}\\_berge.pdf](http://www.windsim.com/documentation/papers{}_presentations/0602{}_ewec/ewec{}_berge.pdf).

- Jean-marie Bettems. COSMO software fieldextra. In *COSMO GM*, number September, Jerusalem, 2017.
- Juliette Blanchet and Anthony C. Davison. Spatial modeling of extreme snow depth. *Annals of Applied Statistics*, 5(3):1699–1725, 2011. ISSN 19326157. doi: 10.1214/11-AOAS464.
- Juliette Blanchet and M. Lehning. Mapping snow depth return levels: smooth spatial modeling versus station interpolation. *Hydrology and Earth System Sciences*, 14(12): 2527–2544, dec 2010. ISSN 1607-7938. doi: 10.5194/hess-14-2527-2010. URL <http://www.hydrol-earth-syst-sci.net/14/2527/2010/>.
- Juliette Blanchet, C. Marty, and M. Lehning. Extreme value statistics of snowfall in the Swiss Alpine region. *Water Resources Research*, 45(5):n/a–n/a, may 2009. ISSN 00431397. doi: 10.1029/2009WR007916. URL <http://doi.wiley.com/10.1029/2009WR007916>.
- Arno J Brand, Joachim Peinke, and Jakob Mann. Turbulence and wind turbines. *Journal of Physics: Conference Series*, 318(7):072005, 2011. ISSN 1742-6596. doi: 10.1088/1742-6596/318/7/072005.
- Anne Sjoerd Brouwer, Machteld Van Den Broek, Ad Seebregts, and André Faaij. Impacts of large-scale Intermittent Renewable Energy Sources on electricity systems, and how these can be modeled. *Renewable and Sustainable Energy Reviews*, 33:443–466, 2014. ISSN 13640321. doi: 10.1016/j.rser.2014.01.076. URL <http://dx.doi.org/10.1016/j.rser.2014.01.076>.
- Anne Sjoerd Brouwer, Machteld van den Broek, Ad Seebregts, and André Faaij. Operational flexibility and economics of power plants in future low-carbon power systems. *Applied Energy*, 156:107–128, 2015. ISSN 03062619. doi: 10.1016/j.apenergy.2015.06.065. URL <http://dx.doi.org/10.1016/j.apenergy.2015.06.065>.
- Anne Sjoerd Brouwer, Machteld van den Broek, William Zappa, Wim C. Turkenburg, and André Faaij. Least-cost options for integrating intermittent renewables in low-carbon power systems. *Applied Energy*, 161:48–74, 2016. ISSN 03062619. doi: 10.1016/j.apenergy.2015.09.090. URL <http://dx.doi.org/10.1016/j.apenergy.2015.09.090>.
- Michael C Brower. Evaluation of four numerical wind flow models. In *EWEA Resource Assessment Workshop 2013*, Dublin, 2013.
- Michael C Brower, Bruce H Bailey, James Doane, and Matthew J Eberhard. *WIND RESOURCE ASSESSMENT A Practical Guide to Developing a Wind Project*. 2012. ISBN 9781118022320.
- Ernst a Brugger, Philipp Dietrich, Rahel Gessler, Kathrin Giger, Patrick Hofstetter, Tony Kaiser, Alexander Wokaun, Energie Trialog Schweiz, and Frau Rahel Gessler. Erneuerbare Energien : Übersicht über vorliegende Studien und Einschätzung des Energie Trialog Schweiz zu den erwarteten inländischen Potenzialen für die Strom-, Wärme- und Treibstoffproduktion in den Jahren 2035 und 2050 inklusive Berücksichtigung der P. Technical report, Energie Trialog Schweiz, Zürich, 2009.

## Bibliography

---

- Bundesamt für Energie. Schweizerische Elektrizitätsstatistik 2014. pages 1–56, 2015. URL [https://www.bundespublikationen.admin.ch/cshop/\\_bbl/b2c/init/\(cquery=\\*805.005.14\\*\)/.do?shopId=BBL00001DE{&}language=DE](https://www.bundespublikationen.admin.ch/cshop/_bbl/b2c/init/(cquery=*805.005.14*)/.do?shopId=BBL00001DE{&}language=DE).
- Bundesamt für Energie BFE. Konzept windenergie Schweiz - Methode der Modellierung geeigneter Windpark-Standorte. Technical report, Bundesamt für Energie BFE, Bern, 2004a.
- Bundesamt für Energie BFE. Konzept windenergie Schweiz. Technical report, Bundesamt für Energie BFE, Bern, 2004b.
- Bundesamt für Energie (BFE). Schweizerische Elektrizitätsstatistik 2016. Technical report, Bundesamt für Energie BFE, 2017. URL [https://www.bundespublikationen.admin.ch/cshop/\\_bbl/b2c/init/\(cquery=\\*805.005.14\\*\)/.do?shopId=BBL00001DE{&}language=DE](https://www.bundespublikationen.admin.ch/cshop/_bbl/b2c/init/(cquery=*805.005.14*)/.do?shopId=BBL00001DE{&}language=DE).
- Bundesamt für Energie BFE. Schweizerische Elektrizitäts Statistik 2017. Technical report, Bundesamt für Energie BFE, Bern, 2017. URL [www.bundespublikationen.admin.ch](http://www.bundespublikationen.admin.ch).
- Bundesamt für Raumentwicklung. Konzept Windenergie. *Sachpläne und Konzepte*, page 33, 2017.
- Swiss Federal Council Bundesrat. Energy Act (EnA), 2017. URL <https://www.admin.ch/gov/en/start/documentation/votes/Popularvoteron21Mai2017/Energy-Act.html>.
- U. Bunse and H. Mellinghoff. Influences of Vertical Wind Profiles on Power Performance Measurements U. pages 1–5.
- Yoreley Cancino-Solórzano, Antonio J. Gutiérrez-Trashorras, and Jorge Xiberta-Bernat. Analytical methods for wind persistence: Their application in assessing the best site for a wind farm in the State of Veracruz, Mexico. *Renewable Energy*, 35(12):2844–2852, 2010. ISSN 09601481. doi: 10.1016/j.renene.2010.05.008. URL <http://dx.doi.org/10.1016/j.renene.2010.05.008>.
- Carlin. The History and State of the Art of Variable-Speed wind Turbine Technology. *Wind Energy*, 6(February):129–159, 2003.
- René Cattin, Beat Schaffner, Matteo Buzzi, and Stefan Kunz. WIND MODELING IN MOUNTAINOUS TERRAIN: VALIDATION BY SODAR. pages 4–7, 2002.
- René Cattin, Beat Schaffner, Stefan Kunz, and Robert Horbaty. Wind measurements and modeling in the Swiss Alps. pages 1–8, 2003.
- René Cattin, Beat Schaffner, and Stefan Kunz. Validation of CFD Wind Resource Modeling in Highly Complex Terrain. In *Ewec 2006*, 2006. ISBN 9781622764679. URL [http://web.windsim.com/documentation/papers/\\_presentations/0602\\_ewec/ewec\\_cattin.pdf](http://web.windsim.com/documentation/papers/_presentations/0602_ewec/ewec_cattin.pdf).
- René Cattin, Russi Markus, and Russi Gabriela. Four years of monitoring a wind turbine under icing conditions. pages 6–10, 2009.



- P Ceppi and C Appenzeller. Extreme Value Analysis of Wind Speed Observations over Switzerland. Technical Report 219, 2008.
- Fotini Katopodes Chow. *Mountain Weather Research and Forecasting: Recent Progress and Current Challenges*. 2013. ISBN 9789400740976.
- Robin T Clark, Philip E Bett, Hazel E Thornton, and Adam A Scaife. Skilful seasonal predictions for the European energy industry (2017 Environ. Res. Lett. 2 024002). *Environmental Research Letters*, 12(11):119602, 2017. ISSN 1748-9326. doi: 10.1088/1748-9326/aa94a7. URL <http://stacks.iop.org/1748-9326/12/i=11/a=119602?key=crossref.fb0be7b83886374f81ae2a14b3709b79>.
- Andrew Clifton, M H Daniels, and M Lehning. Effect of winds in a mountain pass on turbine performance. (August 2013):1543–1562, 2014. doi: 10.1002/we.
- D. John Clyne, Pablo Mininni, Alan Norton, and Mark Rast. Interactive desktop analysis of high resolution simulations: Application to turbulent plume dynamics and current sheet formation. *New Journal of Physics*, 9, 2007. ISSN 13672630. doi: 10.1088/1367-2630/9/8/301.
- Stuart Coles. *An introduction to statistical modeling of extreme values*. 2001. ISBN 1-85233-459-2. doi: 10.1007/978-1-4471-3675-0.
- Stuart Coles and Anthony Davison. Statistical Modelling of Extreme Values. 2008. URL <http://www.cces.ethz.ch/projects/hazri/EXTREMES/talks/colesDavisonDavosJan08.pdf>.
- Consortium for Small-scale Modeling. COSMO model, 2017. URL <http://www.cosmo-model.org>.
- Giorgio Corbetta. EWEA Wind energy scenarios for 2030. *Ewea*, pages 1–8, 2015.
- Megan H. Daniels, Katherine A. Lundquist, Jeffrey D. Mirocha, David J. Wiersema, and Fotini K. Chow. A New Vertical Grid Nesting Capability in the Weather Research and Forecasting (WRF) Model. *Monthly Weather Review*, 144(10):3725–3747, 2016. ISSN 0027-0644. doi: 10.1175/MWR-D-16-0049.1. URL <http://journals.ametsoc.org/doi/10.1175/MWR-D-16-0049.1>.
- A. DeMarrais, Gerard. Wind-Speed Profiles At Brookhaven National Laboratory. *Journal of Meteorology*, 16:181–190, 1958.
- Paul Denholm, Maureen Hand, Maddalena Jackson, and Sean Ong. Land-Use Requirements of Modern Wind Power Plants in the United States Land-Use Requirements of Modern Wind Power Plants in the United States. *National Renewable Energy Laboratory*, Technical (August):46, 2009.
- Martin Densing, Stefan Hirschberg, and Hal Turton. Review of Swiss Electricity Scenarios 2050. Technical Report 14, 2014.

## Bibliography

---

- Silke Dierer, Jan Remund, Beat Schaffner, Vanessa Stauch, and Christophe Hug. Wind power predictions for Switzerland: the performance of different downscaling methods for complex terrain. In *2009 European Wind Energy Conference and Exhibition*, Stockholm, Sweden, 2009. ISBN 9781615677467.
- Caroline Draxl and Georg J. Mayr. Meteorological wind energy potential in the Alps using ERA40 and wind measurement sites in the Tyrolean Alps. In *EWEC2009*, 2009.
- Caroline Draxl and Georg J. Mayr. Meteorological wind energy potential in the Alps using ERA40 and wind measurement sites in the Tyrolean Alps. *Wind Energy*, 14(4):471–489, may 2011. ISSN 10954244. doi: 10.1002/we.436. URL <http://onlinelibrary.wiley.com/doi/10.1002/we.1608/fullhttp://doi.wiley.com/10.1002/we.436>.
- Caroline Draxl, Andrea N. Hahmann, Alfredo Peña, and Gregor Giebel. Evaluating winds and vertical wind shear from Weather Research and Forecasting model forecasts using seven planetary boundary layer schemes. *Wind Energy*, 17(1):39–55, jan 2014. ISSN 10954244. doi: 10.1002/we.1555. URL <http://onlinelibrary.wiley.com/doi/10.1002/we.1608/fullhttp://doi.wiley.com/10.1002/we.1555>.
- Jérôme Dujardin, Annelen Kahl, Bert Kruyt, Stuart Bartlett, and Michael Lehning. Interplay between photovoltaic, wind energy and storage hydropower in a fully renewable Switzerland. *Energy*, 135:513–525, sep 2017. ISSN 03605442. doi: 10.1016/j.energy.2017.06.092. URL <http://linkinghub.elsevier.com/retrieve/pii/S0360544217310861>.
- S Emeis. How Well Does a Power Law Fit to a Diabatic Boundary-Layer Wind Profile ? (26): 59–62, 2005.
- Cornel Ensslin, Michael Milligan, Ieee Hannele Holttinen, Mark O Malley, and Andrew Keane. Current Methods to Calculate Capacity Credit of Wind Power. *IEEE*, pages 1–3, 2008.
- Christophe Etienne, Anthony Lehmann, Stéphane Goyette, Juan-Ignacio Lopez-Moreno, and Martin Beniston. Spatial Predictions of Extreme Wind Speeds over Switzerland Using Generalized Additive Models. *Journal of Applied Meteorology and Climatology*, 49(9):1956–1970, 2010. ISSN 1558-8424. doi: 10.1175/2010JAMC2206.1.
- European Environmental Agency. CORINE Land Cover raster data 2006, 2006. URL <https://www.eea.europa.eu/data-and-maps/data/clc-2006-raster>.
- European Wind Energy Association. Wind Energy Statistics and Targets. 2013. URL [http://www.ewea.org/uploads/pics/EWEA{}\\_Wind{}\\_energy{}\\_factsheet.png](http://www.ewea.org/uploads/pics/EWEA{}_Wind{}_energy{}_factsheet.png).
- Enzo Fanone, Andrea Gamba, and Marcel Prokopczuk. The case of negative day-ahead electricity prices. *Energy Economics*, 35(May 2008):22–34, 2013. ISSN 01409883. doi: 10.1016/j.eneco.2011.12.006. URL <http://dx.doi.org/10.1016/j.eneco.2011.12.006>.
- R. N. Farrugia. The wind shear exponent in a Mediterranean island climate. *Renewable Energy*, 28(4):647–653, 2003. ISSN 09601481. doi: 10.1016/S0960-1481(02)00066-6.

- Federal Department of the Environment Transport Energy and Communications DETEC. DETEC - Energy Strategy 2050, 2018. URL <https://www.uvek.admin.ch/uvek/en/home/energy/energy-strategy-2050.html>.
- Sergio Fernández-González, María Luisa Martín, Eduardo García-Ortega, Andrés Merino, Jesús Lorenzana, José Luis Sánchez, Francisco Valero, and Javier Sanz Rodrigo. Sensitivity analysis of WRF model: wind-resource assessment for complex terrain. *Journal of Applied Meteorology and Climatology*, pages JAMC–D–17–0121.1, 2017. ISSN 1558-8424. doi: 10.1175/JAMC-D-17-0121.1. URL <http://journals.ametsoc.org/doi/10.1175/JAMC-D-17-0121.1>.
- Ebubekir Firtın, Önder Güler, and Seyit Ahmet Akdağ. Investigation of wind shear coefficients and their effect on electrical energy generation. *Applied Energy*, 88(11):4097–4105, 2011. ISSN 03062619. doi: 10.1016/j.apenergy.2011.05.025.
- George Galanis. *Smoothing out the wind power production patterns by connecting different countries within Europe*. MSc Thesis. PhD thesis, Utrecht, 2014.
- Franziska Gerber and Varun Sharma. Running COSMO – WRF on very high resolution over complex terrain. pages 1–20, 2018. doi: 10.16904/envidat.35.Cite.
- Franziska Gerber, Nikola Besic, Varun Sharma, Rebecca Mott, Megan Daniels, Marco Gabella, Alexis Berne, Urs Germann, and Michael Lehning. Spatial variability of snow precipitation and accumulation in COSMO-WRF simulations and radar estimations over complex terrain. *The Cryosphere Discussions*, (March):1–30, 2018. ISSN 1994-0440. doi: 10.5194/tc-2018-50. URL <https://www.the-cryosphere-discuss.net/tc-2018-50/>.
- Giebel. *On the Benefits of Distributed Generation of Wind Energy in Europe*. PhD thesis, 2000.
- Gregor Giebel. Wind power has a capacity credit. *Riso National Laboratory, Roskilde, Dec*, (then 12), 2006.
- Global Wind Energy Council. Global Wind Energy Report: Annual Market Update 2017. 2018. URL [www.gwec.net](http://www.gwec.net).
- J. J. Gómez-Navarro, C. C. Raible, and S. Dierer. Sensitivity of the WRF model to PBL parametrisations and nesting techniques: Evaluation of wind storms over complex terrain. *Geoscientific Model Development*, 8(10):3349–3363, 2015. ISSN 19919603. doi: 10.5194/gmd-8-3349-2015.
- Ingeborg Graabak and Magnus Korpås. Variability Characteristics of European Wind and Solar Power Resources—A Review. *Energies*, 9(6):449, 2016. ISSN 1996-1073. doi: 10.3390/en9060449. URL <http://www.mdpi.com/1996-1073/9/6/449>.
- Christian M. Grams, Remo Beerli, Stefan Pfenninger, Iain Staffell, and Heini Wernli. Balancing Europe’s wind-power output through spatial deployment informed by weather regimes. *Nature Climate Change*, 7(July), 2017. ISSN 1758-678X. doi: 10.1038/nclimate3338. URL <http://www.nature.com/doi/10.1038/nclimate3338>.

## Bibliography

---

- Thomas Grünewald, Silke Dierer, Felix Fundel, and Michael Lehning. Mapping frequencies of icing on structures in Switzerland. *Journal of Wind Engineering and Industrial Aerodynamics*, 108:76–82, 2012.
- Anton Gunzinger. *Kraftwerk Schweiz: Plädoyer für eine Energiewende mit Zukunft*. Zytglogge, Zurich, 2015. ISBN 978-3729608887.
- GWEC. Global Wind Energy Council, 2018. URL <http://gwec.net/>.
- L De Haan and A Ferreira. *Extreme value theory: an introduction*. Springer, 2007. ISBN 9780387239460.
- Berthold Hahn, Michael Durstewitz, and Kurt Rohrig. Reliability of Wind Turbines. *Wind Energy*, pages 1–4, 2007. doi: 10.1007/978-3-540-33866-6\_62. URL [http://link.springer.com/content/pdf/10.1007/978-3-540-33866-6\\_62.pdf](http://link.springer.com/content/pdf/10.1007/978-3-540-33866-6_62.pdf).
- K. B.R.R. Hari Prasad, C. V. Srinivas, T. Narayana Rao, C. V. Naidu, and R. Baskaran. Performance of WRF in simulating terrain induced flows and atmospheric boundary layer characteristics over the tropical station Gadanki. *Atmospheric Research*, 185:101–117, 2017. ISSN 01698095. doi: 10.1016/j.atmosres.2016.10.020. URL <http://dx.doi.org/10.1016/j.atmosres.2016.10.020>.
- Dominik Heide, Lueder von Bremen, M. Greiner, Clemens Hoffmann, Markus Speckmann, and Stefan Bofinger. Seasonal optimal mix of wind and solar power in a future, highly renewable Europe. *Renewable Energy*, 35(11):2483–2489, nov 2010. ISSN 09601481. doi: 10.1016/j.renene.2010.03.012. URL <http://linkinghub.elsevier.com/retrieve/pii/S0960148110001291>.
- N. Helbig, R. Mott, A. Van Herwijnen, A. Winstral, and T. Jonas. Parameterizing surface wind speed over complex topography. *Journal of Geophysical Research*, 122(2):651–667, 2017. ISSN 21562202. doi: 10.1002/2016JD025593.
- Stefan Hirschberg, Christian Bauer, Peter Burgherr, Serge Biollaz, Wilhelm Durisch, Konstantin Foskolos, P Hardegger, Anton Meier, Warren Schenler, Thorsten Schulz, Samuel Stucki, and Frederic Vogel. Neue erneuerbare Energien und neue Nuklearanlagen: Potenziale und Kosten. Technical Report 05, Paul Scherrer Institut PSI, Villigen, 2005.
- Lion Hirth. The benefits of flexibility: The value of wind energy with hydropower. *Applied Energy*, 181:210–223, 2016. ISSN 03062619. doi: 10.1016/j.apenergy.2016.07.039. URL <http://linkinghub.elsevier.com/retrieve/pii/S0306261916309801>.
- Hannele Holttinen. Hourly wind power variations in the nordic countries. *Wind Energy*, 8(2): 173–195, 2005. ISSN 10954244. doi: 10.1002/we.144.
- James Honaker, Gary King, and Matthew Blackwell. AMELIA II : A Program for Missing Data. *Journal Of Statistical Software*, 45(7):1–54, 2011. ISSN 15487660. doi: 10.1.1.149.9611. URL <http://gking.harvard.edu/amelia/>.
- James Honaker, Gary King, and Matthew Blackwell. AMELIA II : A Program for Missing Data, 2015. URL <http://gking.harvard.edu/amelia/>.

- M Hoogwijk and W Graus. Global potential of renewable energy sources: a literature assessment. *Background report prepared by order of ...*, (March), 2008. URL [http://www.researchgate.net/profile/Wina/Crijns-Graus/publication/237576106/GLOBAL\\_POTENTIAL\\_OF\\_RENEWABLE\\_ENERGY\\_SOURCES\\_A\\_LITERATURE\\_ASSESS/links/0deec52f89ed07b2b9000000.pdf](http://www.researchgate.net/profile/Wina/Crijns-Graus/publication/237576106/GLOBAL_POTENTIAL_OF_RENEWABLE_ENERGY_SOURCES_A_LITERATURE_ASSESS/links/0deec52f89ed07b2b9000000.pdf).
- Monique Hoogwijk, Bert de Vries, and Wim Turkenburg. Assessment of the global and regional geographical, technical and economic potential of onshore wind energy. *Energy Economics*, 26(5):889–919, 2004. ISSN 01409883. doi: 10.1016/j.eneco.2004.04.016.
- Monique Maria Hoogwijk. *On the global and regional potential of renewable energy sources*. PhD thesis, 2004. URL [http://np-net.pbworks.com/f/Hoogwijk+\(2004\)+Global+and+regional+potential+of+renewable+energy+sources+\(Thesis+Utrecht\).pdf](http://np-net.pbworks.com/f/Hoogwijk+(2004)+Global+and+regional+potential+of+renewable+energy+sources+(Thesis+Utrecht).pdf).
- S. Jafari, T. Sommer, N. Chokani, and R. S. Abhari. Wind Resource Assessment Using a Mesoscale Model: The Effect of Horizontal Resolution. In *Proceedings of ASME Turbo Expo 2012 GT2012 June 11-15, 2012*, page 987, Copenhagen, Denmark, 2012. ISBN 978-0-7918-4472-4. doi: 10.1115/GT2012-69712. URL <http://proceedings.asmedigitalcollection.asme.org/proceeding.aspx?doi=10.1115/GT2012-69712>.
- Maya Jegen. Energy transition and challenges for wind energy in Switzerland. In *Climate Change and Renewable Energy Policy Workshop, Carleton University, Canada*, pages 2–6, Ottawa, Canada, 2015. URL <https://carleton.ca/ces/wp-content/uploads/Jegen-Maya-Energy-transition-and-wind-energy-in-Switzerland-final.pdf>.
- P. A. Jiménez, J. Dudhia, J. F. González-Rouco, J. P. Montávez, E. García-Bustamante, J. Navarro, J. Vilà-Guerau De Arellano, and A. Muñoz-Roldán. An evaluation of WRF’s ability to reproduce the surface wind over complex terrain based on typical circulation patterns. *Journal of Geophysical Research Atmospheres*, 118(14):7651–7669, 2013. ISSN 21698996. doi: 10.1002/jgrd.50585.
- Pedro A. Jiménez and Jimmy Dudhia. Improving the representation of resolved and unresolved topographic effects on surface wind in the wrf model. *Journal of Applied Meteorology and Climatology*, 51(2):300–316, 2012. ISSN 15588424. doi: 10.1175/JAMC-D-11-084.1.
- Pedro A. Jiménez and Jimmy Dudhia. On the ability of the WRF model to reproduce the surface wind direction over complex terrain. *Journal of Applied Meteorology and Climatology*, 52(7):1610–1617, 2013. ISSN 15588424. doi: 10.1175/JAMC-D-12-0266.1.
- Pedro a. Jiménez, J. Fidel González-Rouco, Elena García-Bustamante, Jorge Navarro, Juan P. Montávez, Jordi Vilà Guerau De Arellano, Jimmy Dudhia, and Antonio Muñoz-Roldan. Surface wind regionalization over complex terrain: Evaluation and analysis of a high-resolution WRF simulation. *Journal of Applied Meteorology and Climatology*, 49(2):268–287, 2010. ISSN 15588424. doi: 10.1175/2009JAMC2175.1.

## Bibliography

---

- Pedro A. Jimenez, Joshua P. Hacker, Jimy Dudhia, Sue Ellen Haupt, Jose A. Ruiz-Arias, Chris A. Gueymard, Gregory Thompson, Trude Eidhammer, and Aijun Deng. WRF-SOLAR: Description and clear-sky assessment of an augmented NWP model for solar power prediction. *Bulletin of the American Meteorological Society*, 97(7):1249–1264, 2016. ISSN 00030007. doi: 10.1175/BAMS-D-14-00279.1.
- Annelen Kahl, Jerome Dujardin, and Michael Lehning. The bright side of PV production in snow-covered mountains. *PNAS*, *in press*, 2018.
- Warren Katzenstein, Emily Fertig, and Jay Apt. The variability of interconnected wind plants. *Energy Policy*, 38(8):4400–4410, 2010. ISSN 03014215. doi: 10.1016/j.enpol.2010.03.069. URL <http://dx.doi.org/10.1016/j.enpol.2010.03.069>.
- Urs Kaufmann. Schweizerische Statistik der erneuerbaren Energien Ausgabe 2017. Technical Report 2017, BFE, Liestal, 2018.
- Janina C. Ketterer. The Impact of Wind Power Generation on the Electricity Price in Germany. 2012.
- Kasim Koçak. A method for determination of wind speed persistence and its application. *Energy*, 27(10):967–973, 2002. ISSN 03605442. doi: 10.1016/S0360-5442(02)00033-6.
- Kasim Koçak. Practical ways of evaluating wind speed persistence. *Energy*, 33(1):65–70, 2008. ISSN 03605442. doi: 10.1016/j.energy.2007.07.010.
- Sara Koller and Tanja Humar. Windpotentialanalyse für Windatlas.ch: Jahresmittelwerte der modellierten Windgeschwindigkeit und Windrichtung. Schlussbericht. Technical report, MeteoTest, BFE, 2016.
- Bert Kruyt, Michael Lehning, and Annelen Kahl. Potential contributions of wind power to a stable and highly renewable Swiss power supply. *Applied Energy*, 192:1–11, apr 2017. ISSN 03062619. doi: 10.1016/j.apenergy.2017.01.085. URL <http://dx.doi.org/10.1016/j.apenergy.2017.01.085><http://linkinghub.elsevier.com/retrieve/pii/S0306261917300922>.
- Bert Kruyt, Jérôme Dujardin, and Michael Lehning. Improvement of Wind Power Assessment in Complex Terrain: The Case of COSMO-1 in the Swiss Alps. *Frontiers in Energy Research*, 6: 102, oct 2018. ISSN 2296-598X. doi: 10.3389/fenrg.2018.00102. URL <https://www.frontiersin.org/article/10.3389/fenrg.2018.00102/full>.
- M. L. Kubik, P. J. Coker, J. F. Barlow, and C. Hunt. A study into the accuracy of using meteorological wind data to estimate turbine generation output. *Renewable Energy*, 51:153–158, 2013. ISSN 09601481. doi: 10.1016/j.renene.2012.08.084. URL <http://dx.doi.org/10.1016/j.renene.2012.08.084>.
- Mohamed Laib and Mikhail Kanevski. Spatial Patterns of Wind Speed Distributions in Switzerland. (November), 2016. URL <http://arxiv.org/abs/1609.05012>.

- Paul G. Leahy and Eamon J. McKeogh. Persistence of low wind speed conditions and implications for wind power variability. *Wind Energy*, 16(4):575–586, may 2013. ISSN 10954244. doi: 10.1002/we.1509. URL <http://onlinelibrary.wiley.com/doi/10.1002/we.1608/fullhttp://doi.wiley.com/10.1002/we.1509>.
- Junhong Lee, Hyeyum Hailey Shin, Song You Hong, Pedro A. Jiménez, Jimy Dudhia, and Jinkyu Hong. Impacts of subgrid-scale orography parameterization on simulated surface layer wind and monsoonal precipitation in the high-resolution WRF model. *Journal of Geophysical Research*, 120(2):644–653, 2015. ISSN 21562202. doi: 10.1002/2014JD022747.
- S Lee, M Churchfield, P Moriarty, and J Jonkman. Atmospheric and wake turbulence impacts on wind turbine fatigue loadings. *Proc. of the 50th AIAA Aerospace Sciences Meeting*, (NREL/CP-5000-53567), 2012. URL <http://arc.aiaa.org/doi/pdf/10.2514/6.2012-540>.
- M. Lehning, H. Löwe, M. Ryser, and N. Raderschall. Inhomogeneous precipitation distribution and snow transport in steep terrain. *Water Resources Research*, 44(7):1–19, 2008. ISSN 00431397. doi: 10.1029/2007WR006545.
- Michael Lehning, Perry Bartelt, Bob Brown, Tom Russi, Urs Stöckli, and Martin Zimmerli. SNOWPACK model calculations for avalanche warning based upon a new network of weather and snow stations. *Cold Regions Science and Technology*, 30(1-3):145–157, 1999. ISSN 0165232X. doi: 10.1016/S0165-232X(99)00022-1.
- Daniel Leuenberger, Marcel Koller, Oliver Fuhrer, and Christoph Schär. A Generalization of the SLEVE Vertical Coordinate. *Monthly Weather Review*, 138(9):3683–3689, 2010. ISSN 0027-0644. doi: 10.1175/2010MWR3307.1. URL <http://journals.ametsoc.org/doi/abs/10.1175/2010MWR3307.1>.
- H. W. Lewis, S. D. Mobbs, and M. Lehning. Observations of cross-ridge flows across steep terrain. *Quarterly Journal of the Royal Meteorological Society*, 134(633):801–816, apr 2008. ISSN 00359009. doi: 10.1002/qj.259. URL <http://onlinelibrary.wiley.com/doi/10.1002/qj.71/abstracthttp://doi.wiley.com/10.1002/qj.259>.
- Peter D. Lund, Juuso Lindgren, Jani Mikkola, and Jyri Salpakari. Review of energy system flexibility measures to enable high levels of variable renewable electricity. *Renewable and Sustainable Energy Reviews*, 45:785–807, 2015. ISSN 13640321. doi: 10.1016/j.rser.2015.01.057. URL <http://dx.doi.org/10.1016/j.rser.2015.01.057>.
- Georg J. Mayr, Laurence Armi, Alexander Gohm, Guenther Zangl, Dale R. Durran, Cyrille Flamant, Sasa Gabersek, Stephen Mobbs, Andrew Rossg, and Martin Weissmann. Gap flows: Results from the Mesoscale Alpine Programme. *Quarterly Journal of the Royal . . .*, 133:937–948, 2007. doi: 10.1002/qj. URL <http://onlinelibrary.wiley.com/doi/10.1002/qj.71/abstract>.
- L. J. Mazzaro, D. Muñoz-Esparza, J. K. Lundquist, and R. R. Linn. Nested mesoscale-to-LES modeling of the atmospheric boundary layer in the presence of under-resolved convective structures. *Journal of Advances in Modeling Earth Systems*, 9(4):1795–1810, 2017. ISSN 19422466. doi: 10.1002/2017MS000912.

## Bibliography

---

- H.-T. Mengelkamp. Wind Climate Simulation over Complex Terrain and Wind Turbine Energy Output Estimation. *Theoretical and Applied Climatology*, 63(3-4):129–139, 1999. ISSN 0177-798X. doi: 10.1007/s007040050098.
- MeteoSchweiz. Automatisches Messnetz, 2016. URL <http://www.meteoschweiz.admin.ch/home/mess-und-prognosesysteme/bodenstationen/automatisches-messnetz.html>.
- MeteoTest. Windenergie-Daten der Schweiz. URL <http://wind-data.ch/messdaten/>.
- METI/NASA. ASTER Global Digital Elevation Model V002, NASA EOSDIS Land Processes DAAC, USGS Earth Re-, 2009. URL <https://search.earthdata.nasa.gov/search>.
- Johan Meyers and Charles Meneveau. Optimal turbine spacing in fully developed wind farm boundary layers. *Wind Energy*, 15(2):305–317, mar 2012. ISSN 10954244. doi: 10.1002/we.469. URL <http://onlinelibrary.wiley.com/doi/10.1002/we.1608/full><http://doi.wiley.com/10.1002/we.469>.
- NASA. U.S. Standard Atmosphere, 1976. URL <http://ntrs.nasa.gov/archive/nasa/casi.ntrs.nasa.gov/19770009539.pdf>.
- Daniel Oppliger, Bruno Dürr, and Stefan Bertsch. Entwicklung einer Methodik zur Erstellung eines Windkatasters mittels CFD Simulationen. Technical report, NTB, Buchs, 2016.
- Miguel A. Ortega-Vazquez and Daniel S. Kirschen. Estimating the Spinning Reserve Requirements in Systems With Significant Wind Power Generation Penetration. *IEEE Transactions on Power Systems*, 24(1):11, 2009. ISSN 0885-8950. doi: 10.1109/tpwrs.2008.2004745.
- J.M.L.M. Palma, F.A. Castro, L.F. Ribeiro, A.H. Rodrigues, and A.P. Pinto. Linear and nonlinear models in wind resource assessment and wind turbine micro-siting in complex terrain. *Journal of Wind Engineering and Industrial Aerodynamics*, 96(12):2308–2326, dec 2008. ISSN 01676105. doi: 10.1016/j.jweia.2008.03.012. URL <http://linkinghub.elsevier.com/retrieve/pii/S0167610508001037>.
- Jp Palutikof, Bb Brabson, Dh Lister, and St Adcock. A review of methods to calculate extreme wind speeds. *Meteorological*, 6:119–132, 1999. ISSN 1469-8080. doi: 10.1017/S1350482799001103. URL <http://journals.cambridge.org/abstract/S1350482799001103>.
- N. Pineda, O. Jorba, J. Jorge, and J. M. Baldasano. Using NOAA AVHRR and SPOT VGT data to estimate surface parameters: Application to a mesoscale meteorological model. *International Journal of Remote Sensing*, 25(1):129–143, 2004. ISSN 01431161. doi: 10.1080/0143116031000115201.
- Jordan G. Powers, Joseph B. Klemp, William C. Skamarock, Christopher A. Davis, Jimy Dudhia, David O. Gill, Janice L. Coen, David J. Gochis, Ravan Ahmadov, Steven E. Peckham, Georg A. Grell, John Michalakes, Samuel Trahan, Stanley G. Benjamin, Curtis R. Alexander, Geoffrey J. Dimego, Wei Wang, Craig S. Schwartz, Glen S. Romine, Zhiquan Liu, Chris Snyder, Fei Chen, Michael J. Barlage, Wei Yu, and Michael G. Duda. The weather research and forecasting



- model: Overview, system efforts, and future directions. *Bulletin of the American Meteorological Society*, 98(8):1717–1737, 2017. ISSN 00030007. doi: 10.1175/BAMS-D-15-00308.1.
- Prognos. Die Energieperspektiven für die Schweiz bis 2050. Technical report, Bundesamt für Energie BFE, 2012.
- N. Raderschall, M. Lehning, and C. Schär. Fine-scale modeling of the boundary layer wind field over steep topography. *Water Resources Research*, 44(9):1–18, 2008. ISSN 00431397. doi: 10.1029/2007WR006544.
- Paula D??az Redondo and Oscar Van Vliet. Modelling the Energy Future of Switzerland after the Phase out of Nuclear Power Plants. *Energy Procedia*, 76:49–58, 2015. ISSN 18766102. doi: 10.1016/j.egypro.2015.07.843. URL <http://dx.doi.org/10.1016/j.egypro.2015.07.843>.
- Shafiqur Rehman and Naif M. Al-Abbadi. Wind shear coefficients and their effect on energy production. *Energy Conversion and Management*, 46(15-16):2578–2591, 2005. ISSN 01968904. doi: 10.1016/j.enconman.2004.12.005.
- Rolando A Rodriguez. *Weather-driven power transmission in a highly renewable European electricity network*. PhD thesis, Aarhus University, 2014.
- Rp-online.de. Stromnetz unter Druck: Starkwind drückt Leistung von 22 Akw ins Netz, 2015. URL <http://www.rp-online.de/wirtschaft/starkwind-drueckt-leistung-von-22-akw-ins-netz-aid-1.4981986>.
- Beat Schaffner and René Cattin. ALPINE WINDHARVEST Report 7-7 CFD modeling evaluation. (April 2005), 2005.
- Beat Schaffner and Ar Gravidahl. Wind modeling in mountains: Intercomparison and validation of models. In *Proc. European Wind Energy ...*, 2003.
- Beat Schaffner and Jan Remund. ALPINE WINDHARVEST Report 7-2: Modeling Approach. Technical Report April 2005, MeteoTest, Bern, 2005.
- Christoph Schär, Daniel Leuenberger, Oliver Fuhrer, Daniel Lüthi, and Claude Girard. A New Terrain-Following Vertical Coordinate Formulation for Atmospheric Prediction Models. *Monthly Weather Review*, 130(10):2459–2480, 2002. ISSN 0027-0644. doi: 10.1175/1520-0493(2002)130<2459:ANTFVC>2.0.CO;2. URL <http://journals.ametsoc.org/doi/abs/10.1175/1520-0493%282002%29130%3C2459%3AANTFVC%3E2.0.CO%3B2>.
- Schweizerischen Eidgenossenschaft. Energiegesetz (EnG 730.0), 2018. URL <https://www.admin.ch/opc/de/classified-compilation/20121295/201801010000/730.0.pdf>.
- V. Sharma, G. Cortina, F. Margairaz, M. B. Parlange, and M. Calaf. Evolution of flow characteristics through finite-sized wind farms and influence of turbine arrangement. *Renewable Energy*, 115:1196–1208, 2018. ISSN 18790682. doi: 10.1016/j.renene.2017.08.075.

## Bibliography

---

- Hyeyum Hailey Shin and Jimy Dudhia. Evaluation of PBL Parameterizations in WRF at Subkilometer Grid Spacings: Turbulence Statistics in the Dry Convective Boundary Layer. *Monthly Weather Review*, 144(3):1161–1177, 2016. ISSN 0027-0644. doi: 10.1175/MWR-D-15-0208.1. URL <http://journals.ametsoc.org/doi/10.1175/MWR-D-15-0208.1>.
- E. Simiu and N. a. Heckert. Extreme Wind Distribution Tails: A “Peaks over Threshold” Approach. *Journal of Structural Engineering*, 122(5):539–547, 1996. ISSN 0733-9445. doi: 10.1061/(ASCE)0733-9445(1996)122:5(539).
- David Siuta, Gregory West, and Roland Stull. WRF Hub-Height Wind Forecast Sensitivity to PBL Scheme, Grid Length, and Initial Condition Choice in Complex Terrain. *Weather and Forecasting*, 32(2):493–509, 2017. ISSN 0882-8156. doi: 10.1175/WAF-D-16-0120.1. URL <http://journals.ametsoc.org/doi/10.1175/WAF-D-16-0120.1>.
- W.C. Skamarock, J.B. Klemp, J. Dudhi, D.O. Gill, D.M. Barker, M.G. Duda, X.-Y. Huang, W. Wang, and J.G. Powers. A Description of the Advanced Research WRF Version 3. *Technical Report*, (June):113, 2008. ISSN 1477870X. doi: 10.5065/D6DZ069T.
- SLF. Measurement and Information System (IMIS), 2016. URL [http://www.slf.ch/ueber/organisation/warnung{}\\_praevention/warn{}\\_informationssysteme/messnetze{}\\_daten/imis/index{}\\_EN](http://www.slf.ch/ueber/organisation/warnung{}_praevention/warn{}_informationssysteme/messnetze{}_daten/imis/index{}_EN).
- RI Smith. Statistics of extremes, with applications in environment, insurance, and finance. *Monographs on Statistics and Applied Probability*, (March):1–62, 2004. ISSN 0960-6696.
- Clara M. St. Martin, Julie K. Lundquist, Andrew Clifton, Gregory S. Poulos, and Scott J. Schreck. Wind turbine power production and annual energy production depend on atmospheric stability and turbulence. *Wind Energy Science Discussions*, 0:1–37, 2016. ISSN 2366-7621. doi: 10.5194/wes-2016-21. URL <http://www.wind-energ-sci-discuss.net/wes-2016-21/>.
- Mária Süveges and Anthony C Davison. Model misspecification in peaks over threshold analysis. *The Annals of Applied Statistics*, 4(1):203–221, 2010. ISSN 1932-6157. doi: 10.1214/09-AOAS292. URL <http://arxiv.org/abs/1010.1357>.
- Swiss Academy of Engineering Sciences (SATW). Road Map Renewable Energies Switzerland: An analysis with a view to harnessing existing potentials by 2050. page 24, 2012.
- Swiss Federal Office of Energy SFOE. Energy Strategy 2050: Chronology 23. 2018. URL <http://www.bfe.admin.ch/themen/00526/00527/index.html?lang=en>.
- Swissgrid. Grid Data 2014. Technical report, 2014.
- Luciano Telesca, Michele Lovallo, and Mikhail Kanevski. Power spectrum and multifractal detrended fluctuation analysis of high-frequency wind measurements in mountainous regions. *Applied Energy*, 162(JANUARY):1052–1061, 2016. ISSN 03062619. doi: 10.1016/j.apenergy.2015.10.187.

- Sven Teske. Energy [r]evolution EUROPEAN RENEWABLE “ will we look into the eyes of our children and confes s that we had the opportunity ,. Technical report, Greenpeace Schweiz, 2013.
- E. Thibaud, R. Mutzner, and a. C. Davison. Threshold modeling of extreme spatial rainfall. *Water Resources Research*, 49(8):4633–4644, 2013. ISSN 00431397. doi: 10.1002/wrcr.20329.
- Heimo Truhetz. *High resolution wind field modelling over complex topography : analysis and future scenarios*. Phd thesis, Graz, 2010.
- Heimo Truhetz, Andreas Krenn, Hans Winkelmeier, Stefan Müller, René Cattin, Tobias Eder, and Markus Biberacher. Austrian Wind Potential Analysis ( AuWiPot ). In *12. Symposium Energieinnovation, 15.-17.2.2012, Graz/Austria*, pages 1–10, Graz, 2012.
- Falko Ueckerdt, Robert Brecha, and Gunnar Luderer. Analyzing major challenges of wind and solar variability in power systems. *Renewable Energy*, 81:1–10, 2015. ISSN 18790682. doi: 10.1016/j.renene.2015.03.002. URL <http://dx.doi.org/10.1016/j.renene.2015.03.002>.
- Franz-Georg Ulmer and Ulrich Bals. Spin-up time research on the weather research and forecasting model for atmospheric delay mitigations of electromagnetic waves. *Journal of Applied Remote Sensing*, 10(1):016027, 2016. ISSN 1931-3195. doi: 10.1117/1.JRS.10.016027. URL <http://remotesensing.spiedigitallibrary.org/article.aspx?doi=10.1117/1.JRS.10.016027>.
- I. Vergeiner and E. Dreiseitl. Valley winds and slope winds - Observations and elementary thoughts. *Meteorology and Atmospheric Physics*, 36(1-4):264–286, 1987. ISSN 01777971. doi: 10.1007/BF01045154.
- D Villanueva, J L Pazos, and A Feijóo. Analysis of the relationship between distance and wind speed correlation in complex terrain cases . *Wind Energy*, 2011.
- VSE. Wege in die neue Stromzukunft - Gesamtbericht. page 128, 2012.
- VSE. Basiswissen Windenergie. Technical Report September 2013, Verband Schweizer Elektrizitätsunternehmen VSE, 2014.
- J W Wagenaar and P J Eecen. Dependence of Power Performance on Atmospheric Conditions and Possible Corrections. In *The European Wind Energy Association*, number March, pages 14–17, 2011. ISBN 9781618399915.
- Wei Wang, Cindy Bruyère, Michael Duda, Jimy Dudhia, Dave Gill, Michael Kavulich, Kelly Keene, Hui-Chuan Lin, John Michalakes, Syed Rizvi, Xin Zhang, Judith Berner, Soyoung Ha, and Kate Fossell. Weather Research & Forecasting ARW Version 3 Modeling System User’s Guide. Technical Report July, NCAR, 2016.
- Wei Wang, Cindy Bruyère, Michael Duda, Jimy Dudhia, Dave Gill, Michael Kavulich, Kelly Werner, Ming Chen, Hui-Chuan Lin, John Michalakes, Syed Rizvi, Xin Zhang, Judith Berner, Domingo Munoz-Esparza, Brian Reen, Soyoung Ha, and Kate Fossell. ARW Version 4

## Bibliography

---

- Modeling System User's Guide. Technical Report July, 2018. URL [http://www2.mmm.ucar.edu/wrf/users/docs/user\\_guide\\_V3.7/ARWUsersGuideV3.7.pdf](http://www2.mmm.ucar.edu/wrf/users/docs/user_guide_V3.7/ARWUsersGuideV3.7.pdf).
- Rudolf O. Weber and Markus Furger. Climatology of near-surface wind patterns over Switzerland. *International Journal of Climatology*, 21:809–827, 2001. ISSN 08998418. doi: 10.1002/joc.667.
- Nicolas Oliver Weidmann. Transformation strategies towards a sustainable Swiss energy system, 2013. URL <http://e-collection.library.ethz.ch/view/eth:7364>.
- Tanja Weusthoff. Weather Type Classification at MeteoSwiss - Introduction of new automatic classification schemes. *Arbeitsberichte der MeteoSchweiz*, (235):46, 2011.
- D J Wiersema, K A Lundquist, and F K Chow. A framework for WRF to WRF-IBM grid nesting to enable multiscale simulations. Technical report, 2016.
- Andrew Williams. Improving wind farm availability Better performance and increased ROI through accurate availability measurement Improving wind farm availability. *Wind Energy Update*, 2014. URL <http://www.windenergyupdate.com/operation-maintenance-onshore-report/pdf/WEUSciemusWP.pdf>.
- Wind Europe. European Wind Energy Generation, first half of 2017. 2017.
- WindSim. WindSim, 2018. URL <https://windsim.com/>.
- Hans Winkelmeier, Andreas Krenn, and Florian Zimmer. Das realisierbare windpotential Österreichs für 2020 und 2030. Technical report, FFG Österreichische Forschungsförderungsgesellschaft mbH, 2014.
- Adam Winstral, Tobias Jonas, and Nora Helbig. Statistical Downscaling of Gridded Wind Speed Data Using Local Topography. *Journal of Hydrometeorology*, 18(2):335–348, feb 2017. ISSN 1525-755X. doi: 10.1175/JHM-D-16-0054.1. URL <http://journals.ametsoc.org/doi/10.1175/JHM-D-16-0054.1>.
- John C. Wyngaard. Toward Numerical Modeling in the “Terra Incognita”. *Journal of the Atmospheric Sciences*, 61(14):1816–1826, 2004. ISSN 0022-4928. doi: 10.1175/1520-0469(2004)061<1816:TNMITT>2.0.CO;2.
- Bowen Zhou, Jason S. Simon, and Fotini K. Chow. The Convective Boundary Layer in the Terra Incognita. *Journal of the Atmospheric Sciences*, 71(7):2545–2563, 2014. ISSN 0022-4928. doi: 10.1175/JAS-D-13-0356.1. URL <http://journals.ametsoc.org/doi/abs/10.1175/JAS-D-13-0356.1>.

## Curriculum Vitae

Kruyt, Albertus Christiaan (Bert)  
Grünenstrasse 13,  
7270 Davos Platz, Switzerland.

Telephone: +41 (0)76 671 98 91  
E-mail: bertkruyt@gmail.com  
Nationality: Dutch  
Date of birth: 25/06/1982  
Gender: Male



---

### Professional experience

- Dec 2014 – 2018* PhD researcher at **École Polytechnique Fédérale de Lausanne (EPFL)**.  
Supervised by Prof. Dr. Michael Lehning.
- 2014 – current* Guest researcher at **WSL Institute for Snow and Avalanche Research SLF**.
- 2013 – 2014* Programmer at **Utrecht University**. Review of the TIMER model, an energy systems model, simulating the global energy system.
- 2012 – 2013* Consultant at **Ernst & Young Cleantech and Sustainability Services**.  
Energy efficiency and renewable energy consultancy projects in various industrial sectors. Data analysis, monitoring and the development of software tools to these ends.
- 2010 – 2012* Consultant at **Beco**. Tasks and responsibilities as described above. In October 2012, Beco became part of Ernst & Young.
- 2008 – 2009* Programmer at the **Netherlands Environmental Assessment Agency**,  
Department of Climate and Global Sustainability (KMD). Development of the TIMER energy systems model. Development a web-based User Support System for the IMAGE model.
- 2007 – 2008* Intern at both the **Energy Research Centre for the Netherlands** as well as the **Netherlands Environmental Assessment Agency**. Work on indicators for energy security, theoretical and modelling.

### Education

- 2006 – 2008* **MSc Energy Science**, Utrecht University.  
Topics: Energy economics, energy system analysis, energy conversion technology, energy policies, (mitigation of) climate change, ETS, IPCC, scenario-based modelling, sustainable development & global change, LCA, cost-benefit analysis.  
MSc Thesis: “ Indicators for energy security”
- 2001 – 2005* **BSc Physics**, Utrecht University. (With distinction)  
Optional courses: - 2 months teaching physics at high school  
- Communication and didactics in science  
- Special program on economics and business.  
BSc Thesis: “Magnetohydrodynamic propulsion”
- 1994 – 2000* Grammar School ( “Gymnasium” ), Utrecht.

## Additional training and education

2016	<b>Ski Touring Instructor</b> , Royal Dutch Mountaineering federation NKBV
2013	<b>Time management</b> , in-house training at Ernst & Young
2012	<b>Acquisition skills</b> , in-house training at Beco
2010	<b>Professional consulting</b> , in-house training at Beco
2008	<b>Presentation skills</b> , training by Helma Coolman Communicatie & Advies.
2001	<b>Studio Sound Certificate</b> , audio engineering program at the School of Audio Engineering (SAE).

## Languages

Dutch	Fluent (mother tongue)
English	Fluent
German	Advanced
Spanish	Intermediate
French	Beginner

## Computer skills

Programming	Python, R, Matlab, VBA, C, M, html (basic), Java (basic)
-------------	--

## Other

Free time	Rock climbing, backcountry skiing & freeride, mountaineering, yoga
Driving license	Holder of a clean EU category B drivers licence

## Selected publications and referred scientific articles

- B Kruyt, J Dujardin, M Lehning (2018) Improvement of wind power assessment in complex terrain: The case of COSMO-1 in the Swiss Alps, *Frontiers in Energy Research* 6, 2018, doi: [10.3389/FENRG.2018.00102](https://doi.org/10.3389/FENRG.2018.00102)
- B Kruyt, A Kahl, M Lehning (2017) Potential contributions of wind power to a stable and highly renewable Swiss power supply, *Applied Energy* 192, doi: [10.1016/j.apenergy.2017.01.085](https://doi.org/10.1016/j.apenergy.2017.01.085)
- J Dujardin, A Kahl, B Kruyt, S Bartlett, M Lehning (2017) Interplay between photovoltaic, wind energy and storage hydropower in a fully renewable Switzerland, *Energy* 135, 2017 doi: [10.1016/j.energy.2017.06.092](https://doi.org/10.1016/j.energy.2017.06.092)
- S. Bartlett, B. Kruyt, A. Kahl, M Lehning, (2015) Risks and Reliability in a Fully Renewable Switzerland, ESREL proceedings
- Benjamin K Sovacool (ed.) (2010) *The Routledge Handbook of Energy Security*, Chapter 15 doi: [10.4324/9780203834602.ch15](https://doi.org/10.4324/9780203834602.ch15)
- Kruyt, B., D.P. van Vuuren, H.J.M. de Vries and H. Groenenberg, (2009) Indicators for Energy Security, *Energy Policy*, Volume 37, Issue 6, June 2009, Pages 2166-2181, doi: [10.1016/j.enpol.2009.02.006](https://doi.org/10.1016/j.enpol.2009.02.006)
- Indicators for Energy Security, MSc Thesis, Utrecht University, 2008



